Author/s:
Titchener, Samuel Andrew

Title:
Oculomotor Behaviour and Perceptual Localisation in Retinal Prostheses

Date:
2020

Persistent Link:
https://hdl.handle.net/11343/262680

Oculomotor Behaviour and Perceptual Localisation in Retinal Prostheses

Samuel Andrew Titchener

ORCiD: 0000-0001-8312-2924

Submitted in total fulfilment for the degree of Doctor of Philosophy

September 2020

Department of Medical Bionics

Faculty of Medicine, Dentistry & Health Sciences

University of Melbourne

Abstract

Prosthetic vision is an emerging technology aiming to provide artificial vision to the profoundly blind. Present-day visual prostheses provide useful assistance in everyday life but the quality of vision is poor, with only fractional visual field coverage and limited resolution of detail. The retina, optic nerve, or primary visual cortex are electrically stimulated using implanted electrodes to elicit artificial visual percepts. Eye movements cause movement of the percept within the visual field, however, in many devices, electrode activity is modulated by images captured by a head-mounted camera that does not move in conjugate with eye movement. Percept locations are therefore dissociated from the real-world, leading to localisation errors. Users must be trained to use head movement, rather than eye movement, to control the camera, potentially increasing the difficulty of using the device for every-day activities. This thesis explores oculomotor behaviour in prosthetic vision and investigates the use of eye tracker feedback to redirect the video input in real time ('gaze compensation') to restore naturalistic control of gaze.

The first study presented in the thesis investigated the effect of visual field loss on eye and head movement coordination in low-vision subjects with retinitis pigmentosa (RP), the current primary indication for retinal prostheses. Visual field loss was found to be associated with a habitually confined range of eye movement and a greater reliance on head movement. This has implications for training and rehabilitation in visual prostheses, as recipients with RP express atypical eye and head scanning behaviour.

An investigation of the oculomotor behaviour of retinal prosthesis recipients in a forced-choice localisation task and a motion discrimination task is also presented. Although the participants were aware of the potential for eye movements to impair task performance, systematic eye movements were observed in response to the task stimuli. These were interpreted as reflexive eye movements made in response to the static and dynamic stimuli, as would be expected in normal vision, suggesting preserved oculomotor capacity. This is a promising indication for the naturalistic integration of artificially evoked percepts into the visual system, but the primary purpose of these eye movements, namely foveation, cannot be fulfilled without gaze compensation.

Following the demonstration of naturalistic eye movement in retinal prosthesis users and the finding that suppression of eye movement was difficult or impossible, the thesis then examines the effect of eye movement on localisation and the possible benefits of gaze compensation. It was found that eye movement lead to localisation errors in a target localisation task in simulated prosthetic vision, but the introduction of gaze compensation resolved this. A subsequent pilot study in retinal prosthesis recipients is also presented, in which no benefit of gaze compensation for localisation was observed, possibly because the subjects had learned compensatory strategies. However, some methodological problems were identified, and similar studies from a different group do show a benefit of gaze compensation. Overall the thesis advances the understanding of the perceptual experience and oculomotor behaviour of visual prosthesis users and argues for the integration of gaze compensation in camera-based visual prostheses.

Declaration

I declare:

i. This thesis comprises only original work towards the degree of Doctor of Philosophy, except where indicated in the preface.
ii. Due acknowledgement has been made in the text to all material previously written or published by another person.
iii. The thesis is fewer than the maximum word limit in length, exclusive of tables, bibliographies, and appendices.

Samuel Andrew Titchener

Preface

All of the work presented in the thesis was carried out during my postgraduate candidature and was first-authored by myself. This thesis contains published and unpublished work that was carried out in collaboration with others. Chapters that have been published or submitted for publication are indicated in the text. The contributors to each published or in-review study are named at the beginning of the relevant chapter, and their specific contributions are listed below. The studies presented in Chapter 4, Chapter 6, and Chapter 7 have been published in peer reviewed journals (Chapter 4: IOVS, 2019; Chapter 6: TVST 2020; Chapter 7: TVST, 2018) and the author-accepted version of those manuscripts are included unabridged. Chapter 8 presents unpublished material not submitted for publication. Chapter 5 presents analyses that featured in a published article first-authored by Dr. Mohit Shivdasani in which I was named as a co-author (IOVS, 2017). Only my own contributions to this study are included in the thesis, and the presentation has been changed from the published version to respect copyright.

My own contributions to this work include the design and planning of psychophysical experiments in simulated prosthetic vision, low vision subjects, and retinal implant recipients. I was responsible for developing the necessary software and hardware tools to execute these experiments, and for carrying out the experiments. I developed data analysis techniques to process and interpret the eye and head position data collected in the course of these experiments. I produced three peer-reviewed journal articles and presented my work at local and international conferences. This was possible due to the valuable contributions of the following individuals:

Dr. Matt Petoe: Visual psychophysics lead in the 44-channel retinal implant clinical trial. Contributed to study design and provided intellectual input into data analysis and editing. Aided in carrying out psychophysical experiments in low vision subjects and retinal implant users.

Dr. Mohit Shivdasani: Contributed to study design and provided intellectual input into data analysis and editing. Also contributed to development of the 24-channel and 44-channel retinal implant.

A/Prof. James Fallon: Contributed to study design and provided intellectual input into data analysis and editing.

Dr. Lauren Ayton, Dr. Carla Abbott: Contributed to study design and aided in carrying out psychophysical experiments in low vision subjects. Also contributed to the development and clinical trial of the 24-channel and 44-channel suprachoroidal retinal implant.

Maria Kolic, Elizabeth Baglin, Dr. Jessica Kvansakul, Stephanie Epp: Contributed to the clinical trial of the 44-channel suprachoroidal retinal implant. Aided in psychophysical experiments in retinal implant users.

Emily Caruso, Pyrawy Sivarajah: Aided in acquiring ocular health data from experiment participants with retinitis pigmentosa.

Dr. David Nayagam, A/Prof. Chris Williams, A/Prof. Nick Barnes, William Kentler, A/Prof. Chi Luu, A/Prof. Penny Allen, Nick Sinclair, Dr. Thushara Perara, Damien Pardinas-Diaz, Prof. Peter Blamey, Dr. Lisa Gillespie: Contributed to the development and testing of the suprachoroidal retinal implant.

Acknowledgement of funding:

My candidature was supported by the Australian Government Research Training Program Scholarship and the Melbourne Neuroscience Institute Strategic Australian Postgraduate Award.

Publications

Journal articles

Shivdasani M. N., Sinclair N. C., Gillespie L. N., Petoe M. A., **Titchener S. A.**, Fallon J. B., Perara T., Pardinas-Diaz D., Barnes N. M., Blamey P. J. Identification of Characters and Localization of Images Using Direct Multiple-Electrode Stimulation With a Suprachoroidal Retinal Prosthesis. *Investig Ophthalmol Vis Sci*. 2017;58(10):3962-3974.

Titchener S. A., Shivdasani M. N., Fallon J. B., Petoe M.A. Gaze Compensation as a Technique for Improving Hand–Eye Coordination in Prosthetic Vision. *Transl Vis Sci Technol*. 2018;7(1):2.

Titchener S. A., Ayton L. N., Abbott C. J., Fallon J. B., Shivdasani, M. N., Caruso E., Sivarajah P., Petoe M. A. Head and Gaze Behavior in Retinitis Pigmentosa. *Invest Ophthalmol Vis Sci*. 2019;60(6):2263-2273.

Titchener, S. A., Kvansakul, J., Shivdasani, M. N., Fallon, J. B., Nayagam, D. A. X., Epp, S. B., Williams, C. E., Barnes, N., Kentler, W. G., Kolic, M., Baglin, E. K., Abbott, C. J., Luu, C. D., Allen, P. J., Petoe, M. A. Oculomotor responses to dynamic stimuli in a 44-channel suprachoroidal retinal prosthesis. *Transl Vis Sci Technol.* 2020;9(13):31

Conference abstracts

Titchener, S. A., Shivdasani, M. N., Sinclair, N. C., Petoe, M. A., Fallon, J. B., Pardinas-Diaz, D., & Blamey, P. J. (2016). Oculomotor Behaviour of Patients Implanted with a Suprachoroidal Retinal Prosthesis During a Spatial Discrimination Task. *The Eye and the Chip - World Congress on Artificial Vision.* Detroit, MI.

Titchener, S. A., Sinclair, N. C., Gillespie, L., Petoe, M. A., Fallon, J. B., Pardinas-Diaz, D., … Shivdasani, M. N. (2016). Oculuomotor behaviour of suprachoroidal retinal implant patients during a spatial discrimination task. *4th International Conference on Medical Bionics.* Brisbane, Australia.

Titchener, S. A., Petoe, M. A., Kvansakul, J., Shivdasani, M. N., Nayagam, D. A. X., Epp, S. B., Williams, C. E., Barnes, N., Kentler, W. G., Kolic, M., Baglin, E. K., Abbot, C. J., Luu, C. D., Allen, P. J. (2019). Perception of motion in a 2nd generation suprachoroidal retinal implant. *Artificial Vision*. Aachen, Germany.

Petoe, M. A., **Titchener, S. A.**, Shivdasani, M. N., Fallon J. B., Abbott, C. J., Ayton, J. N. Visual Scanning in Retinitis Pigmentosa. (2018). *Investigative Ophthalmology & Visual Science.* 59 (9), 1946-1946

Acknowledgements

My endless gratitude goes to my partner, Haley, for being with me every step of the way. I'm humbled by your support and commitment, and by your incredible patience while I walked around with my head in the clouds.

I would also like to acknowledge my primary supervisor Matt, and co-supervisors James and Mohit, without whom this work would not have been possible. Matt, a close friend and role model, provided guidance and freedom in just the right balance and tutored me in the important skill of figuring things out as I go along. Thank you for the long days in the psychophysics booth and the long evenings at the pub. Thanks to James and Mohit for sharing a wealth of knowledge and expertise, and for sacrificing so much of your time to keep me on track.

Thanks to all the excellent people from the Bionics Institute, CERA, and the University of Melbourne, who made the BVT clinical trial a fantastic experience – Maria, Liz, Penny, Carla, Lauren, Kiera, Matt, Jessica, Dave, Steph, and William. Thanks also to the Mollison house picnic table and all the characters who filled its seats. A special mention to Tom, Ella, Angus, Caitlin, Claire, and Chrystal, for camaraderie, solidarity, and hilarity.

And finally, to my family for their unfaltering support always.

Contents

List of Figures

Chapter 1

Introduction

The visual system processes an astonishing amount of information and is the primary means by which we understand the world around us. From reading and writing, to walking down the street, to recognising friends and interpreting body language, the activities we perform every day depend upon vision to such a tremendous degree that it can be difficult to imagine life without sight.

Vision impairment is a growing problem in many developed countries with aging populations. A survey study in 2009 estimated that 575,000 Australians aged over 40 suffered vision loss, with 66,500 of those meeting the legal criteria for blindness. That number was projected to rise to 801,000 impaired and 102,750 blind by 2020.[1] Not only do these people experience loss of independence and agency, blindness is also associated with mental health issues, social isolation, and poor general health. The estimated financial burden of visual disorders in Australia in 2009 was A$16.6 billion, up from A$9.85 billion in 2004. This figure includes A$9.4 billion in loss of wellbeing, A$2.98 billion in health system costs, and A$4.2 billion in indirect costs such as carer's costs, lost productivity, and welfare payments.[1–3] Many vision impairment conditions are easily treated – for example, cataracts can be removed with a relatively simple and safe surgery. But for some other conditions there is currently no effective treatment, representing about 10% of cases of vision impairment in Australia. These conditions include retinitis pigmentosa, age-related macular degeneration, diabetic retinopathy, and glaucoma.[4]

Visual prostheses have recently emerged as a tool for providing artificial vision to those visually impaired by otherwise untreatable conditions. These devices electrically stimulate neurons in the visual pathway in order to elicit artificial visual percepts. Retinal implants are currently the predominant type of visual prosthesis. They target neurons in the retina and require a functional optic nerve to carry signals to the higher visual centres, and therefore are only suitable for diseases that primarily impact photoreceptor cells and spare the remaining network, for example retinitis pigmentosa or age-related macular degeneration.[5,6] Cortical implants, targeting neurons in the primary visual cortex, have begun to receive greater attention in recent years. Cortical implants could be applicable in a much wider range of blindness conditions, even when the eye and optic nerve are severely damaged, with the obvious trade-off of requiring brain surgery. Implants that target the optic nerve or the thalamus are also possible, but have received less research focus due to inherent practical constraints.[7]

Though there is variation between different devices, many visual prostheses comprise the same basic components. An external camera, usually mounted on a spectacle frame, captures images of the scene in front of the user. Images from the camera are sent to a portable vision processing unit that determines the electrical stimulation required to produce a useful visual percept based on the captured image. Stimulation commands are then transmitted wirelessly to an implanted stimulator, which generates the electrical stimulation that is delivered to the retina, optic nerve, thalamus, or visual cortex, resulting in a visual percept. One notable exception to this design pattern is photovoltaic retinal implants. In these devices, electrode activity is modulated by ambient or projected light that enters the eye and is received by a photosensitive implanted photodiode array. Designs using ambient light (rather than artificially projected light) may forego the head-mounted camera.

To date several hundred individuals worldwide have received visual prostheses, mostly retinal implants. These devices have proven to be useful in everyday life, providing assistance in navigation, social interaction, and other everyday activities. For many users the impact on their quality of life has been profound.[8] However, present-day visual prostheses are crude compared to the incredible intricacies of natural vision. Spatial resolution is limited by the relatively large size of the stimulating electrodes, which flood large areas of the retina (or visual cortex) with electric current, activating large populations of interconnected neurons. Visual neurons of many types and functions are activated indiscriminately. The resulting visual percept can be indistinct, lack form, and covers only a small fraction of the visual field.[5,9,10]

An understanding of the visual experience of users is vital for optimising stimulation parameters, evaluating the effectiveness of new developments, and training users to interpret their unfamiliar new artificial sense. Verbal accounts from users are valuable but inescapably subjective, making them a poor basis for design decisions if not supported by objective measurement. Instead, psychophysics techniques are used to systematically quantify and characterise artificial vision, answering questions about some particular aspect of artificial vision, such as resolution of detail or perception of motion, in an objective way. This provides a framework for research and design decisions and is the primary means by which the effectiveness of any development can be evaluated.

Oculomotor behaviour (eye movement) plays an important role in visual psychophysics due to its intimate coupling with perception and attention. Our eyes are in constant motion, although we may not often be conscious of it. Humans possess an area of high acuity central vision, the fovea, capable of resolving fine detail, surrounded by low acuity peripheral vision. It is eye movement that enables us to direct the fovea around the field of view to examine features that catch our attention and track objects as they move.[11] Eye movement also plays an important role in perceptual localisation and spatial updating, the maintenance of a consistent three-dimensional map of the space around us. The orientation of the eyes is monitored and fed back into the visual system to stabilise the perception of the world.[12] Without this functionality the entire world would appear to shift each time we moved our eyes. Thus the oculomotor system plays a role in the interpretation of visual percepts in addition to planning and executing eye movements. Observing the type, size, and frequency of eye movements can grant valuable insight into an individual's visual experience.

Oculomotor behaviour has particular significance in visual prostheses due to the separation between the retina and the image sensor of the head-mounted camera. Just as in normal vision, eye position is used to determine the location of a percept; visual stimuli are interpreted as originating from whichever direction the eye is pointing in. This means that eye movements cause a corresponding movement of the percept within the visual field since the stimulating array is retinally fixed. However, the camera remains fixed in place, capturing only what is directly ahead regardless of any eye movement. Thus, eye movements change the location, but not the content, of the percept. The result is that percept locations are dissociated from the real-world axes, leading to localisation errors, and that eye movement cannot be used for visual search because eye movement has no effect on the camera orientation. This, coupled with the highly limited field of view afforded by present day retinal implants, makes exploration of the visual environment a difficult and unintuitive task. Visual prosthesis recipients must learn head scanning strategies to systematically sample their environment and localise objects relative to the camera instead of the eye.[13]

This thesis presents a number of visual psychophysics experiments in retinal prosthesis recipients, low vision subjects, and simulated prosthetic vision. The experiments were conducted in the context of the development and clinical trial of a retinal implant (Bionic Vision Technologies, Australia). The thesis aims to characterise oculomotor behaviour in order to further our understanding of perception in prosthetic vision and inform future developments in the field. Eye movements are analysed in order to understand visual perception and particular focus is given to the unusual perceptual side-effects introduced as a consequence of the fixed-position camera in visual prostheses.

1.1. Thesis outline

Chapter 2 reviews the relevant literature to provide context for the original works in the thesis. The fundamental concepts underlying visual prostheses are introduced and the current state of the field is summarised, including a discussion of the various devices that exist and their clinical successes and limitations. Literature relating to the perceptual experience of prosthetic vision is also reviewed. Experimental methodologies relevant to several of the studies are detailed in Chapter 3. The remaining chapters present a series of studies that constitute the original contributions of the thesis. Three of these chapters were published in peer-reviewed journals and a fourth featured as an original contribution to a co-authored journal article.

The first study, presented in Chapter 4, investigates the coordination of eye and head movement in retinitis pigmentosa. Statistical and neural models of eye movement planning contend that much of eye movement is driven by visual saliency.[14] It is thought that visual field loss would interfere with this process, changing oculomotor behaviour. However, the few existing studies addressing eye movement in low vision have conflicting results, small sample sizes, and differing methodologies. This study aimed to characterise the effect of visual field loss on eye-head coordination, and the range of eye movements made, in a large cohort using a repeatable methodology. The findings can inform the design and clinical practice of retinal implants because retinitis pigmentosa is currently the primary indication for retinal implants, and the limited visual field afforded by retinal implants bears resemblance to peripheral visual field loss.[15]

Chapter 5 and Chapter 6 investigate oculomotor behaviour in recipients of a suprachoroidal retinal implant during spatial localisation and motion discrimination tasks. These studies explore the effects of eye movement on performance in the tasks and make inferences about the visual experiences of the participants based on the types of eye movements observed in response to the task stimuli. We show that the participants made significant eye movements in response to the stimuli, and some of those movements appeared naturalistic and suggest preserved oculomotor capacity.[16]

Chapter 7 and Chapter 8 investigate the relationship between eye movement and spatial localisation in prosthetic vision. The preceding studies suggested that eye movements were difficult to suppress, and previous work has shown that eye movement causes electrically-evoked percepts to move about the visual field.[13] Chapter 7 used simulated prosthetic vision to demonstrate that this leads to errors in reaching for a target, but that this could be corrected by shifting the camera image in parity with eye movement (termed 'Gaze Compensation').[17] Chapter 8 comprises a pilot study aiming to repeat the findings of Chapter 7 in retinal implant recipients.

Chapter 9 reviews the findings of the thesis in the wider context of the visual prostheses and considers the implications of the thesis for future developments in the field.

Chapter 2

Literature review

2.1. The visual system

The visual system encompasses the eye and associated components of the nervous system that work together to acquire and process visual information. This includes the structures of the primary visual pathway (the retina, optic nerve, lateral geniculate nucleus, and the visual cortex) which process the visual signal and give rise to visual perception. Also included are peripheral systems that control other visual functions such as eye movement, pupillary dilation and contraction, and circadian rhythm. This section outlines the structure of the visual system and the function of its main components, focussing on the retina, primary visual pathway, and oculomotor system.

2.1.1. Anatomy of the eye

The body of the eye, the vitreous chamber, is roughly spherical in shape and filled with a clear jelly-like substance called vitreous humour. The wall of the eye, enclosing the vitreous chamber, consists of three layers of tissue. The outermost layer is the sclera, a tough fibrous tissue that provides structure and protection. Directly beneath the sclera is the choroid, which consists mostly of blood vessels and connective tissue. The innermost later is the retina, containing a network of neurons and light-sensitive photoreceptors. The front of the eye hosts the pupil, an

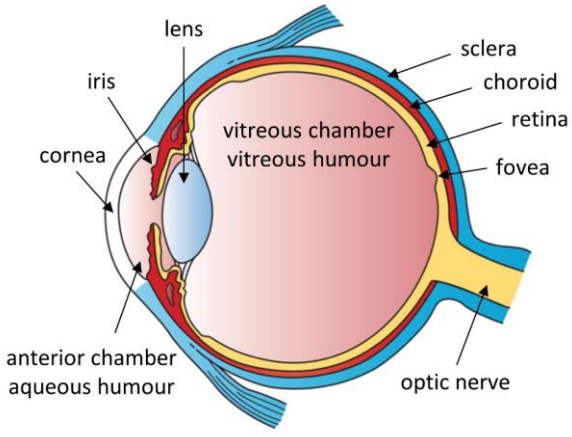

Figure 2.1: Anatomy of the eye. The eye consists of three main layers: the sclera, a tough fibrous outer layer; the choroid, mainly connective tissue and blood vessels; and the retina, which has photoreceptors and networks of neural cells. Adapted with permission from Holly Fischer [CC BY 3.0].[240]

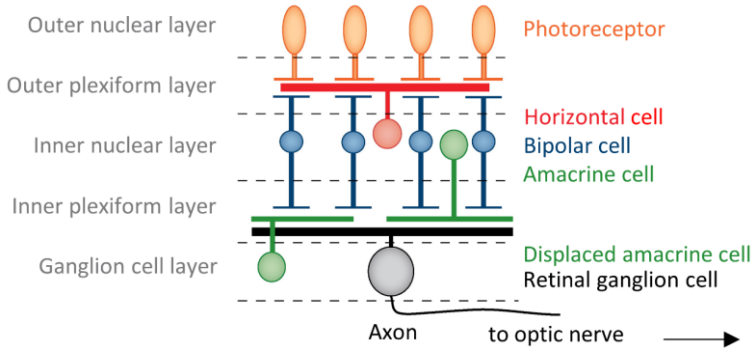

Figure 2.2: Simplified diagram of the organisation of the retina. Adapted with permission from Wei (2018).[188]

opening through which light can enter the eye, as well as the cornea and lens to focus the incoming light onto the retina (Figure 2.1).[18]

The retina contains the eye's sensory cells and is itself a layered structure, as shown in Figure 2.2. Incident light is received by photoreceptors and transduced to electrochemical signals that make their way through the retina and exit the eye via the optic nerve. The macula, the area of the retina responsible for high resolution central vision, contains a high density of cone (chrominance) photoreceptors which is greatest in a small region at the centre of the macula known as the fovea. The more peripheral areas of the retina have fewer photoreceptors and contain a relatively higher proportion of rod (luminance) photoreceptors. Interestingly, the photoreceptors are sub-optimally located in the posterior layer of the retina such that incident light is attenuated by its passage through the other layers of the retina before reaching the photoreceptors. Signals from the photoreceptors are transmitted to bipolar cells in the inner nuclear layer and then to the ganglion cell layer, which runs adjacent to the retina surface. Ganglion cell axons exit the retina via the optic disc, forming the optic nerve, and carry the visual signal to the higher visual centres.[19]

A substantial amount of signal processing occurs in the retina before the visual signal leaves the eye, performed by many different types of retinal visual neurons. The region of photoreceptors that affect the activity of any particular visual neuron is referred to as its receptive field. Horizontal cells in the outer plexiform layer integrate the input from many photoreceptors to form contrast-sensitive networks that modulate bipolar cell activity. The principle of activation is referred to as 'centre-surround', such that each bipolar cell will respond either to a spot of light in the centre of its receptive field surrounded by a dark ring (ON bipolar cell), or to a spot of darkness in the centre of their receptive field surrounded by a ring of light (OFF bipolar cell).[20] Amacrine cells in the inner plexiform layer form horizontal connections between the outputs of bipolar cells, and these networks perform further signal processing. More than twenty types of amacrine cell have been identified in the mammalian retina and many of their functions are not yet well understood.[21] By the time the visual signal reaches the optic nerve it contains separately encoded elements representing visual features such as contrast, luminance, chrominance, size, orientation, speed of motion, and direction of motion.[22]

2.1.2. Visual pathway

The optic nerve projects towards the higher visual centres via the optic chiasma. At this point the visual signal is divided in the left and right hemispheres of the visual field, each to be processed in parallel by the opposing hemisphere of the brain – the left visual field is processed

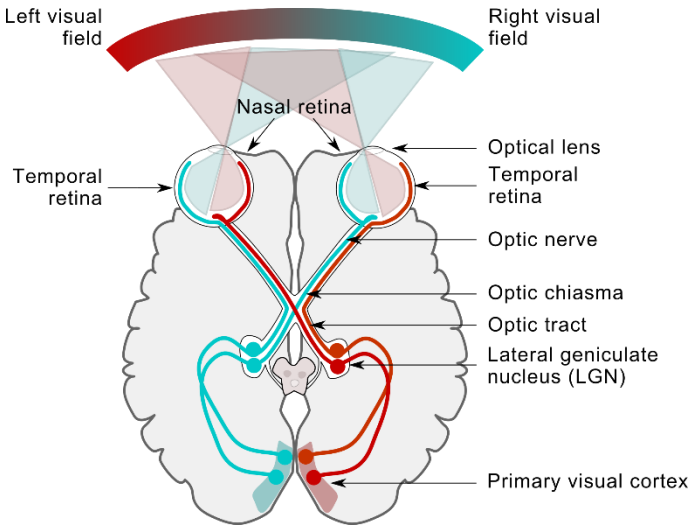

Figure 2.3: Illustration of the primary visual pathway. Adapted with permission from Miquel Perello Nieto [CC BY-SA 4.0].[241]

by the right hemisphere of the brain and the right visual field is processed by the left hemisphere of the brain. To achieve this, the two optic nerves meet at the optic chiasma and exchange half of their axons as shown in Figure 2.3. The axons originating in the left side of the right eye, and those originating in the right side of the left eye (that is, both nasal sides) cross the chiasma and join the nerve on the opposite side. Exiting the optic chiasma, the left optic tract consists of axons originating in the nasal retina of the right eye and the temporal retina of the left eye, while the right optic tract consists of axons originating in the nasal retina of the left and the temporal retina of the right eye. The result is that information from each eye is represented in both hemispheres of the brain but the left and right visual fields are separated, each only represented in the opposite hemisphere.[18]

Once it exits the eye, the primary point of termination of the optic tract is the lateral geniculate nucleus (LGN) of the thalamus. Other destinations are not considered part of the primary visual pathway because their functions are not directly related to the formation of an image, for example the pretectum, which is responsible for controlling pupil dilation, the hypothalamus, which modulates the circadian rhythm, and the superior colliculus, which coordinates head and eye movements. As the optic tract reaches the LGN the axons are segregated based on their functional group, giving the LGN a layered structure with distinct functions per layer.[23] There are two LGNs, one in each hemisphere of the brain, each containing a representation of only half of the visual field because they receive input from only one optic tract each. The LGN was once thought to be a simple relay between the retina and visual cortex but it is now argued that it plays a role in such functions as attentional modulation and integration of the binocular visual signal into a single image.[24] Neurons in the LGN project their axons to the primary visual cortex (V1). Integration and processing of the visual signals occurs in the visual cortex, ultimately resulting in the experience of vision.[18] Each point on the primary visual pathway – the retina, optic nerve, LGN, and primary visual cortex – is retinotopically arranged. That is, the visual field is spatially mapped onto each of these areas according to the spatial map of the retina.[18] This is a crucial concept in the field of visual prostheses, as it means that the retinotopic location of stimulation determines the perceived location in the visual field.

2.1.3. The oculomotor system

Eye movements play an important role in visual perception. From saccades - the abrupt shifts in gaze used to foveate on a new target, to smooth pursuit - the steady movements made when tracking a moving target, our eyes are constantly in motion.[11] Even when fixating intently we make constant eye movements, too small to be perceptible. These 'fixational' eye movements help to counteract percept fading due to neural adaption by shifting the image across the retina, modulating neural activity.[11,25,26] Other eye movements are reflexive, such as the vestibulo-ocular movements that stabilise our gaze during head movements and the reflexive saccades that snap our attention towards startling stimuli, bright colours, and sudden movement.[11]

The primary purpose of saccades is to redirect the fovea towards a stimulus or area of interest. They are abrupt, rapid movements of around 20-200ms in duration that reach velocities as high as 900°/s. Saccades are usually described as "ballistic" movements because, once initiated, the movement cannot be altered or adjusted until it has completed.[27] In fact, visual processing is suspended during saccades in a process called "saccadic masking", such that the movement is not perceivable at all.[28] Large saccades are often followed by subsequent corrective saccades to compensate for any inaccuracy in the initial saccade or movement of the target.

In contrast to the ballistic nature of saccades, smooth pursuits are smooth continuous movements that act to maintain foveation on a moving target. The velocity and trajectory of a smooth pursuit is determined by the target, although smooth pursuits faster than approximately 30°/s are not possible in humans. Unlike saccades, smooth pursuits are closed-loop movements that are controlled and adjusted during the movement and are often interspersed with small "catch-up" saccades that correct for any drift between the target and fovea. Generally, it is not possible to initiate a smooth pursuit movement without the presence of a moving visual target.[11,27]

Motor commands for eye movement and eye-head coordination are primarily generated in the superior colliculus (SC), which is one of the terminations of the optic nerve and contains a retinotopic map of the visual field. The presence of a salient visual stimulus (typically something that contrasts with its surroundings) in the visual field causes activity at the corresponding location in the SC, leading to the generation of a saccade toward the stimulus. Auditory and somatosensory inputs are also systematically mapped in the SC, enabling the generation of saccades towards other salient sensory cues.[11,29]

Computational models that incorporate these saliency cues have been shown to be effective predictors of eye movement; however, humans express a wide range of complex oculomotor behaviours that depend on context and intent, not saliency alone. It is thought that the response to salient stimuli is modulated in the SC by other factors, such as attention and cognition. Thus oculomotor behaviour depends on a combination of saliency based "bottom-up" inputs and volitional "top-down" control.[14,30,31] A number of other brain structures are also implicated in eye movement control, such as the frontal eye field (within the frontal cortex), the paramedian pontine reticular formation (of the brainstem), and the dorsolateral pontine nucleus (also of the brainstem).[32]

Eye movements also play an important role in perceptual localisation and spatial updating – the assimilation of visual information into a coherent three-dimensional spatial map. Perceptual

localisation is important in localising objects in space, hand-eye coordination, navigation, mobility, and spatial awareness more generally. Eye and head movements change the angle of incident light, causing visual stimuli to move across the retina, transforming their position in the field of view. Importantly, oculomotor information is used to compensate for these movements to maintain a stable and consistent representation of space. Thus the oculomotor system is not just responsible for planning and executing eye movement, but also plays a role in the localisation of percepts.

Oculomotor information for the stabilisation reflex/process comes from two sources: as proprioceptive information from the extraocular muscles ('inflow'), and as an internal copy of the muscle innervation signals for voluntary eye movements ('outflow'). Inflow was aptly demonstrated by Gauthier et al in a simple experiment wherein participants had one eye patched and passively rotated using a suction cup. When the participants attempted to point to a target seen with their non-patched eye the pointing error was skewed towards the direction in which the patched eye was deviated.[33] Outflow has been anecdotally demonstrated in paralysed subjects, who reportedly perceive a confusing sense of motion of their entire visual field when attempting (but failing) to move their eyes.[34] The interplay of the two information streams is complex, and both affect perceptual localisation.

2.1.4. Retinal degeneration

Retinitis pigmentosa is an inherited condition characterised by the gradual degeneration of the retinal photoreceptor cells.[35] Approximately 1 in 4000 people are affected by retinitis pigmentosa, equating to around 1.5 million people worldwide.[36] Progression of the disease is highly variable, but symptoms usually begin in adolescence or early adulthood with a loss of night vision. Peripheral vision loss follows, resulting in "tunnel vision" that gradually narrows as the degradation spreads, eventually progressing to profound blindness. Most cases lead to legal blindness due to restricted field of view by 40 years of age, and to loss of central vision by age 60.[37]

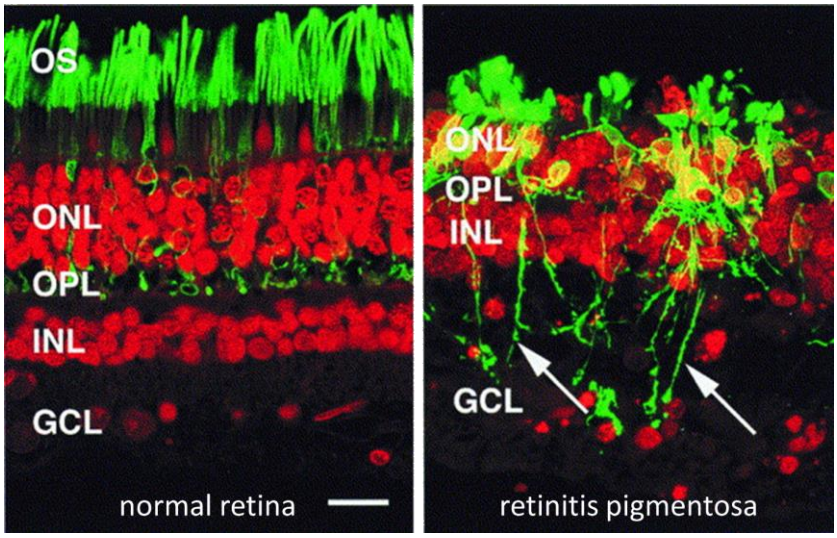

Figure 2.4: Histological imaging comparing a healthy retina (left) to a retina affected by retinitis pigmentosa (right). Colours show immuno-labelling of rod photoreceptors with anti-opsin (green) and staining of nuclei in the outer nuclear layer (ONL), inner nuclear layer (INL), and ganglion cell layer (GCL) with propidium iodide (red). The photoreceptor cells are severely degraded. The neuronal cells in the inner nuclear layer and the ganglion cell layer are largely preserved. Scale bar = 25µm. Adapted with permission from Fariss et al (2000).[242]

A gene therapy treatment for retinitis pigmentosa is currently in clinical trials in the USA, marketed under the name “Luxturna”. Initial results show some efficacy of the treatment for restoring vision, but it remains to be seen whether these benefits are maintained long-term.[38] Importantly, the Luxturna treatment is indicated in only a small minority of cases because it targets just one particular genetic mutation known to cause retinitis pigmentosa, while mutations in over 40 different genes have been associated with other presentations of the disease.[39,40] Gene therapy treatments for the other forms of retinitis pigmentosa may arise in the future. An additional pharmacological intervention is vitamin A supplementation which can slow the progression of the disease, extending useful vision for an estimated seven years on average, but profound blindness is still the inevitable outcome.[41,42]

In the absence of any effective treatment for retinitis pigmentosa, retinal implants have emerged as a technology for providing artificial vision to the blind. Retinitis pigmentosa leads to near-total loss of photoreceptor cells but the neuronal cells of the inner retina remain relatively preserved, as shown in Figure 2.4. A histological study of post-mortem retinae with severe retinitis pigmentosa reported a preservation rate of 30% for retinal ganglion cells and 78% for cells in the inner nuclear layer,[43] and higher preservations rates would be expected in subjects with less advanced degeneration. Retinal prostheses are designed to interface with these surviving inner retinal neurons in order to provide artificial vision.[44]

2.2. Visual prosthesis technology

Visual prostheses are implantable medical devices that aim to provide artificial vision to the blind. Neurons in the visual pathway are stimulated by implanted electrodes to elicit the perception of localised flashes of light called “phosphenes” in the visual field. Combinations of phosphenes can be used to create geometric patterns that convey useful information to the subject. It is easiest to conceptualise phosphenes as behaving like pixels; discrete independent points of light that can represent an image when used in large numbers. This is known as the “scoreboard model” of phosphene vision and is useful as a conceptual tool but has a number of limitations that are discussed later in this chapter.

The conventional design of a visual prosthesis is illustrated in Figure 2.5. The user wears an external camera, usually mounted on a pair of glasses. Images captured from the camera are sent to a processing unit that determines the appropriate pattern of electrode stimulation to

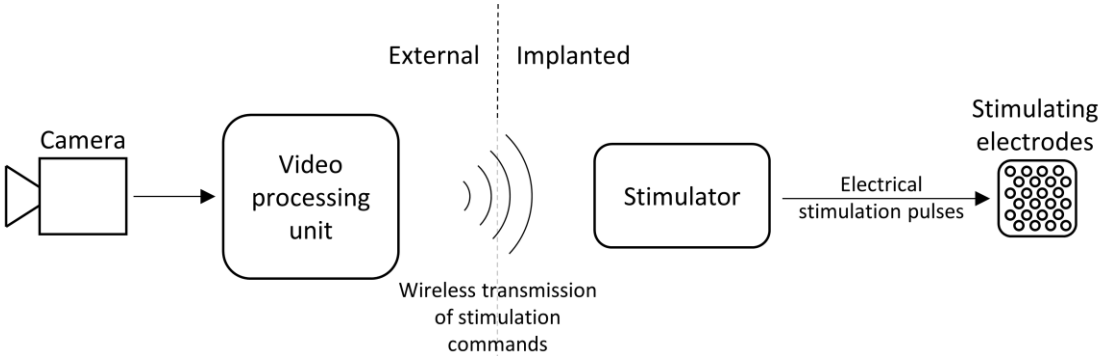

Figure 2.5: Flow chart of a conventional visual prosthesis. Images captured by an externally worn camera are sent to a video processing unit that determines the appropriate stimulation. Stimulation commands are transmitted wirelessly to the implanted stimulator, which then generates the actual electrical stimulation pulses. The electrical pulses travel to the implanted electrodes, stimulating visual neurons to elicit a percept.

elicit a percept that approximates the image. Often the captured image is first processed for easier interpretation, for example by contrast enhancement, saliency enhancement, feature extraction, or depth processing. Stimulation commands are then sent from the processor via a wireless link to an implanted stimulator that generates the actual stimulation pulses. These pulses travel to the stimulating electrodes, which interface with visual neurons at some point in the visual pathway, resulting in a visual percept.

Currently, a wide variety of visual prostheses exist at various stages of development and commercialisation. They vary in several specifications, most notably the anatomical location of the implanted electrode array, the number and size of stimulating electrodes, and the method of sampling the visual environment. The field of visual prosthetics still in its infancy – the visual experience delivered by modern devices can be confusing and unintuitive, and patient outcomes have thus far been convincing but modest – but as the state of the art progresses there is hope that visual prostheses may one day match the successes of cochlear implants in providing reliable sensory input. This section reviews the accomplishments and limitations of modern visual prostheses, the main challenges in the field today, and the promising developments on the horizon.

2.2.1. History of artificial vision

The notion that electrical stimulation can give rise to visual percepts has existed since at least 1755, when French physician Charles Le Roy attempted to treat a blind patient by passing electrical current through the patient's body via electrodes attached the head and leg. The patient reported seeing "flames passing rapidly downwards" and, unsurprisingly, experienced a loud bang and intense pain.[45] A second example of early experimentation with phosphenes comes from Alessandro Volta, esteemed inventor of the battery, who in the year 1800 wrote excitedly to the royal society about his new invention (emphasis mine):

> *"… hold the metallic plate between the lips and in contact with the tip of tongue; since, when you afterwards complete the circle in the proper manner, you excite at once, if the apparatus is sufficiently large and in good order, and the electric current sufficiently strong and in good course,* ***a sensation of light in the eyes****, a convulsion in the lips, and even in the tongue, and a painful prick at the tip of it, followed by a sensation of taste".*[46]

The first attempt to use this phenomenon in a controlled manner for the purpose of artificial vision dates back to 1929, when German Neurosurgeon Otfrid Foerster electrically stimulated the exposed occipital lobe of a patient, inducing a localised perception of light, termed a 'phosphene' in the shape of 'stars', 'clouds', and 'pinwheels'.[47] Other early experimenters in prosthetic vision include Australian Graham Tassicker, who in 1956 described the implantation of a single patient with a photo-sensitive selenium cell behind the retina, and Brindley and Lewin of Cambridge University, who implanted multiple electrodes in the occipital lobe of a single blind patient. In both cases, the patients experienced phosphenes, and Brindley and Lewin were able to demonstrate that by stimulating multiple electrodes simultaneously they could present simple geometric patterns of phosphenes to the subject.[48,49]

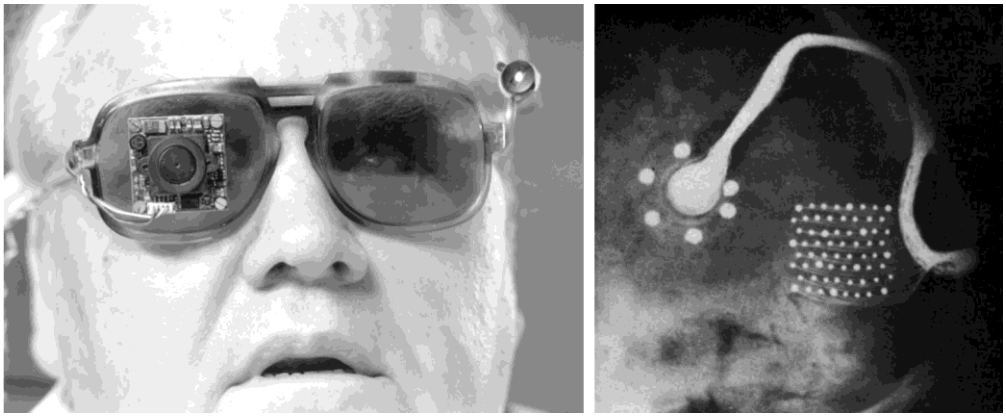

Figure 2.6: The Dobelle bionic eye. (Left): a blind subject wearing glasses with attached video camera. (Right): X-ray image showing the percutaneous connector and array of cortical electrodes. Reused with permission from Dobelle (1976, 2000).[52,243]

Over the following decades, a group led by William Dobelle expanded on the work of Brindley et al in a series of experiments involving stimulation of the occipital lobe in sighted and non-sighted subjects.[50–54] By the year 2000, Dobelle had developed a permanently implantable array of occipital lobe electrodes that were connected to an external stimulator via a percutaneous connector (Figure 2.6). A head mounted video camera connected to the stimulator allowed the subjects to sample their visual environment through the implant. Sixteen subjects received the Dobelle bionic eye and experienced phosphene vision, representing a significant milestone for visual prosthetics, but the project was beset by technical and financial issues and medical malpractice. The recipients, who had personally paid hundreds of thousands of dollars to be involved in the program, have alleged that Dobelle exaggerated the likely benefits of the device in his pitch, ignored seizures that were caused by the device in some subjects, failed to provide some subjects with the external hardware required to actually use the device, withheld refunds for operations that never went ahead, and threatened to eject disgruntled participants from the project.[55] When Dobelle died in 2004 the program was halted, leaving the participants out of pocket and with the defunct implanted hardware still in place, including the infection-prone percutaneous connector. Significant advances have been made since the Dobelle bionic eye, certainly regarding ethics and patient welfare, but also in surgical methods and device design.

2.2.2. Present-day visual prostheses

To date, three visual prostheses have received regulatory approval for commercial sale, with hundreds of patients treated worldwide. Several other devices are in varying stages of development. Generally visual prostheses are categorised by the anatomical placement of the stimulating array, which may be the retina, optic nerve, thalamus, or visual cortex; however, they also vary in a number of other parameters, such as surgical approach, size, method for sampling the visual environment, and the number, size, pitch, and shape of the stimulating electrodes. Figure 2.7 depicts the possible stimulation targets and lists the devices that target each area. An important feature of each of these anatomical targets is their retinotopic architecture, meaning the visual field is spatially mapped in each structure. This is a necessary criterion for a stimulation target to produce a localised percept.

Visual prosthesis recipients have shown improvement in tasks of localisation, orientation and mobility, and activities of daily living.[56] However, visual acuity is very limited. Object recognition,

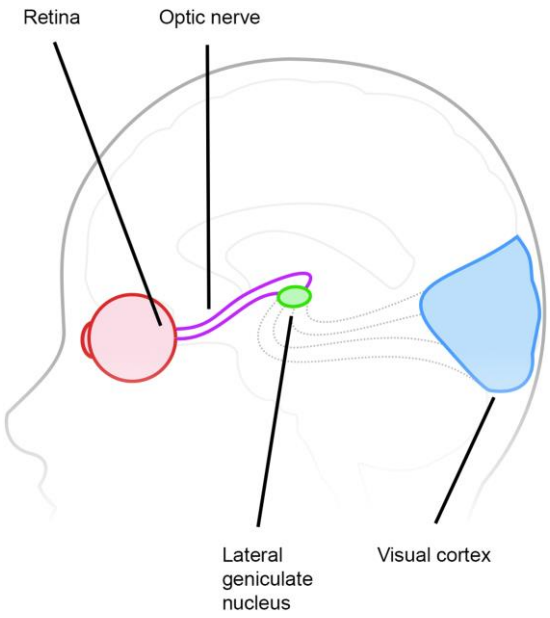

Figure 2.7: Depiction of the possible electrical stimulation targets for visual prostheses. Stimulating electrodes may be implanted in the retina, optic nerve, lateral geniculate nucleus, or visual cortex. Reused with permission from Nguyen et al (2016).[107]

face recognition, and reading are still out of reach for present day devices. This section reviews the visual prostheses currently available or under development. The list of devices presented is not comprehensive but includes the most prominent devices as well as some that illustrate interesting concepts. Functional outcomes for each device will be commented on briefly in this section, while a more comprehensive discussion of functional outcomes is included in Section 2.3.

Retinal prostheses

Retinal prostheses have been the prevailing approach in visual prosthetics so far, principally because the eye is much more surgically accessible than the brain or optic nerve. They are only suitable in blindness caused by retinal degeneration, which causes photoreceptor death while leaving the neuronal population of the retina relatively intact (see Section 2.1.4). Those surviving neuronal cells, which include bipolar cells, horizontal cells, and retinal ganglion cells, are the target of the electrical stimulation. This approach also requires the optic nerve to be intact. One advantage of targeting the retina is that the processing power of the residual horizontal networks of the retina may be utilised, at least in theory, whereas devices that target the higher areas of the visual pathway bypass these networks entirely. Stimulating electrodes for retinal prostheses may be implanted at several different sites within the laminar structure of the retina (Figure 2.8).

Epiretinal implants

The Argus II epiretinal implant (Second Sight Medical Products Inc., USA) was the first visual prosthesis to attain regulatory approval for commercial use, first in the European Economic area (2011) and then in USA (2013).[57] To date, more than 350 patients have received an Argus II. A 6x10 array of platinum electrodes are implanted flat on the epiretinal surface within the macular, ideally covering the fovea, and secured by a titanium tack that pierces the retina.[57,58] A scleral buckle encircles the eye, housing a receiver coil antenna and a stimulator that is

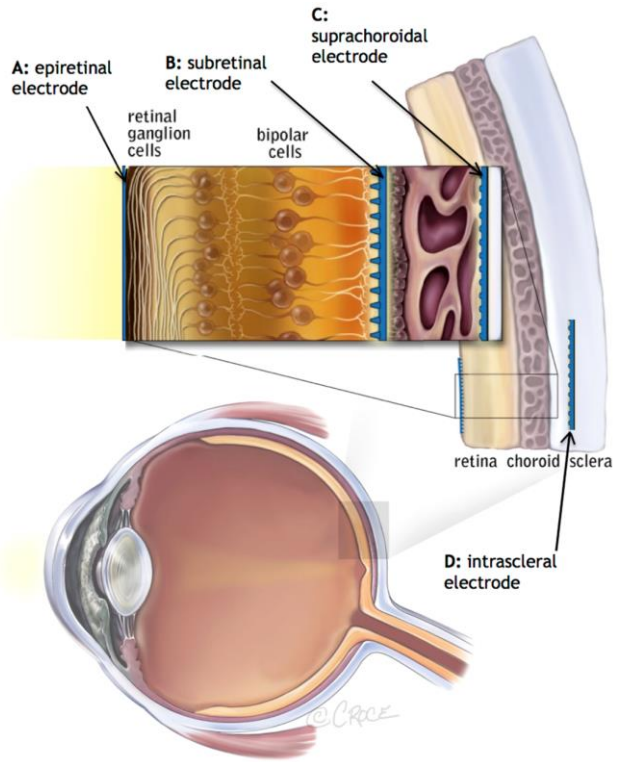

Figure 2.8: Exploded view of the retina depicting the possible implantation sites for retinal prostheses. Stimulating electrodes may be epiretinal, subretinal, suprachoroidal, or intrascleral. Reused with permission from Ayton et al (2014).[88]

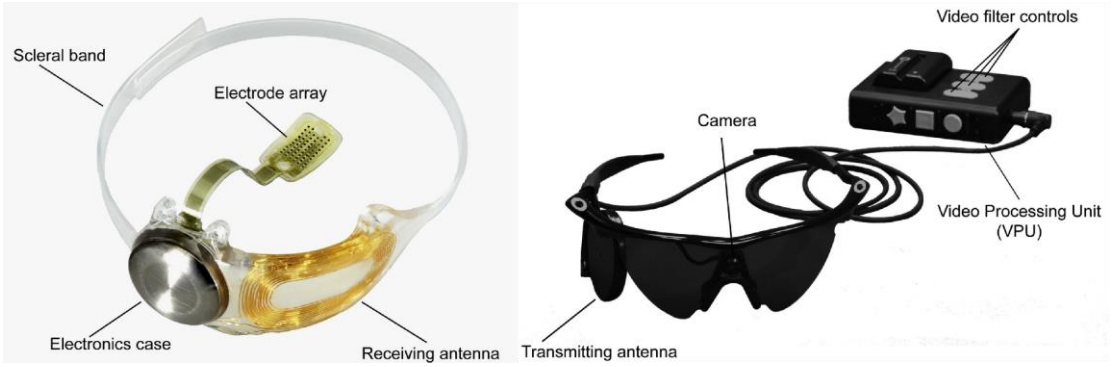

Figure 2.9: Implanted (left) and externally worn (right) components of the Argus II epiretinal implant. Adapted with permission from da Cruz et al (2016).[59]

connected to the implanted electrode array via a ribbon cable passing through the pars plana. Externally worn components include a camera mounted to a pair of glasses, a pocket-sized video processing unit, and a transmitting coil (also mounted to the glasses) that couples with the implanted receiver coil to transmit stimulation commands (Figure 2.9).

The Argus II has so far proven to be generally safe and stable, though a number of adverse events have been reported. In a cohort of 30 recipients, by five years post-implantation two implants had failed due to damage to the receiving coil antenna and three other recipients opted for explant – two due to recurring conjunctival erosion and one due to chronic hypotony and ptosis.[59] In a different cohort of 20 recipients, by 24 months post-implantation fibrosis had developed on the retinal surface beneath the array in 10 recipients (50%), and in nine of those the fibrosis eventually lead to retinoschisis; however, this did not appear to affect visual function

with the device.[60] Improvements in the device design and surgical procedure made since the first Argus II implantations have also reduced the incidence of complications.[58,59,61,62] For the majority of recipients any complications are treatable and the device remains safe and operational for many years. In 2016 it was reported that the longest-running Argus II was still operational 8.4 years after implantation.[59]

A battery of assessment tasks has been used to assess the functional benefit of the Argus. Recipients have demonstrated improved performance with the device on compared to off in localisation, motion detection, and mobility tasks.[58,59,63,64] An assessment that combined self-reporting with expert observation of recipients in the home environment showed that 80% experienced a "positive" or "mild positive" benefit from the device at one year post-implantation and 65.2% at three years.[8,61,65] Second Sight Medical Products have now ceased manufacture of this device in order to focus on their Orion cortical implant, citing the potential for a much larger market for cortical devices due to the wider range of indications.[66]

A second epiretinal implant, the IRIS II (Pixium Vision SA, France), obtained CE approval in 2016. The IRIS II is similar to the Argus II with a few unique innovations. The camera uses a "neuromorphic" image sensor, which encodes temporal pixel changes as well as intensity in order to mimic retinal processing. A novel iterative calibration technique, dubbed "retinal encoding", maps image space to retinotopic space.[67] Stimulation commands are transmitted to the intraocular components through the iris via an infra-red link, although mutually coupled coils are still required to transmit power to the implant so the need for a trans-scleral cable remains. Ten subjects received the device in a clinical trial beginning in 2016 and preliminary psychophysical results were promising[68], however, the lifetime of the device was found to be less than anticipated and the clinical trial was halted.[69] The specific benefits of neuromorphic image sensors and retinal encoding have not been reported.

Other notable epiretinal implants include the EPIRET3 (EPIRET GmBH, Germany) and the NR-600 (Nano Retina Ltd., Israel). The EPIRET3 was the first fully wireless intraocular retinal prosthesis, and featured 25 surface electrodes and an implanted stimulator that communicated wirelessly with an external processor in much the same fashion as the Argus II. Six patients received the device in a four week clinical trial, and all reported visual percepts as a result of electrical stimulation. The device was explanted at the end of four weeks.[70,71] The NR-600 features a relatively high density array of 600 electrodes, which unlike the surface electrodes of the Argus II, IRIS II, and EPIRET3, are designed to penetrate the retina to achieve lower activation thresholds. In a recent Nano Retina press release, the first two patients to receive the NR-600 as part of an ongoing clinical trial were both said to have perceived phosphenes following activation of the device. Further results are anticipated from up to 20 patients.[72]

Subretinal photovoltaic implants

The Alpha IMS (Retina Implant AG GmbH, Germany) subretinal implant became the second visual prosthesis to obtain regulatory approval in Europe in 2013. A chip comprising 1500 photodiode-amplifier-electrode units is implanted in the subretinal space. The activity of each electrode is independently modulated by the light that naturally enters the eye and strikes the photodiode array, eliminating the requirement for an externally worn camera. A bias voltage to amplify the photodiode signal is necessary because the photodiode current generated from

ambient light is usually below perceptual levels.[73] To supply this bias voltage, a power supply cable exits the eye through the choroid and sclera, connecting the subretinal array to subdermal coil on the ipsilateral skull. An external coil, magnetically coupled to the subdermal coil, provides power and data transfer from a pocket-sized battery and control unit.[74]

Alpha IMS recipients have demonstrated functional improvement in localisation, motion discrimination, object recognition, activities of daily living.[74–76] However, problems with hermetic chip encapsulation led to a very short operational lifetime of the device, with only 32% of devices functioning after 12 months.[77] The Alpha IMS was superseded by the Alpha AMS, featuring 1600 stimulating electrodes and modified encapsulation which greatly improved longevity.[78,79] The predicted median device lifetime for Alpha AMS is 4.7 years and 81% of devices were still functional after 12 months.[80] However, in 2019 Retina Implant AG discontinued business activities and production of the Alpha AMS ceased.[81]

When compared to other visual prostheses, the photovoltaic approach of the Alpha AMS presents an interesting trade-off. The number of externally worn components is minimised by eliminating the camera, and the natural coupling between eye position and perception is maintained because the implanted image sensor moves in parity with the eye (discussed in more depth in Section 2.5). Subretinal electrodes are optimally positioned to stimulate the bipolar, amacrine, and horizontal cells of the inner nuclear layer, which in theory employs the natural signal processing capabilities of the retina, while epiretinal electrodes, located adjacent to the ganglion cell layer, are more likely to stimulate ganglion cells directly and bypass any retinal signal processing. These advantages come at the expense of flexibility of stimulation parameters; in camera-based retinal implants, thresholds are determined for each electrode separately and gains can be individually set to normalise brightness across the field of view, while the Alpha IMS/AMS only provisions for a global amplification and gain. Additionally, the

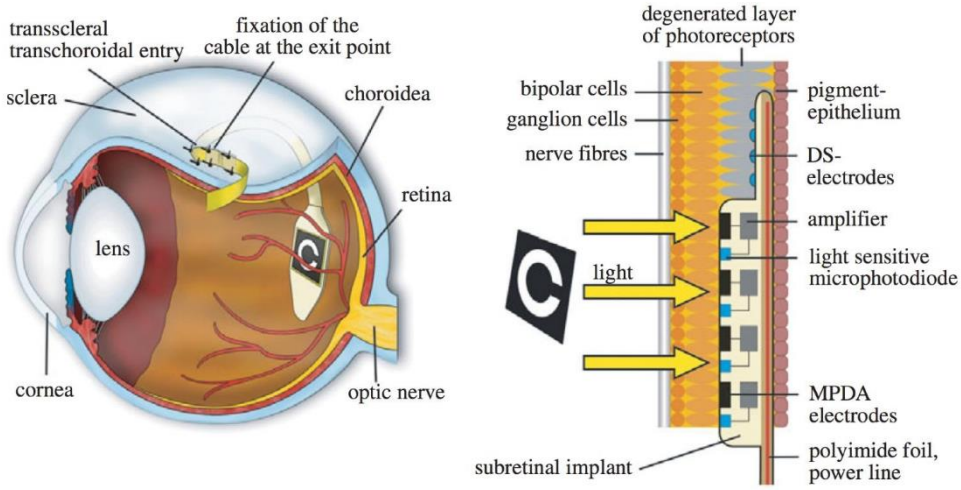

Figure 2.10: Alpha IMS photovoltaic subretinal implant. (Left): the electrode array is implanted behind the macula and power is provided via a transscleral transchoroidal cable. (Right): cross-sectional view of the retina showing the placement of the stimulating array and demonstrating the principle of operation of a photovoltaic visual prosthesis. The array is placed in the subretinal space, between the choroid and retina. Each pixel unit on the array comprises a photodiode, amplifier, and electrode. Electrode activity is modulated by photocurrents generated by ambient light that is incident with the implanted photodiodes. The photocurrents are too small to elicit a percept, so powered amplification is required. This differs from the PRIMA (Pixium Vision SA, France), in which near-infra-red light is projected onto the photodiode array with enough intensity to produce a percept without an external power supply. Reused with permission from Hafed et al (2016).[145]

use of implanted photodiodes precludes any image processing such as feature extraction and depth processing.

The PRIMA photovoltaic subretinal implant (Pixium Vision SA, France), offers innovative solutions to some of the problems faced by other retinal implants. A 1mm^2 chip containing 378 photodiode-electrode units is implanted in the subretinal space but, unlike the Alpha IMS/AMS, the photodiode signal does not require amplification. Instead, images captured by an external camera are projected onto the photodiodes via a near-infra-red projector, amplifying photocurrents above perceptual thresholds. This is likely to improve safety and stability by eliminating the need for a trans-scleral cable and allowing the implanted components to be completely intraocular. Processing of the captured image is also possible, unlike the Alpha IMS/AMS. At 1mm^2, the electrode array covers a smaller field of view than most other retinal implants (the Argus II electrode array spans 16.5mm^2)[82] but it is intended that multiple arrays can be implanted at once to provide wide field of view coverage. Like the Alpha IMS/AMS, the image sensor moves in parity with eye movement, however, the sensor must stay within the relatively narrow arc of the projector, limiting the practical oculomotor range. A clinical trial to assess the safety and functional outcomes of the PRIMA began in 2017.[83] Five subjects with age-related macular degeneration have each been implanted with a single chip beneath the macula. Promising results up to 12 months post-implantation have recently been published, with four of the five subjects able to discriminate Landolt-C optotypes.[84]

Suprachoroidal retinal implants

In suprachoroidal retinal implants the stimulating electrodes are implanted in the suprachoroidal space, between the sclera and choroid. One advantage of this approach is in the simplicity of the surgery and the stability of the device: unlike epiretinal and subretinal devices, no vitrectomy is required; no components are placed between the choroid and the retina (risking separating the retina from its blood supply); and the natural adherence between the sclera and choroid mean that no retinal tack is required to anchor the electrode array. However, suprachoroidal electrodes are relatively distant from the target neurons, requiring a greater stimulating current in order to reach perceptual thresholds. Currents passing through the choroid also spread tangentially, increasing the extent of activated retinal neurons well beyond the circumference of the stimulating electrode. As relatively large circumference electrodes are required in order to meet safe charge density criteria, the spatial selectivity of suprachoroidal stimulation is constrained.[85–87]

A 24 channel suprachoroidal retinal implant (Bionic Vision Australia) underwent a clinical trial in three participants with retinitis pigmentosa between 2012-2014.[88] Power and stimulation commands were provided to the implant via a percutaneous connector, limiting the duration of implantation to 2 years after which the percutaneous connector was removed, rendering the remaining ocular components inactive. During the trial all three participants experienced electrically-evoked phosphenes and the implant was well tolerated in the eye, with the sole serious adverse event being an infection at the site of the percutaneous connector. The participants demonstrated improvements in light localisation, character identification, and discrimination of direction of motion.[16] Following the success of the first clinical trial intellectual property rights were licenced to Bionic Vision Technologies Pty Ltd (Australia) and a fully implantable device was developed, now featuring 44 stimulating electrodes and implanted

receiver coils instead of a percutaneous connector. A clinical trial for this 2nd generation device commenced in four subjects with retinitis pigmentosa in 2018. Preliminary results up to 44 weeks post-implantation show a good safety profile[89] and positive psychophysical[90] and functional vision results.[91]

A similar device, the Suprachoroidal Transretinal Stimulation (STS) retinal implant (Artificial Vision Project and NIDEK Co., Japan) is implanted in a scleral pocket, rather than between the sclera and choroid. A unique feature of this device is its 49 "bullet" electrodes that protrude from the array to more optimally increase surface area and improve the electrode-tissue interface.[92] A one-year clinical trial was undertaken in three subjects with retinitis pigmentosa. No major complications were reported, and subjects showed improvement in object detection, object discrimination, and reach and grasp tasks.[93]

Optic nerve implants

Artificial vision can also be achieved by stimulation of the optic nerve. Within the cylindrical structure of the nerve bundles forming the optic nerve, different parts of the visual field are represented at different axial angles and different radii from axis. Spiral cuff electrodes can be implanted on the intracranial[94,95] or intraorbital optic nerve.[96] The cuff wraps around the surface of the nerve, locating each of the stimulating electrodes at a different angle around the circumference of the nerve in order to achieve spatially distinct phosphenes (Figure 2.11A). However, retinotopy is not systematic in the optic nerve[97], such that the location of a phosphene in the field of view cannot be easily predicted by the location of the stimulating electrode, unlike in retinal implants.[9,98] Instead, manual mapping of the phosphene locations is required post-implantation.[99] A second challenge is that in the optic nerve, in comparison to the retina or visual cortex, the entire visual field is represented within a very small cross sectional area, which could lead to very large phosphenes unless current spread is carefully controlled. Cuff electrode optic nerve implants were trialled in subjects with retinitis pigmentosa, enabling recognition of simple patterns, but have not been pursued since.[100,101]

More recently, penetrating electrodes for optic nerve stimulation were proposed, whereby an array of electrodes within the vitreous cavity penetrate directly into the optic nerve head (Figure 2.11B).[102,103] Penetrating electrodes are expected to reduce perceptual thresholds and limit current spread, resulting in greater spatial resolution, and the full cross section of the optic nerve (i.e. full visual field) is available for stimulation. Further, retinotopy in the optic nerve is more predictable at the optic nerve head, possibly simplifying phosphene mapping.[97,104] The use of

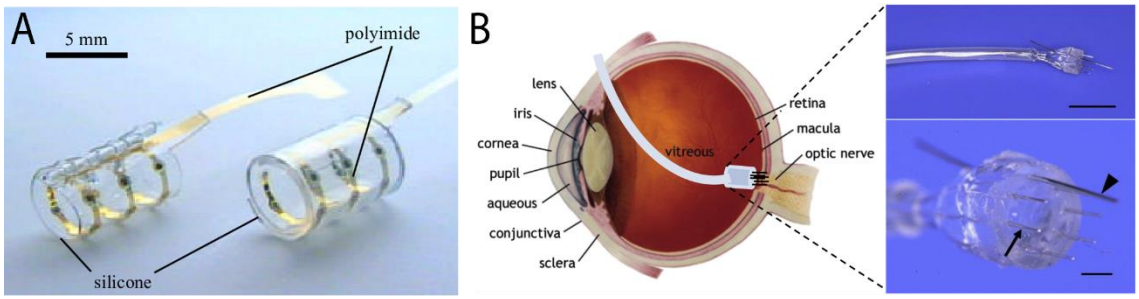

Figure 2.11: Stimulating electrodes for optic nerve implants. (A): an example of a spiral cuff electrode designed for peripheral nerve stimulation. The electrodes are housed in a silicon cuff that wraps around the nerve. Reused with permission from Schuettler (2001).[244] *(B): penetrating electrodes for optic nerve stimulation. The electrodes are placed within the vitreous cavity and penetrate the optic nerve head. Reused with permission from Nishida (2015).*[105]

penetrating electrodes, and the trans-scleral cable needed to power them, could compromise the long-term stability in this approach relative to spiral cuff optic nerve implants. Pilot studies have demonstrated that electrical stimulation with these penetrating electrodes led to the perception of phosphenes in a blind subject[102,105]. It remains to be seen whether clinical trials will progress.

Thalamic implants

The lateral geniculate nucleus (LGN) of the thalamus has been proposed as a potential site for electrical stimulation for artificial vision.[106] Several features of the structure of the LGN make it a promising target. Firstly, the LGN is unique in the visual system in that it is divided into several layers corresponding to different visual functionalities; M type (luminance, motion, depth), P type (red and green chrominance, fine detail), and K type (blue chrominance) retinal ganglion cells each project to distinct regions of the LGN.[23] ON-centre and OFF-centre cells are also spatially segregated in the LGN. This presents the potential for functionally selective stimulation, which is not presently possible in retinal or cortical implants.[107] Secondly, the spatial representation of the visual field in the LGN is proportional to the density of retinal ganglion cells in the corresponding area of the retina, such that a proportionately larger area of the LGN is dedicated to representing central vision compared to peripheral vision. Therefore, a uniform electrode array would yield high density of phosphenes in the central visual field and a lower density in the periphery, similar to the acuity of natural vision.[108] Finally, thalamic implants would be suitable even in cases blindness caused by trauma or complete loss of the eye and optic nerve.

Despite these benefits, the development of thalamic implants lags that of retinal, cortical, and optic nerve implants. Primate model experiments have shown that stimulation of the LGN can elicit phosphenes[109] but there do not appear to be any devices intended for human use currently under development. This is largely due to small size of the LGN, approximately 250mm^3 or 6mm along each dimension, and its anatomical position 8cm below the surface of the brain, which make the LGN a difficult surgical target. The compressed representation of the visual field in the LGN relative to the retina or visual cortex may also limit the number of stimulating electrodes that can be implanted. Additionally, the left and right LGN each represent opposing halves of the visual field, requiring bilateral implantation if the full visual field is to be covered.[107] However, high-precision implantation of electrodes for deep brain stimulation is fast becoming an established procedure for treatment of Parkinson's disease and other movement disorders,[110] and these advances may prove useful for future thalamic implants.

Cortical implants

The primary visual cortex (V1) has been considered as a target for electrical stimulation since the early work of Brindley and Lewin in 1968.[49] Cortical implants could be applicable in a wide range of blindness conditions as they bypass the retina and optic nerve entirely. From a surgical perspective, surface electrodes provide the least invasive means of stimulating V1. Penetrating electrodes, which require less current to reach perceptual thresholds and therefore enable a greater density of electrodes and improve spatial resolution, have been tested in human and animal models[111–113] but may not be as well tolerated in chronic implantation. The representation of the visual field is greatly expanded in V1 compared to the retina, making it a viable site for large numbers of stimulating electrodes; however, approximately 67% of the

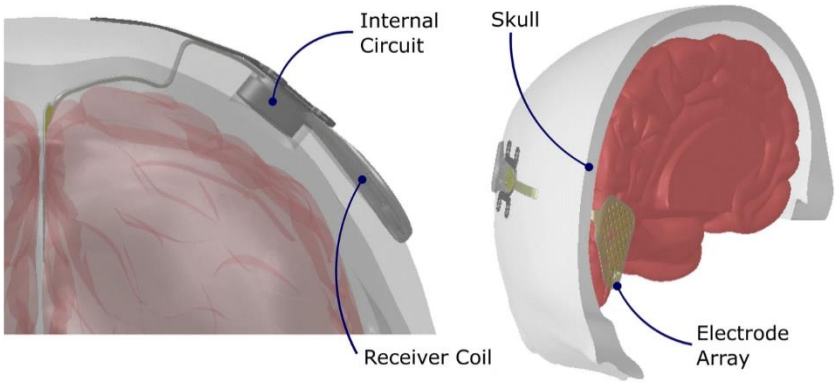

Figure 2.12: Schematic of the Orion cortical visual prosthesis (Second Sight Medical Products Inc., USA). The stimulating surface electrodes are located over the medial occipital lobe. Reused with permission from Niketeghad (2019).[245]

surface area of V1 is concealed within sulci and therefore inaccessible to surface electrodes.[114] Although neurons in V1 are retinotopically arranged, they are organised in a layered three-dimensional structure that differs between individuals, making it difficult to predict the position of a phosphene within the visual field based on 2-dimensional electrode position. Therefore, manual mapping of phosphene locations is required. The obvious downside of cortical implants relative to retinal implants is that neurosurgical implantation of electrodes in the brain carries a risk of brain haemorrhage and infection. Other risks include stimulation-induced seizures, as previously observed in humans[55] and in cats.[115]

A clinical trial for the Orion cortical implant (Second Sight Medical Products Inc., USA) is currently underway following a successful chronic safety study in one subject.[116] The device comprises 60 flat electrodes implanted on the surface of V1 (Figure 2.12), an implanted stimulator, wireless link, head-worn camera and video processing unit. Six participants received the device in 2018, and preliminary results at 12 months post-implantation were promising; perceptual thresholds were stable, and three out of four participants were capable of object localisation and motion detection with the device. One seizure while under lab supervision was reported.[117]

The CORTIVIS project, supported by the Commission of the European Communities, aims to develop a cortical visual prosthesis utilising the Utah array – a widely-used penetrating electrode array that already has FDA approval for long-term human implantation. Early human experiments in 12 patients with epilepsy or brain tumours have demonstrated that implantation can be performed without major complications and electrical stimulation of the occipital lobe with the array produces phosphenes.[112] No long-term implantation in blind patients has yet been reported.

Table 2.1: Summary of visual prostheses that have been tested in chronic implantation in humans. The 'gaze contingent' column indicates whether the image sensor moves in parity with eye movement.

Device	Company	Implant location	Number of electrodes	patients implanted	Gaze contingent	Current status
Argus II[57]	Second Sight Medical Products Inc., USA	Epiretinal	60	>350	no	FDA and CE mark approval. Commercially available. Ceased manufacture in 2019
IRIS II[68]	Pixium Vision SA, France	Epiretinal	150	10	no	CE mark approval. Discontinued due to short device lifetime
EPIRET3[71]	EPIRET GmBH, Germany	Epiretinal	25	6	no	Acute (28 day) clinical trial completed. No further clinical trials planned
NR-600[72]	Nano Retina Ltd., Israel	Epiretinal (penetrating)	600	2	limited	Ongoing clinical trial in up to 20 patients
Alpha IMS[75]	Retina Implant AG GmbH, Germany	Subretinal	1500	30	yes	CE mark approval. Superceded by Alpha AMS
Alpha AMS[79]	Retina Implant AG GmbH, Germany	Subretinal	1600	28	yes	CE mark approval. Discontinued in 2019
PRIMA[84]	Pixium Vision SA, France	Subretinal	378	5	limited	Ongoing clinical trial in five patients
STS[118]	Artificial Vision Project and NIDEK Co., Japan	Suprachoroidal trans-scleral	49	3	no	12 month clinical trial completed
BVT 2nd gen.[89–91]	Bionic Vision Technologies Ltd, Australia	Suprachoroidal	44	4	no	Ongoing clinical trail in 4 patients
ORION[116]	Second Sight Medical Products Inc., USA	Cortical (V1)	60	6	no	Ongoing clinical trial in six patients

2.3. Evaluation of visual prostheses

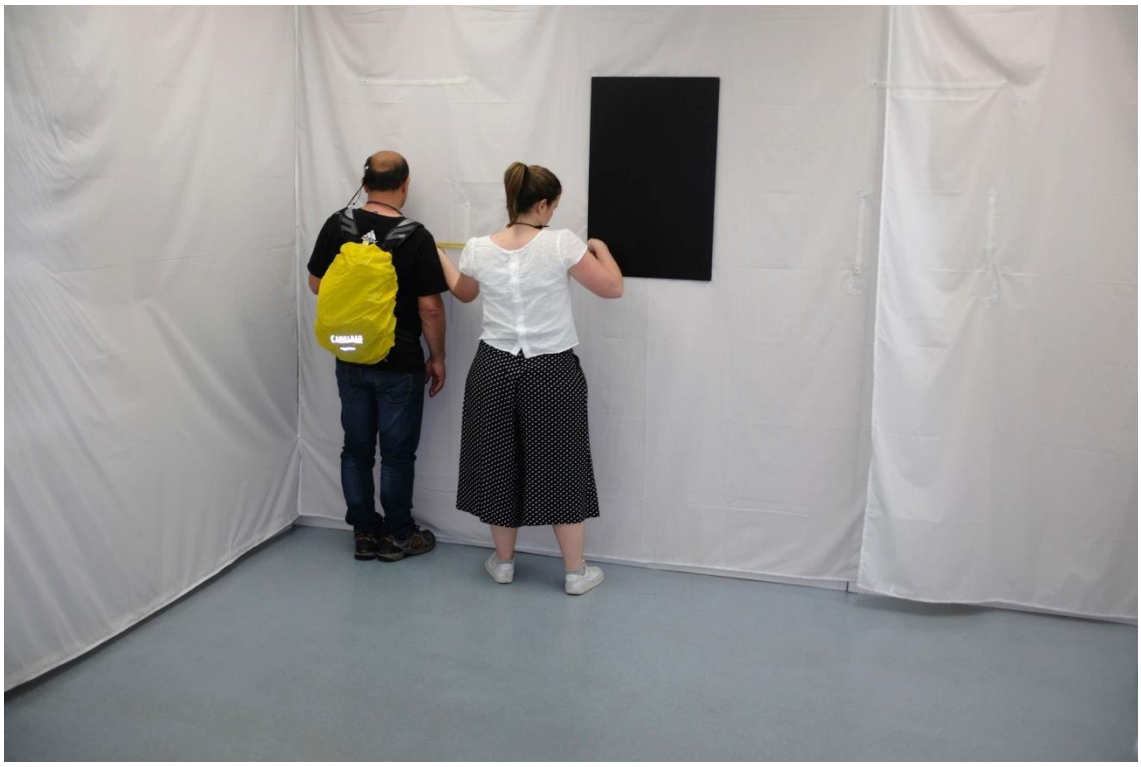

Figure 2.13: A user of the Bionic Vision Technologies 2nd Generation Suprachoroidal Retinal Implant performs a synthetic "doorway detection" task as a measure of patient outcomes. The participant must search for a mock door (block rectangle) in a white room. A researcher (right) measures the distance from the door to the final position of the user (left).

As with any visual aid the goal of a visual prosthesis is to enhance the quality of life of the patient, either by enabling them to independently perform tasks that were previously not possible, or by making previously difficult tasks easier. The degree to which the patient can effectively utilise artificial vision in everyday life should always be the determining factor in the success of a visual prosthesis. Of course, this is a difficult premise to quantify as it depends on the individual's specific rehabilitative goals, their level of motivation and commitment to rehabilitation, their lifestyle and the environment in which they typically use the device, and their own subjective perception of the impact the device has had on their lives. Observation of the patient using their device in the home environment plays an important role in outcome assessment, but this is supplemented by controlled laboratory-based testing in order to more fully understand the capabilities and limitations of a visual prosthesis. This testing usually involves assessment of visual function, orientation and mobility, and activities of daily living. These outcome assessments are the primary means by which the effectiveness of visual prostheses can be measured and compared.

2.3.1. Device fitting

Camera-based visual prostheses generally allow a clinician to directly control stimulation to individual electrodes, bypassing the camera. For photodiode devices a similar effect can be achieved by projecting calibrated optical patterns onto the implanted sensor.[119] This is a useful tool for characterising the dictionary of phosphenes available to the patient and establishing optimal stimulation parameters. For example, the perceptual threshold for an electrode can be

determined by varying charge levels according to a staircase procedure.[120] This is then used to set the operational charge range for that electrode. Phosphene mapping tasks can also be performed, in which electrodes are activated individually and the patient indicates the location of the resultant phosphene. Phosphene mapping is especially important for cortical implants, as phosphene locations are not easily predicted from cortical electrode locations.[99] The clinician may also use direct-to-array stimulation to identify and disable electrodes that do not yield a phosphene to minimise the total charge delivered, and may consider disabling electrodes that produce confusing or indistinct phosphenes if these interfere with the interpretation of other more useful phosphenes. Visual function assessment

Light localisation

Light localisation is generally assessed using a square localisation task in which the patient attempts to search for a square white target against a black background and point to the centre of the target with their finger. Usually the targets are displayed on a touchscreen monitor and the patient response is collected via the touchscreen. The primary measure of performance on the task is the average pointing error – the distance between the target and the point the patient touched. The Basic Light and Motion (BaLM) 'Location' task, a forced-choice task within the BaLM test suite[121] in which the patient must determine which wedge segment of a circle on a monitor is illuminated, is another commonly used light localisation task.

Light localisation is perhaps the most basic requirement for a visual prosthesis. It does not require any form vision, motion detection, or resolution of detail. In fact, a single phosphene is enough to complete most light localisation tasks. This is reflected in the success of most patients in these tasks. In a cohort of 30 Argus II patients, pointing accuracy in a square localisation task was better with system on versus system off in 93% of patients tested at 1 year post-implantation, 89.3% of patients tested 3 years post-implantation, and 80.9% at 5 years post-implantation.[59,64] Light localisation was also achievable for many Alpha IMS patients, although a confound was observed between surgical placement and task performance. Overall, only 17/29 (59%) of Alpha IMS patients tested could pass the BaLM location task. However of these, 100% of patients with foveal array placement passed the assessment, suggesting parafoveal array placement was associated with poor outcomes.[75,122] In the subsequent clinical trial of the next generation Alpha AMS system the array placement was foveal in all patients, and all patients tested passed the BaLM location task.[79] Preliminary results from the Orion cortical implant

Figure 2.14: Light localisation tasks. (Left): Example of a BaLM 'Location' stimulus presented to a user of the Bionic Vision Australia 1st generation suprachoroidal retinal implant in a four alternative forced-choice task. The wedge-shaped stimulus could be oriented right (shown), left, up, or down. The red dots indicate the locations in the image that were sampled to determine the electrode activity. Reused with permission from Barnes (2016).[185] (Right): Photograph of a healthy-sighted subject performing a target localisation task under stimulated prosthetic vision. The white target appeared in random locations on the screen, and the subject was required to find it and touch it with their finger. Reused with permission from Titchener (2018) [CC BY 4.0].[17]

clinical trial (Second Sight Medical Products Inc., USA) show that three out of four patients performed better in a square localisation task with system on versus system off at one year post-implantation.[117]

As the outcome measure includes the direction and magnitude of pointing errors, the square localisation task may also be used to align the camera with the patient's perception. It is optimal that the location of a percept in the visual field aligns with the real-world location of the stimulus. To this end, it is necessary to carefully align the camera, either mechanically or by shifting the sampled region in software. Misalignments between the camera and the patient's perception manifest in the square localisation task as a systematic offset between the target and the touch point.[123]

Motion discrimination

Motion discrimination tasks measure the ability of the patient to determine the direction of motion of moving stimuli. This is usually tested using a high contrast stimulus moving at a constant speed across the field of view, but the specific method varies between research groups. Second Sight Medical Products (Argus II epiretinal implant and Orion cortical implant) use a moving bar task in which a white bar moves across a black background in a randomly selected direction (0-360°) on a touchscreen monitor. The patient responds by swiping their finger across the touchscreen in the perceived direction of motion. The error between the movement angle and the response angle is compared between system on and system off. Between 50% and 56% of Argus II patients, depending on specific cohort and time-point, perform better on this task with the system on than off.[58,59,61,63] In these tests the speed of the bar ranged 7.9°/s to 31.6°/s and was selected for each patient according to their best performance. In preliminary reports from the Orion clinical trial, three out of four patients performed better in this task with system on versus system off.[117]

A four alternative forced choice (4AFC) adaptation of the moving bar task has been used in the clinical trials of Bionic Vision Technologies' suprachoroidal retinal implant. In this task the bar moves in one of the four cardinal directions and the patient responds by pressing the corresponding button on a keypad. One out of three patients with a 24-channel suprachoroidal implant, and two out of four patients with a 44-channel suprachoroidal implant, achieved a pass score (accuracy ≥ 62.5%) for bar speeds between 7°/s and 64°/s.[16,124] Patients implanted with the Alpha IMS and Alpha AMS subretinal implants have been tested using the 4AFC BaLM 'Motion' task, in which a randomised field of white dots move across a black background at a constant speed between 3.3 to 35°/s. Only 6/28 (21%) of Alpha IMS patients tested and 2/13 (15%) of Alpha AMS patients achieved a passing score,[75,79] however, this task is likely to be more difficult than moving bar tasks because some level of visual acuity is necessary in order to discriminate the multiple dot stimuli.

Motion discrimination is more complex than light localisation, and the smaller number of patients capable of motion discrimination reflects this. In fact, light localisation is a prerequisite for motion discrimination, as localisation of the moving stimuli on at least two time points is necessary to appreciate motion. Moving bar tasks are theoretically possible with only a single phosphene (i.e. no requirement for any spatial resolution) through strategic head scanning. However, it was reported that scrambling the spatial information of the stimulation was

detrimental to performance of Argus II patients in a motion detection task, suggesting that the patients did utilise retinotopic information in the task.[63] The temporal characteristics of stimulation sequences may also affect motion discrimination, though the effect of this has not been systematically studied.

Visual acuity

Despite recent advances, the spatial resolution and visual acuity realised in visual prostheses remains modest at best. Patients have found use for the present capabilities of artificial vision in a range of activities of daily living, but tasks such as reading, recognising faces, and resolving fine detail remain beyond reach. In theory, visual acuity in retinal implants is determined by the density of stimulating electrodes and hence the theoretical visual acuity of a retinal implant can be calculated directly from the electrode pitch – the spacing between neighbouring electrodes (in µm) determines the expected spacing between phosphenes in the visual field (in degrees of visual arc).[9,125,126] No present-day devices offer acuity better than the threshold for legal blindness (1.0 logMAR), and in practice, visual acuity is expected to be well below the theoretical maximum due a number of factors including current spread and the fact that usually only a subset of electrodes is utilised.

Acuity of visual prostheses is typically assessed using a grating acuity task or a Landolt-C optotype acuity task. In the grating acuity task the patient must identify the orientation of a set of alternating black and white stripes, and the narrowest gauge of grating (measured in cycles per degree of visual arc, cpd) that can be reliably perceived is the acuity measure. In the Landolt-C optotype recognition task the patient must identify the orientation of a ring broken by a gap (i.e. a letter 'C' optotype) and the minimum reliably perceivable gap width is taken as the acuity measure (measured in logMAR).

Table 2.2 summarises the visual acuity outcomes for several different visual prostheses. For each device the best reported optotype acuity is comparable to the theoretical maximum for that device. For example, one patient with an Alpha IMS implant and one patient with an Alpha AMS implant could discriminate Landolt-C optotypes up to 20/546 (1.44 logMAR), compared to a theoretical limit of 20/280 (1.15 logMAR) for those devices,[75,79] and one patient implanted with a 24-channel suprachoroidal retinal prosthesis could discriminate Landolt-C optotypes up to 20/4451 (2.35 logMAR) compared to a theoretical limit of 20/4242 (2.33 logMAR).[88] However, it is important to note this is not representative of the average user for any particular device – visual acuity is not near the theoretical maximum for most individuals, and many have no

Table 2.2: Summary of visual acuity measures reported in visual prosthesis clinical trials. Theoretical acuity limits are calculated from the pitch of the stimulating electrodes. Hyphens (-) indicate that no data have been reported. No acuity measures have been reported for the STS retinal implant, IRIS epiretinal implant, or Orion cortical implant.

Device			Landolt-C acuity		Grating acuity	
Name	Electrode pitch (um)	Theoretical acuity (logMar)	% of patients able to perform task	Highest reported (logMAR)	% of patients able to perform task	Highest reported (logMAR)
BVT 24-ch[63]	1000	2.33	33%	2.35	-	-
Argus II[66]	575	1.9	-	-	48%	1.8
PRIMA[91]	100	1.37	60%	1.36	-	-
Alpha IMS[82]	70	1.15	14%	1.44	48%	0.96
Alpha AMS[86]	70	1.15	15%	1.44	92%	0.96

measurable acuity at all (48% of Argus II and Alpha AMS users). The Alpha IMS/AMS are the only devices for which both grating and Landolt-C acuities have been reported, and for both devices the best reported grating acuity is much better than the best optotype acuity.[75,79] It has been suggested that this is because the two tests measure different aspects of spatial discrimination, since grating cues are spread over a large area of the visual field whereas discrimination of optotypes requires discrimination of a single feature.[75]

Compared to Alpha IMS patients, a much greater proportion of Alpha AMS patients can discriminate grating stimuli (Table 2.2).[75,79] This can be explained by the placement of the array on the retina, as it was found that parafoveal placement in the initial Alpha IMS cohort was associated with worse visual function when compared to foveal placement and the surgical procedure was altered accordingly for subsequent patients.[122] A similar result has been reported from the Pixium Vision PRIMA trial, in which three patients with foveal array placement could discriminate Landolt-C optotypes and two others with more peripheral array placement could not.[84] The integrity of the inner retina is also likely to play an important role in determining a patient's visual acuity, though this is more difficult to measure.

It is also interesting to note that the highest reported grating acuity scores for the Alpha IMS, Alpha AMS, and Argus II devices are better than the theoretical limit determined by the electrode pitch (Table 2.2).[59,75,79] It is thought that this 'hyperacuity' is possible through the parsing of temporal cues created by strategic head scanning (and eye scanning, for photovoltaic devices).[56] This suggests that visual acuity in artificial vision may not be directly comparable to visual acuity in normal vision, as visual prosthesis users may depend upon a different set of cues and techniques to sighted individuals.[88] Nevertheless, it can be said that some patients are able to use artificial vision to resolve features that are comparable to the theoretical limits of their device.

2.3.2. Orientation and mobility

Functional outcome measures include mobility and navigation tasks, hand-eye coordination, and object recognition and identification. Typically, these tasks are carried out in synthetic laboratory set-ups featuring high contrast stimuli and minimal distractors to enable a controlled comparison of performance on the task with the system on and off. The tasks are carefully selected to emulate some task or activity in which the patient might utilise artificial vision in the daily life and, despite their synthetic nature, it is expected that performance on these tasks correlates with real-world outcomes. Results from various retinal implant clinical trials show improved performance with system on versus off in such tasks as following a line on the floor, finding a mock door in an empty room (Figure 2.13), and counting and locating the number of items on a tabletop.

Recognition of objects is more challenging. For example, Alpha IMS patients could count and locate the number of geometric shapes on a table but could not reliably identify the shapes.[59,75,79,118,127] This is unsurprising given the limitations of present electrical stimulation strategies. These results support the notion that modern visual prostheses can be useful for everyday tasks such as navigation and localisation of objects but are unlikely to be useful for tasks that require resolution of fine detail.

2.3.3. Activities of daily living

Perhaps the most important measure of functional vision is the Functional Low-Vision Observer Rated Assessment (FLORA, Second Sight Medical Products Inc., USA).[8,65] This assessment combines a self-report questionnaire with expert observation of the patient in the home environment by a low vision rehabilitation specialist. The FLORA assessment can quantify quality-of-life (QoL) impacts, both in terms of expert-assessed performance with activities of daily living and in subjective patient-reported outcomes (PROs).

To administer the FLORA, the rehabilitation specialist first interviews the patient to gauge their subjective experience with the device and identify rehabilitative goals. The patient is then observed performing a number of activities of daily living in their home environment. The observations and interview are then rated by an independent evaluator on a scale of "positive" to "negative" to summarise the impact the device has had on the life of the patient. Results from the Argus II clinical trial show that 80% of patients had a "positive" or "mild positive" outcome at one year post implantation, dropping to 65% at three years post implantation. The remaining patients had either a "neutral" outcome or a "prior positive" outcome (self-reported positive outcomes that could not be replicated at the time of the test).[61] According to preliminary results from the ORION cortical implant clinical trial four out of four patients tested at one year post-implantation had a "positive" or "mild positive" FLORA outcome.[117] The FLORA is also a primary outcome measure for the ongoing clinical trial of the Bionic Vision Technologies 44-channel suprachoroidal retinal implant (NCT NCT03406416). In an assessment similar to the FLORA, Alpha IMS patients were asked to self-report their visual experiences, and 45% of patients reported useful new daily life experiences with the device.[75]

2.4. Anticipated developments

Novel electrode designs may lead to improved spatial resolution, as conventional platinum electrodes cannot safely stimulate neurons when the electrodes are small. Coating the surfaces of platinum electrodes with other materials can improve the electrochemical properties of the electrode, allowing for smaller electrodes. Possible coatings include conductive polymers, carbon nanotube, graphene, and diamond.[128,129] The geometry of the electrode can also improve spatial resolution, for example, three-dimensional electrode geometries use vertical column-like return electrodes to separate stimulating electrodes and contain the path of the current, reducing current spread (Figure 2.15).[130–132]

Other studies have investigated novel stimulation strategies to improve spatial resolution without necessarily changing the electrode design. These studies aim to use carefully selected stimulation waveforms to selectively activate cell subtypes,[133,134] for example addressing on-type and off-type cells separately. Electric field shaping exploits the interaction of the electric fields from neighbouring electrodes and has been proposed as a method for more precise control over stimulation. Some groups are investigating the notion of using electric field shaping to construct "virtual electrodes" that produce phosphenes in the spaces between electrodes[135], while others are attempting to move away from the concept of phosphenes as distinct light points and instead use global (whole array) electrical field shaping based on models of retinal activation.[136]

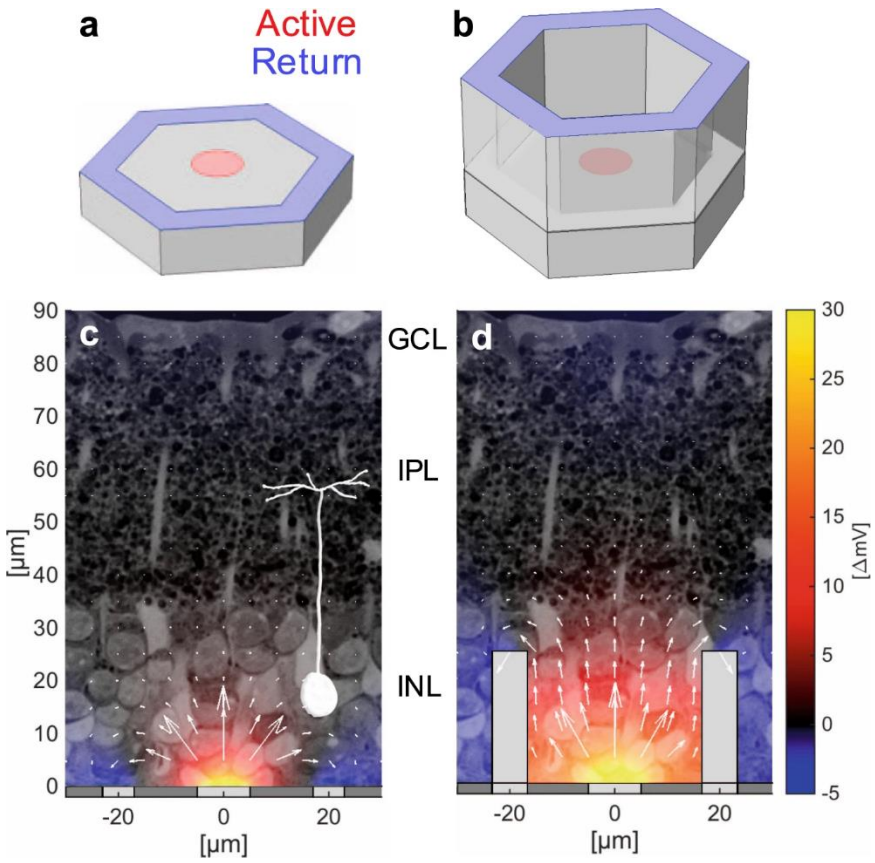

Figure 2.15: Flat (a) and honeycomb (b) configurations of the return electrode for a subretinal prosthesis. (c) Planar pixels with circumferential returns generate locally confined electric fields with shallow vertical penetration. Electric potential (shown in false color scale for 68 nA current) is represented with respect to potential in the middle of IPL, where axon terminals of bipolar cells reside. (d) Return electrodes on top of the insulating walls create a vertical dipole confined to the pixel volume and thereby maximize the vertical potential drop across the target cell layer. Current magnitude (arrow length) is shown in log scale. Reused with permission from Flores (2019)[130] [CC BY 4.0].

Improved video processing may be another useful way to improve user experiences, as present visual prostheses generally only apply simple contrast enhancement or edge detection to captured images. Some methods aim to improve comprehension of the percept by identifying salient stimuli and eliminating distracting stimuli. Depth cameras enable segmentation of the ground plane, foreground, and background, so that obstacles or items of interest that are immediately relevant (foreground) can be isolated and presented without distracting activity from background objects. A depth-based approach to video processing has been shown to improve performance in a mobility task in recipients of a suprachoroidal retinal implant but is not yet available in any commercial devices.[137] Similarly, thermal imaging may be useful for detecting people against noisy backgrounds.[138] Feature extraction using machine learning may also be a viable method for identifying salient stimuli.[139] Other methods attempt to mimic the processing that occurs in the retinal circuits in normal vision in order for stimuli to more closely resemble a natural signal.[140,141]

2.5. Eye movements in prosthetic vision

Anyone who has ever had the afterimage of a lightbulb filament lingering in their vision may have experienced the bizarre frustration of seeing the image dance away whenever they turn their eyes towards it. Ordinarily, eye movements are useful for exploring a visual scene because

they allow light from different locations to refract onto the fovea. In the case of the filament afterimage, the lingering perception is caused by the specific area of the retina that was overexposed to light and is therefore perfectly stationary on the retina – eye movement does not change the part of the retina receiving the stimulus. Moving one's eyes towards the afterimage only causes it to jump further away by the same amount. The afterimage appears to move against the ambient visual scene because its source is fixed in place with respect to the retina, while the rest of the visual scene is not.

The phenomenon of visual perceptions appearing to remain retinotopically stable applies to visual prostheses also. In one of the first clinical trials for a cortical visual prosthesis, Brindley and colleagues noted that "During voluntary eye movements, the phosphenes move with the eyes"[49] just as the lightbulb filament afterimage does. The same phenomenon is observed in retinal implants because the stimulating electrodes are affixed to the retina. Retinal stability of phosphenes is in fact problematic because it can cause the location of the percept within the visual field to be dissociated from the actual location (in the real-word axes) of the stimulus captured by the camera.

Only when the user's gaze is directed straight ahead, aligned with the camera axis, are the apparent percept location and actual stimulus location aligned. Eye position therefore plays an important role in perceptual localisation (as discussed in Section 2.1.3), and eye movement in retinal implant recipients can compromise perceptual localisation and hand-eye coordination. When Argus II recipients were asked to point at a target while intentionally holding their gaze in an eccentric position, their direction of pointing was significantly skewed towards the direction of the eye movement.[142] As it stands, retinal implant users must be trained to keep their gaze fixed centrally and explore their visual environment using only head movements in order to reduce the incidence of eye-camera misalignments. Users have difficulty maintaining central gaze and find keeping a fixed gaze very unintuitive, especially since they have no visual feedback with which to gauge their eye position.[143]

Oculomotor function is largely preserved in many forms of acquired blindness[144], and subjects implanted with the Alpha IMS subretinal implant (which uses implanted photodiodes instead of an external camera and hence does not suffer from eye-camera misalignments) exhibit "qualitatively normal" eye movements when compared to normal sighted subjects.[145] Thus there is reason to believe that resolving misalignments between the eye and camera orientations in camera-based retinal implants could improve coordination and perceptual localisation abilities and allow recipients to use naturalistic eye movements to redirect their gaze. One group has proposed replacing the external camera with an intraocular camera so that the camera bearing is contingent on gaze, though the surgical feasibility of such a system has not been established.[146,147] Alternatively, the sampled region of an image captured by a wide field of view camera could be shifted to compensate for eye movement, monitored by an eye tracker. This method is referred to as "gaze compensation". As an added benefit, gaze-compensated systems might help to counteract percept fading, as eye movement was correlated with reduced incidence of percept fading in subjects implanted with the Alpha IMS subretinal implant.[145]

Some studies have investigated the benefits of gaze compensation in visual prostheses. Shivdasani et al (2015) found that retinal implant recipients performed significantly better on a spatial discrimination task after gaze compensation was enabled.[148] McIntosh (2015) found a significant improvement in subject performance on a reach and grasp task in simulated prosthetic vision after enabling gaze compensation, but only for phosphene densities much higher than is currently feasible.[146] This result was possibly because the tasks were too complex (with many distractor objects) to be completed easily with low resolution regardless of gaze compensation. In a much simpler square localisation task, gaze compensation was associated with improved localisation accuracy in Argus II recipients.[149]

Acquired vision loss is often associated with pathological oculomotor conditions such as nystagmus (rapid involuntary eye movements, most often in a repetitive to-and-fro 'beating' pattern) and strabismus (misalignment of the eyes).[144] Nystagmus can degrade vision by preventing stable fixation, and in prosthetic vision would presumably cause the artificial percept to be unsteady.[150] Strabismus in natural vision can cause double vision and interfere with depth perception – neither of which are relevant to present-day monocular visual prostheses. However, the eye used to focus on an object can alternate, which could conceivably confound attempts to determine direction of gaze in visual prosthesis users.[151] To my knowledge no studies investigating the perceptual effects of nystagmus or strabismus in visual prosthesis users have been published.

Chapter 3

Methods and apparatus

This chapter describes general experimental methodology that is relevant to many of the studies presented in subsequent chapters. Each study chapter also includes a description of the methods specific to that chapter.

3.1. Suprachoroidal retinal implant

The thesis presents a number of studies in subjects implanted with a suprachoroidal retinal implant. The implant was developed first by the Bionic Vision Australia consortium, and more recently by Bionic Vision Technologies. Chapter 5 presents results from two subjects implanted with the prototype 24-channel suprachoroidal retinal implant (NCT01603576, 2012-2014). Chapter 6, and Chapter 8 present results from four subjects implanted with the 2nd generation 44-channel surprachoroidal retinal prosthesis (NCT03406416, 2018-2020).

3.1.1. The 24-channel suprachoroidal retinal implant

The 24-channel suprachoroidal retinal implant, shown in Figure 3.1, was a prototype device developed by the Bionic Vision Australia consortium. A clinical trial in three subjects with end-stage retinitis pigmentosa took place in 2012-14 with the intent of proving the safety, stability, and efficacy of the suprachoroidal approach.

The intraocular components of the device comprise 35 platinum disc electrodes (20 active, 13 ganged-return, 2 return) embedded in silicone and implanted in the suprachoroidal space. A trans-scleral lead wire connected the electrode array to a percutaneous connector behind the ear. Stimulation was provided by a non-portable external multi-channel stimulator,[152] meaning the system was not fully implantable and could only be used in the laboratory under research supervision.

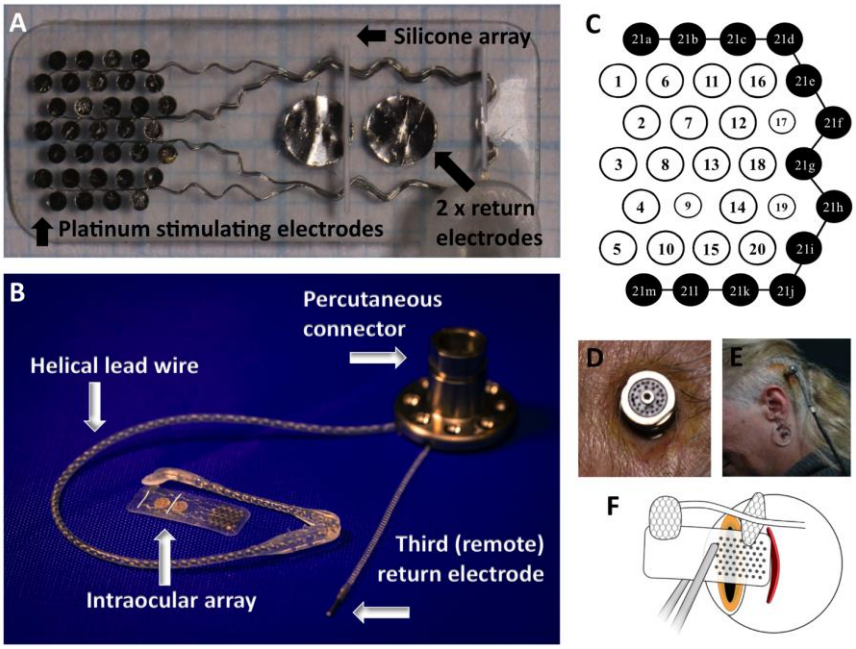

Figure 3.1: The intraocular electrode array of the suprachoroidal device (A) and the entire device (B), showing the array connected to the percutaneous connector via a helical lead wire. The electrodes on the intraocular array (C) were numbered for analysis, with the black electrodes (21a to 21m) being ganged to provide an external ring for common ground and hexagonal stimulation parameter testing. Note electrodes 9, 17 and 19 were smaller (400 mm vs. 600 mm). The percutaneous connector protruded through the skin behind the ear (D), allowing direct connection to the neurostimulator via a connecting lead (E). The scleral incision was made 9 mm to 10 mm posteriorly from the sclero-corneal limbus. Reused with permission from Ayton (2014)[88] [CC BY 4.0].

3.1.2. The 44-channel suprachoroidal retinal implant

Following the successful phase I clinical trial a fully implantable suprachoroidal retinal implant system was developed, featuring 44 active electrodes instead of only 20, a wider field of view, and implantable stimulator units (Figure 3.2). Four subjects with end-stage retinitis pigmentosa were implanted with the device in 2018 as part of a clinical trial to demonstrate its utility in daily life, including unsupervised use outside the lab.

The retinal implant comprised 44 platinum disc electrodes embedded in silicone (Figure 3.2) implanted in the suprachoroidal space, connected via a lead-wire to a pair of subcutaneous stimulators behind the ear. Figure 3.3 shows an example of the placement of the array with respect to the macula. A psychophysical fitting procedure established the stimulation parameters for each individual, which were then used for all lab assessments, training, and at-home use. The fitting procedure involved selecting the subset of electrodes that produced the optimal experience for the individual. Electrodes were excluded from the configuration if they did not yield a phosphene within safe charge limits or if the phosphene was confusing, indistinct, or not easily discriminable from other phosphenes. Any two neighbouring electrodes could optionally be operated as a shorted pair to increase the effective surface area and raise the safe charge limit, allowing for phosphenes in areas of the retina that did not respond optimally to single-electrode stimulation.

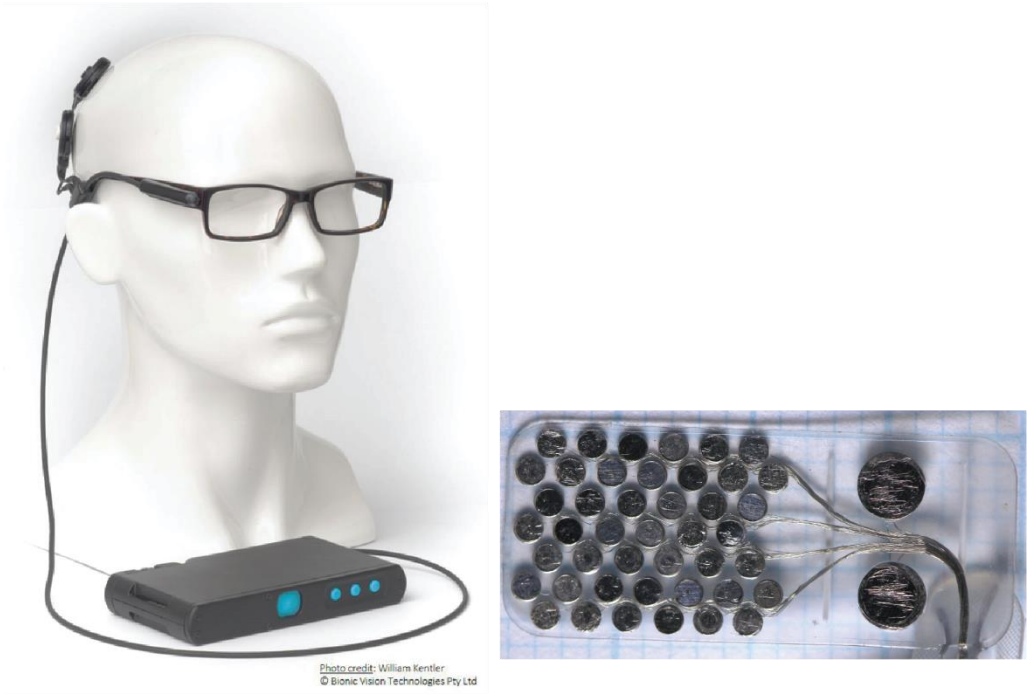

Figure 3.2: The fully implantable suprachoroidal retinal implant currently in phase II clinical trial in four subjects (Bionic Vision Technologies Ltd., Australia). (Left): the external components include a camera mounted on a pair of glasses, a pocket-sized processing unit, and a pair of coils to communicate with the implanted stimulators. (Right): the intraocular component of the device, comprising 46 platinum disc electrodes embedded in silicone, of which 44 (small size) are stimulating electrodes and two (large size) are return electrodes. Photo credit: William Kentler and David Nayagam ©Bionic Vision Technologies Pty Ltd.

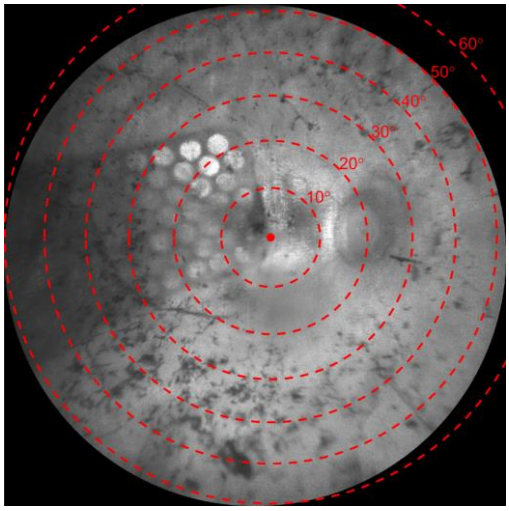

Figure 3.3: Fundus image showing the 44-channel suprachoroidal electrode array implanted within the eye. The electrodes are visible as bright circles. The large red dot indicates the estimated location of the fovea and concentric red circles indicate 10° eccentricities of visual field according to the Drasdo and Fowler schematic eye.[125,126]

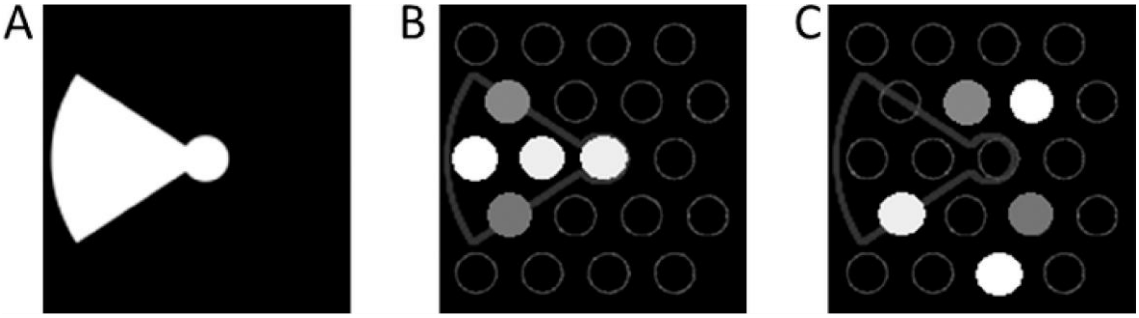

Figure 3.4: Image-to electrode mapping for Normal and Scrambled video processing. (A): captured image. (B): Normal (retinotopic) conditions, where the intensity values are mapped to electrodes in the corresponding location. (C): In the Scrambled condition, the mapping was purposefully corrupted to be non-retinotopic but contain the same number and intensity of phosphenes as for Normal. Adapted with permission from Petoe (2017)[154] [CC BY 4.0].

3.1.3. Video processing

Stimulation could either be directly controlled by the research software ("direct-to-array") or modulated by images captured by a head-mounted camera. Camera images were processed using a Lanczos2 antialiasing filter[153] and contrast enhancement. In normal operation ("Normal" condition) the spatial mapping from camera image to electrodes was uniform, such that electrode activity was determined by sampling the processed image at locations directly corresponding to the retinotopic location of each electrode. A "Scrambled" condition was also used, in which the same sampling locations were randomly assigned to the electrodes every five seconds to disrupt the spatial structure of the image while maintaining similar field of view, overall brightness, and number of phosphenes – allowing a functional assessment of retinotopic discrimination as described in our previous work.[154] The charge delivered in each stimulation pulse was determined by a linear mapping of pixel brightness (0-255) to the dynamic range of each phosphene.

3.2. Eye and head tracking

The studies presented in the subsequent chapters employ a video-oculography eye tracking apparatus (Arrington Research, AZ, USA) to monitor eye position. The system uses head-mounted cameras that face towards the eyes to sample the position of the pupil at 60Hz. These cameras are mounted to a purpose-built spectacle frame for low vision subjects (Chapter 4) and retinal implant users (Chapters Chapter 5,Chapter 6,Chapter 8), or are integrated into the head-mounted-display for participants using simulated prosthetic vision (Chapter 7). A conversion from sampled pupil position (pixels) to gaze angle was possible after a calibration routine, but as this required the subject to fixate on visual targets it was therefore only possible to calibrate for sighted participants (Chapters 4 and Chapter 7). For blind participants (Chapter 5, Chapter 6, and Chapter 8) the system was instead configured to output the raw position of the pupil in the camera image, with (0, 0) representing the bottom left corner and (1, 1) representing the top-right corner of the image. A tactile calibration was attempted in three retinal implant users and is described in more detail in Section 8.2.3. A magnetic motion tracker (Ascension Technology Corporation, VT, USA) was used to monitor the head position and orientation at 20Hz. The motion tracker was fastened to the spectacle frame above the implanted eye for retinal implant users or on the nose-bridge for low vision patients. The motion tracker system did not require calibration.

Chapter 4

Head and gaze behaviour in retinitis pigmentosa

Published as:

Titchener S. A., Ayton L. N., Abbott C. J., Fallon J. B., Shivdasani M. N., Caruso E., Sivarajah P., Petoe M. A. Head and Gaze Behavior in Retinitis Pigmentosa. *Invest Ophthalmol Vis Sci*. 2019;60(6):2263-2273.

Purpose: Peripheral visual field loss (PVFL) due to retinitis pigmentosa (RP) decreases saccades to areas of visual defect, leading to a habitually confined range of eye movement. We investigated the relative contributions of head and eye movement in RP patients and normal sighted controls to determine whether this reduced eye movement is offset by increased head movement.

Methods: Eye-head coordination was examined in 18 early-moderate RP patients, 4 late-stage RP patients, and 19 normal sighted controls. Three metrics were extracted: 1) the extent of eye, head, and total gaze (eye+head) movement while viewing a naturalistic scene; 2) head gain, the ratio of head movement to total gaze movement during smooth pursuit; 3) the customary oculomotor range (COMR), the orbital range within which the eye is preferentially maintained during a pro-saccade task.

Results: The late-stage RP group had minimal gaze movement and could not discern the naturalistic scene. Variance in head position in early-moderate RP was significantly greater than in controls while variance in total gaze was similar. Head gain was greater in early-moderate RP than in controls, while COMR was smaller. Across groups, visual field extent was negatively correlated with head gain and positively correlated with COMR. Accounting for age effects, these results demonstrate increased head movement at the expense of eye movement in participants with PVFL.

Conclusion: Retinitis pigmentosa is associated with an increased propensity for head movement during gaze shifts, and the magnitude of this effect is dependent on the severity of visual field loss.

4.1. Introduction

Visual scanning using a coordinated combination of head and eye movement is critical to human vision. For individuals with peripheral visual field loss (PVFL) due to retinitis pigmentosa (RP), exploring a visual scene necessarily requires a greater degree of scanning. The eye-head coordination of RP patients during visual scanning is of interest to clinicians and orientation and mobility specialists who could train patients to scan their surroundings more effectively.

Studies on the effect of PVFL on eye and head movement have yielded conflicting results. The hypothesis that PVFL may disrupt the generation of reactive saccades to visually salient targets (bottom-up saccade control) is supported by the finding that patients with simulated and actual PVFL make fewer than expected saccades into areas of visual defect in a visual search task[155,156] and have a more confined range of eye movement during locomotion.[157] Contrarily, in a different study PVFL patients made beyond-visual-field saccades frequently during locomotion, and there was no difference in eye movement behaviour between PVFL patients and normal sighted controls.[158] Furthermore, the degree of gaze (eye+head) movement was found to be greater in PVFL patients compared to controls in an indoor walking task[159] but smaller in a traffic gap judgement task.[160] In the only PVFL study to our knowledge that has considered the relative contributions of eye and head movement, participants with RP employed increased horizontal head movement and a similar eye movement during locomotion compared to healthy sighted controls.[161] None of the aforementioned studies have considered age or field of view extent as possible correlates for eye and head behaviour in RP. It is known that healthy subjects can adapt to artificial restrictions of the field of view or oculomotor range by increasing the relative contribution of head movement to overall gaze movement but it remains unclear whether this effect is observed in retinitis pigmentosa.[162–165]

In the present study we investigated the relative contributions of head and eye movement in RP patients and normal sighted controls during three head-unrestrained tasks. Three measures of head movement propensity were extracted: the extent of eye, head, and gaze (eye+head) movement while viewing a naturalistic scene; head gain (the ratio of head movement to total gaze movement) during a smooth pursuit task[166]; and the customary oculomotor range (COMR), which measures the orbital range within which the eye is preferentially maintained during a saccade task.[167] We hypothesised that peripheral visual field loss due to RP would lead to greater reliance on head movement and therefore visual field extent would be negatively correlated with propensity for head movement.

4.2. Methods

4.2.1. Participants

18 early to moderate stage retinitis pigmentosa (RP) patients (early-moderate RP group, aged 31-84), four late-stage RP patients (late RP group, aged 55-82) and 19 normal sighted participants (control group, aged 30-82), took part in the study. The RP patients were categorised as early-moderate RP or late RP based on their ability to perform a central fixation task for eye tracker calibration. Participants in the control group all had best-corrected visual acuity (BCVA) better than 6/12 in both eyes. Ten patients in the early-moderate RP group used no mobility aid regularly, six used a long cane, one used an identification cane, and one used

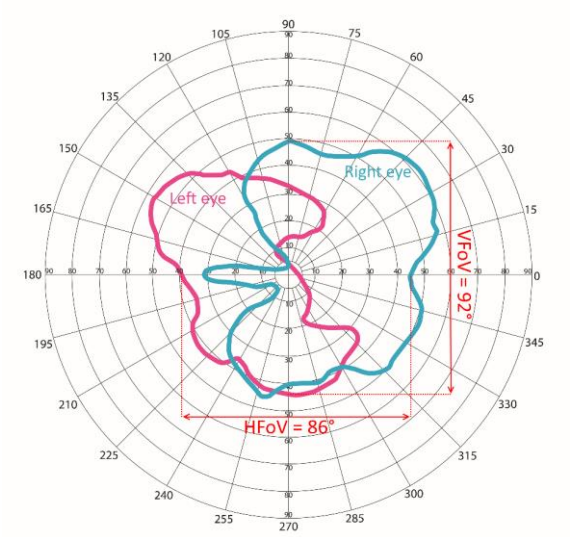

Figure 4.1: Example of Goldmann perimetry for a retinitis pigmentosa patient. The visual fields of the left eye (magenta) and right eye (blue) are overlaid on the same chart using the methodology of Turano (2005)[168] and the binocular horizontal and vertical fields of view (HFoV and VFoV, red arrows) are taken as the width along the horizontal and vertical meridians of the binocular visual field. Peripheral islands were not included in the calculated field of view.

both a long cane and a guide dog. All participants in the late RP group used a long cane regularly and one used both a long cane and a guide dog. None of the participants in any group exhibited nystagmus, amblyopia, or strabismus. The study was approved by the Royal Victorian Eye and Ear Hospital Human Research and Ethics Committee, and was carried out in accordance with the tenets of the Declaration of Helsinki with the informed consent of all participants.

The residual visual field of each RP patient was measured with the Goldmann manual kinetic perimetry test by an experienced examiner using a size 5 target, chosen so as to be similar in size to the task stimuli. We defined the horizontal and vertical field of view (HFoV, VFoV) as the width of the binocular visual field along the horizontal and vertical meridian lines respectively when the field of view of both eyes were overlaid with the retinal fixation points aligned (Figure 4.1), as described in Turano et al (2005).[168] Confrontation testing and optometric examination performed by an experienced clinician confirmed that the control group were without significant visual field loss or retinal or optic nerve disease.

4.2.2. Eye and head tracking

A head-mounted infrared eye tracker (Arrington Research, AZ, USA) tracked the eye-in-head angle of both eyes at 60 Hz. The system was calibrated by presenting a series of targets at predefined locations spanning approximately 80x50°, upon which the participant was required to fixate while keeping their head stationary in a chin rest. The chin rest was removed after the calibration was complete. Four RP patients were unable to complete the fixation task independently due to poor central fixation. In these cases it was necessary for the researcher to verbalise the target location (e.g.: “top right”) and to tap on the target to provide a directional audio cue for localisation. These patients were allocated to the late RP group on account of their poor central fixation. Goldmann perimetry data for these participants included at most only a single detection at the origin, corresponding to a horizontal and vertical field of view smaller than 1°. An electromagnetic tracking tag (Ascension Technology Corporation, VT, USA) fastened to the eye tracker headset worn by the participant recorded the head position and orientation

at 20Hz. Head tracker data was up-sampled to 60Hz using a linear interpolator to match the sample rate of the eye tracker.

4.2.3. Experiment procedure

Participants wore the eye and head tracking apparatus and were seated 1 metre in front of a large projector screen that spanned 88x57° of visual arc, and were free to move their heads for the duration of the experiment except during eye tracker calibration. Five participants in the control group and one participant in the early-moderate RP group wore corrective spectacle lenses during the experiment. Stimuli were presented on the screen in a naturalistic scene task, a smooth pursuit task, and a saccade task, each described below. The smooth pursuit and saccade tasks occurred in both horizontal and vertical configurations. All participants performed the naturalistic scene task first, and then performed the saccade and smooth pursuit tasks in each configuration once. This was then repeated so that each task and configuration was performed twice in total. The configuration of each smooth pursuit task was prescribed by a balanced-random schedule, and each smooth pursuit task was followed by a saccade task in the same configuration. The late RP group completed two repetitions of the naturalistic scene task but could not perform the smooth pursuit and saccade tasks.

Naturalistic scene task

The participant was required to passively watch a short computer-generated film that featured streams of moving traffic crossing a busy intersection in a single continuous shot from an elevated angle ("Rush Hour", Fernando Livschitz).[169] The film was 63 seconds in duration and was preceded by a 4° circular white fixation target that was presented in the centre of the display for 10 seconds. From the observer's perspective, traffic moved along both the horizontal and vertical medians, covering most of the lower two-thirds of the projected image.

Smooth pursuit task

The participant was required to track a 4° circular white target with their gaze as it moved smoothly along a 1 dimensional horizontal or vertical path. The target began in the centre of the display and remained stationary for 3 seconds before describing three full sinusoidal oscillations of equal amplitude along the path, and then stopped in the central position again. After pausing in the central position for 3 seconds the target completed another set of three oscillations with greater amplitude than the first set. This was repeated until five sets had been completed with incrementally increasing amplitudes. In the horizontal configuration of the task the five sets had amplitudes of ±8°, 16°, 24°, 32°, 40°, while in the vertical configuration the five sets had amplitudes of ±5°, 10°, 15°, 20°, 25° (limited by the aspect ratio of the projected display). Figure 4.2A plots the target position for a full execution of the horizontal configuration of the task. The period of oscillation was constant regardless of amplitude, such that the peak velocity (velocity at zero-crossing) increased with oscillation amplitude up to a maximum of 40°/s (Table 4.1).

Table 4.1: Amplitude, period, and peak velocity of the oscillating smooth pursuit target

Path orientation	Amplitude (°)	Period (s)	Velocity at zero-crossing (°/s)
Horizontal	8	6.28	8
	16	6.28	16
	24	6.28	24
	32	6.28	32
	40	6.28	40
Vertical	5	7.18	8
	10	7.18	16
	15	7.18	24
	20	7.18	32
	25	7.18	40

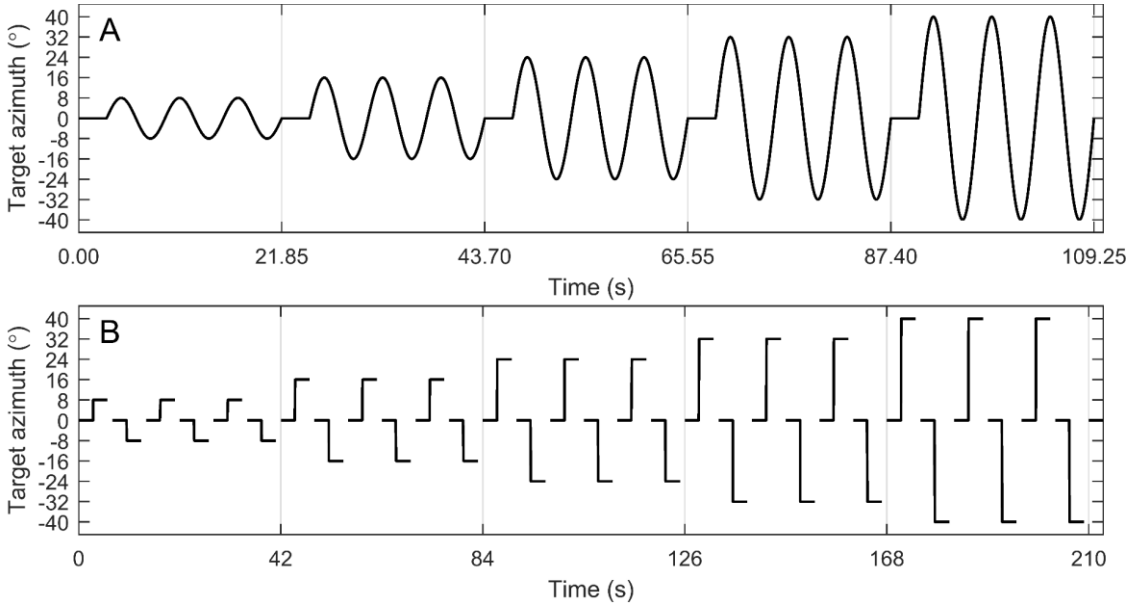

Figure 4.2: Target position during a single execution of the horizontal smooth pursuit task (top) and horizontal saccade task (bottom). Vertical grey lines delimit triplets of equal-amplitude oscillations. The targets followed an obvious pattern so as to accommodate participants with peripheral visual field loss.

Saccade task

The participant was required to fixate on 4° circular white targets as they appeared in predefined locations on a 1 dimensional horizontal or vertical path. In each trial a fixation target was presented in the central position for three seconds. Then the central target was extinguished and an eccentric target appeared simultaneously. After a presentation period of three seconds the eccentric target was extinguished, at which time the subject was required to return their gaze to the remembered location of the central target. This was accompanied by an audio cue to prompt participants who had not successfully located the eccentric target to return their gaze to the centre. One second after the offset of the eccentric target the central target was re-presented, marking the beginning of the next trial. The eccentric targets appeared in sets of six, with constant amplitude and alternating polarity within a set. The task finished when five sets (thirty eccentric targets total) had been presented. As in the smooth pursuit task, the target amplitude increased incrementally with each set. In the horizontal version of the task the five sets had amplitudes of ±8°, 16°, 24°, 32°, 40°, while in the vertical version the five sets had amplitudes of ±5°, 10°, 15°, 20°, 25°. Figure 4.2B plots the target position for a full execution of

the horizontal configuration of the task. The target locations followed an easily predictable to-and-fro pattern in a single plane so as to accommodate participants with peripheral visual field loss.

4.2.4. Data analysis

Eye and head tracking

Eye-in-head (orbital) azimuth and elevation (°) were measured using the eye tracker, and head-in-space position (mm), azimuth angle (°), and elevation angle (°) were measured using the motion tracker. Eye tracker data was processed to remove blink artefact, then for each trial one eye was nominated for further analysis based on a quality statistic reported by the eye tracker system. Motion tracker measurements were found to be free of artefact without any processing. For the smooth pursuit and saccade tasks only head and eye movements in the direction congruent with target movement were analysed.

Naturalistic scene task

Eye and head position measurements were summated to produce the gaze position at all time points during the task. The dispersion of gaze locations during the task was quantified by the area of the bivariate contour ellipse encompassing 68% of the gaze locations measured over the duration of the task (Figure 4.3).[170] Gaze dispersion was calculated separately for each repetition of the task and then averaged to produce a single measure for each participant. Eye position dispersion and head position dispersion were similarly defined for the eye and head components of gaze separately, allowing for an assessment of the relative contributions of the eye and head movement to overall gaze movement.

Smooth pursuit head gain

The contribution of head movement to smooth pursuit was quantified by the head gain, as described by Proudlock (2004).[166] Horizontal head gain (HHG) was calculated from the horizontal component of gaze during the horizontal variant of the task while vertical head gain (VHG) was calculated from the vertical component of gaze during the vertical variant of the task. For each full oscillation of the smooth pursuit target we found the difference between the two most

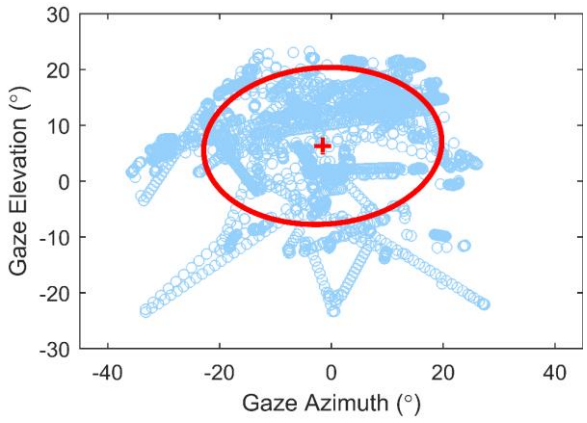

Figure 4.3: Gaze location of a control subject during the naturalistic scene task. Eye and head position measurements were summated to produce the gaze point relative to the centre of the projector screen at all time points (light blue dots). The dispersion of gaze positions is quantified by the area of the bivariate contour ellipse (red) that encompasses 68% of the gaze position measurements over the trial. Eye and head position dispersion were similarly defined for the eye and head components of gaze separately. The display spanned approximately 88°x57° of visual arc.

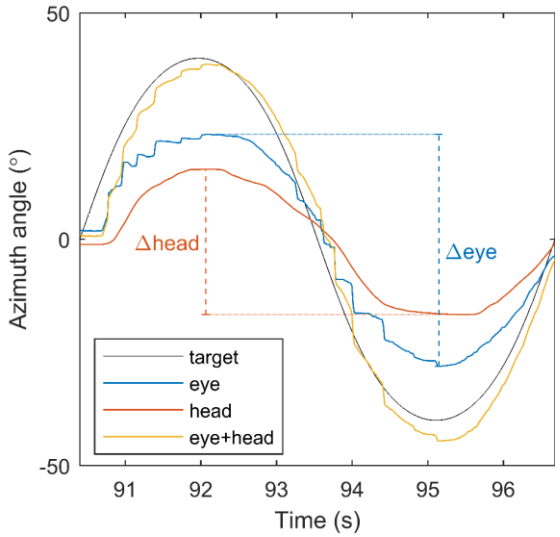

Figure 4.4: Eye and head movement during a single oscillation of the smooth pursuit target (±40° eccentricity). ΔH and ΔE were measured between the leftmost and rightmost excursions of the head and eye and were used to calculate the head gain for the trial, equal to $\Delta head/(\Delta eye + \Delta head)$ as per Proudlock (2004).[166] Head gain could range from 0 (no head movement, entirely eye movement) to 1 (no eye movement, entirely head movement).

extreme excursions of the head ($\Delta head$) and eye (Δeye) as shown in Figure 4.4. The head gain for the trial was then given by $HeadGain_{trial} = \frac{\Delta head}{\Delta eye + \Delta head}$ and could range from 0 (no head movement, entirely eye movement) to 1 (no eye movement, entirely head movement). The mean head gain over the entire stimulus set was used as a measure of head movement propensity and is referred to simply as "head gain" from this point onward.

Saccade task COMR

Each presentation of an eccentric saccade target constituted a single trial, and resulted in a single gaze shift. These gaze shifts were used to calculate the customary oculomotor range (COMR) of each subject as described by Stahl (1999).[167] Retrograde saccades to central targets at the conclusion of each trial were not included in the analysis. Horizontal COMR (HCOMR) was calculated from the horizontal component of gaze during the horizontal variant of the saccade task while vertical COMR (VCOMR) was calculated from the vertical component of gaze during the vertical variant of the task.

A gaze shift was defined as the summation of an eye movement ($\Delta eye = eye_{final} - eye_{initial}$) and a head movement ($\Delta head = head_{final} - head_{initial}$) as shown Figure 4.5. Eye saccades were defined as any period of eye movement with velocity exceeding 30°/s, and head saccades were defined as any period of head movement with velocity exceeding 5°/s. The first eye saccade made within 800ms of target onset was nominated as the response eye saccade for each trial. The eye saccade end point was extended to capture any subsequent corrective eye saccades that were initiated up to 130ms after the offset of the initial eye saccade. Then, if a head saccade was initiated up to 100ms before or 50ms after the response eye saccade the gaze shift was classified as a combined eye-head saccade, and the start and end points of the gaze shift were chosen to fully enclose both the eye and head saccades. If no head saccade occurred then the gaze shift was classified as eye-only, and the start and end points were equal to the eye saccade onset and offset. If no eye saccade occurred, or if the initial eye saccade was in the wrong direction, then the trial was discarded. The accuracy of a gaze shift (the proximity of the

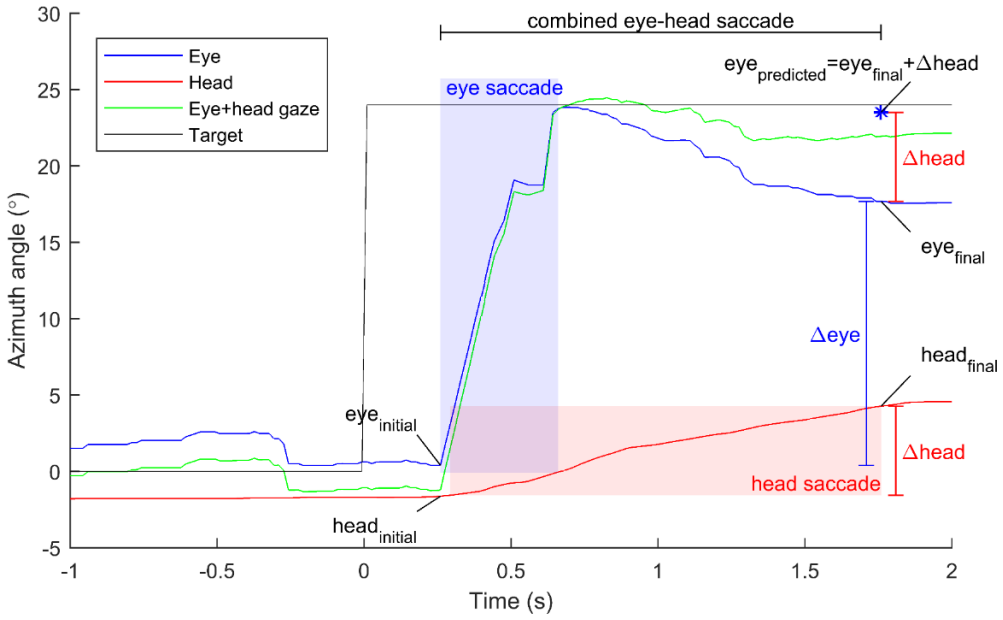

Figure 4.5: Eye and head azimuth of an RP participant in this study during a combined eye-head saccade to an eccentric target during the horizontal saccade task. An eye saccade (blue shaded region) and a slower head saccade (red shaded region) together comprise an eye-head saccade (black bar). The eye saccade includes an initial large saccade followed a short time later by a smaller corrective saccade.

final gaze point to the target) was unimportant, as the fixation targets simply acted as prompts to elicit saccadic gaze movement over a range of eccentricities.

The predicted orbital eccentricity, $eye_{predicted}$, is defined in Stahl (1999)[167] as the eccentricity that would have occurred if a gaze shift of the same amplitude had been executed with no contribution from head movement; that is,

$$\begin{aligned} eye_{predicted} &= eye_{final} + \Delta head \\ &= eye_{initial} + \Delta eye + \Delta head \end{aligned}$$

For an accurate saccade to an eccentric target $eye_{predicted}$ is therefore approximately equal to the target location relative to the initial head position. Stahl's method is predicated on the theory that head movement acts to confine actual orbital eccentricity at the conclusion of the gaze shift (eye_{final}) to some comfortable central range, the COMR, and therefore head movements only occur during gaze shifts that would otherwise result in the eye falling beyond that range ($eye_{predicted}$ outside of COMR).[167] This gives rise to the characteristic plot of $\Delta head$ against $eye_{predicted}$ (Figure 4.6A) featuring a flat central region of almost no head movement in which $eye_{predicted}$ is approximately equal to eye_{final}, flanked by two sloping lobes in which head movements act to confine eye_{final} to the COMR. Note that it is possible for $eye_{predicted}$ to exceed the maximum target amplitude of ±40° depending on the initial eye and head position.

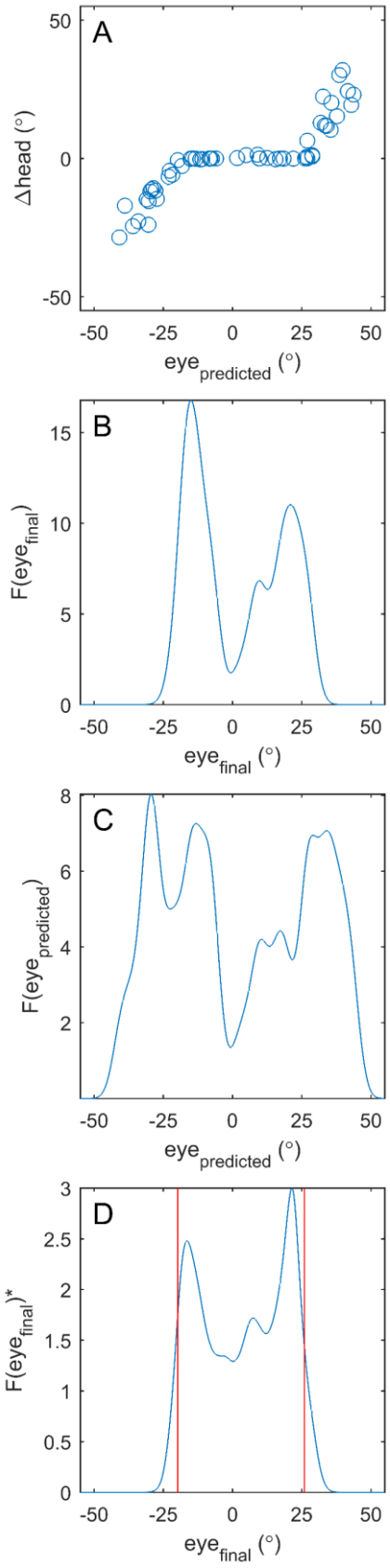

Figure 4.6: Derivation of COMR using the methodology of Stahl (1999).[167] *(A): Head movement against* $eye_{predicted}$*, the eye eccentricity that would have occurred if a gaze shift of the same amplitude had been executed with no contribution from head movement. This plot characteristically features a central flat region in which head movements do not occur and two flanking sloped regions in which head movements are used to confine the orbital eccentricity to some central range. (B): Frequency of occurrence of* eye_{final}*, the final eye eccentricity at the conclusion of the gaze shift. (C): Frequency of occurrence of* $eye_{predicted}$*. (D): Normalised frequency of occurrence of* eye_{final}*, calculated by pointwise division of* $F(eye_{final})$ *by* $F(eye_{predicted})$ *to eliminate the effect of the task-specific distribution of targets. The COMR (red lines) is the range enclosing 90% of the area under the curve.*

The COMR was calculated from $F(eye_{final})$, the distribution of frequency of occurrence of eye_{final} (Figure 4.6B), and $F(eye_{predicted})$, the distribution of frequency of occurrence of $eye_{predicted}$, (Figure 4.6C), both approximated using kernel density estimation. $F(eye_{final})$ was then divided pointwise by $(eye_{predicted})$to normalise against the effect of the task-specific distribution of targets, resulting in $F(eye_{final})$*. The COMR was then defined as the range of orbital eccentricities encompassing the central 90% of the area beneath $F(eye_{final})$* (Figure 4.6D). In theory, head movements are employed to ensure that eye position falls within the COMR at the conclusion of a gaze shift 90% of the time.

Statistical analyses

Participants were divided into three groups for statistical analysis: Control (n=19), early-moderate RP (n=18), and late RP (n=4). Gaze, eye, and head position dispersion during the naturalistic scene task were compared between the three groups using one-way ANOVAs with Tukey's test for multiple comparisons. Visual inspection of the residual normal Q-Q plots confirmed that the residuals were approximately normally distributed for each test with the exception of the test on head position dispersion. The analysis on head position dispersion was therefore repeated using a non-parametric Kruskal-Wallis ANOVA on ranks with Dunn's test for multiple comparisons.

Head gain and COMR were then compared between the early-moderate RP group and the control group. We tested the effect of group (early-moderate RP or control) on head movement propensity using a generalized linear model (gamma distribution, log link function) on COMR and head gain with group as a factor and age as a continuous predictor. We then tested the correlation between field of view and head movement propensity using a generalized linear model (gamma distribution, log link function) on COMR and head gain with age and field of view as continuous predictors. Note that as group and field of view were highly correlated they could not both be included as predictors in the same model. Vertical and horizontal data were analysed separately. For the control group a normal healthy field of view of 200x135° was inferred from their lack of retinal or optic nerve disease.[171] All statistical analyses were performed with Minitab18 statistics software (Minitab Inc., PA, USA).

4.3. Results

Participants in the early-moderate RP and Control groups were able to complete all tasks. The four participants in the late RP group only performed the naturalistic scene task. None of these participants were able to accurately describe any content of the scene. Means, standard deviations, and ranges for visual assessment results and head movement propensity measures are presented in Table 4.2. The mean (±SD) BCVA was 0.36±0.29 logMAR for early-moderate RP and 1.00±0.60 logMAR for late RP, and the mean visual field extent was 29±31° by 28±29° for early-moderate RP and 0.25±0.43° by 0.25±0.43° for late-RP.

Table 4.2: Descriptive statistics of visual assessment results and task outcomes. Head gain and COMR values are not given for the late RP group as they did not perform the smooth pursuit and saccade tasks. For the control group a normal healthy field of view of 200x135° was inferred from their lack of retinal or optic nerve disease.[171]

	Early-moderate RP (n=18)				Control (n=19)				Late RP (n=4)			
Measure	**Min.**	**Max.**	**Mean**	**S.D.**	**Min**	**Max**	**Mean**	**S.D.**	**Min**	**Max**	**Mean**	**S.D.**
Age	31	84	59	17	30	82	59	16	55	82	70	11
HFoV (°)	0	128	29	31	200	200	200	0	0	1	0.25	0.43
VFoV (°)	0	111	28	29	135	135	135	0	0	1	0.25	0.43
BCVA (logMAR)	0.00	1.00	0.36	0.29	-0.30	0.20	-0.06	0.12	0.40	2.00	1.00	0.60
Gaze disp.	521.9	1743.3	943.3	301.5	473.1	1233.4	949.6	213.1	49.0	361.4	201.5	114.8
Eye pos. disp.	295.8	1268.7	640.8	249.1	427.1	1104.6	786.5	217.1	45.1	237.0	134.2	69.8
Head pos. disp.	4.8	306.2	114.5	101.9	2.5	147.5	36.8	44.1	0.3	166.2	52.5	66.6
HHG	0.02	0.65	0.25	0.23	0.01	0.66	0.12	0.16	-	-	-	-
VHG	0.02	0.60	0.19	0.18	0.01	0.67	0.10	0.16	-	-	-	-
HCOMR (°)	17.8	81.8	57.1	18.2	27.3	95.1	72.7	21.3	-	-	-	-
VCOMR (°)	12.1	75.7	48.5	19.0	23.8	80.0	61.8	15.8	-	-	-	-

4.3.1. Gaze while viewing a naturalistic scene

None of the late RP group were able to accurately describe any details of the scene in the naturalistic scene task. An example of gaze position during the task and the calculation of gaze dispersion is given in Figure 4.7. Comparing the late RP group to the control group and early-moderate RP group, gaze and eye position dispersion were significantly smaller in the late RP group ($p<0.001$) while head position dispersion was not significantly different ($p=1.000$ vs. control; $p=0.286$ vs. early-moderate RP). Head position dispersion in the early-moderate RP group was significantly greater than in the control group ($p=0.022$) but there was no significant difference in gaze or eye position dispersion between the early-moderate RP and control groups (eye: $p=0.148$; gaze: $p=1.000$).

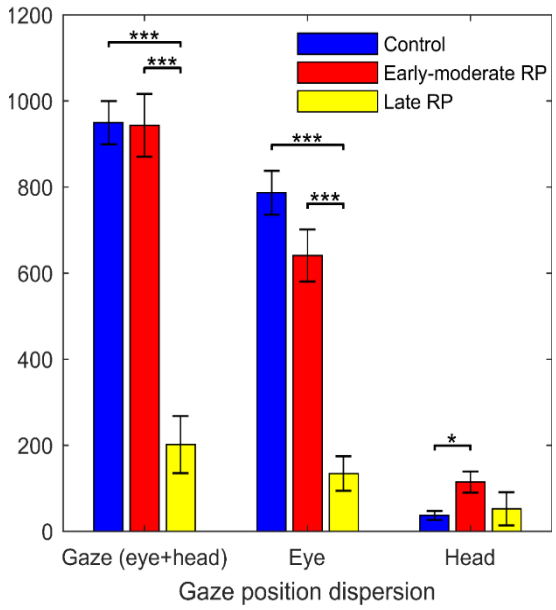

*Figure 4.7: Comparison of mean (±s.e.m.) gaze, eye, and head position dispersion between the control group, early-moderate RP group, and late RP group. Asterisks indicate significant differences (*p<0.05; **p<0.01; ***p<0.001).*

4.3.2. Factors affecting head movement propensity

A positive correlation was found between horizontal head gain and vertical head gain (Pearson's R^2=0.65, p<0.001) and between horizontal COMR and vertical COMR (R^2=0.69, p<0.001). Head gain was negatively correlated with COMR in the horizontal direction (R^2=0.63, p<0.001) and in the vertical direction (R^2=0.65, p<0.001), demonstrating consistency between the two measures of head movement propensity. Horizontal and vertical head gain (VHG, HH) and COMR (HCOMR, VCOMR) are plotted against field of view and age in Figure 4.8. The results of a generalized linear model on head gain and COMR with group and age predictors are presented in Table 4.3, while the results of a generalized linear model on head gain and COMR with field of view and age as predictors are presented in Table 4.4. Age, group, and field of view extent each had a significant effect on horizontal and vertical head gain and COMR, however, a large degree of variation among individuals is evident (Figure 4.8). There was no significant difference in variance in head gain or COMR between the two groups (Bonnett's test, p>0.05).

*Table 4.3: Summary of results of a general linear model on horizontal and vertical head gain (HHG, VHG) and customary oculomotor range (VCOMR, HCOMR) with group as a factor and age as a continuous predictor. The results of an F-test demonstrating improvement over the null model are presented, along with p values for each predictor included in the model. Significant results are denoted by asterisks (*p<0.05; **p<0.01; ***p<0.001). Age and group both had a significant effect on horizontal and vertical head gain and COMR.*

	Model (Age, Group)			
Measure	**$F_{2,34}$**	**Model *p***	**Factor**	**Factor *p***
HHG	22.16	< 0.001***	Age	< 0.001***
			Group	0.040*
HCOMR	5.82	0.007**	Age	0.024*
			Group	0.017*
VHG	21.53	< 0.001***	Age	< 0.001***
			Group	0.026*
VCOMR	7.11	0.003**	Age	0.007**
			Group	0.018*

*Table 4.4: Summary of results of a general linear model on horizontal and vertical head gain (HHG, VHG) and customary oculomotor range (VCOMR, HCOMR) with age and field of view extent as continuous predictors. The results of an F-test demonstrating improvement over the null model are presented, along with p values for each predictor in the model individually. Significant results are denoted by asterisks (*p<0.05; **p<0.01; ***p<0.001). Age and field of view both had a significant effect on horizontal and vertical head gain and COMR.*

	Model (Age, FoV)			
Measure	**$F_{2,34}$**	**Model p**	**Factor**	**Factor p**
HHG	23.34	< 0.001***	Age	< 0.001***
			HFoV	0.022*
HCOMR	6.63	0.004**	Age	0.027*
			HFoV	0.008**
VHG	21.96	< 0.001***	Age	< 0.001***
			HFoV	0.031*
VCOMR	7.33	0.002**	Age	0.010*
			HFoV	0.013*

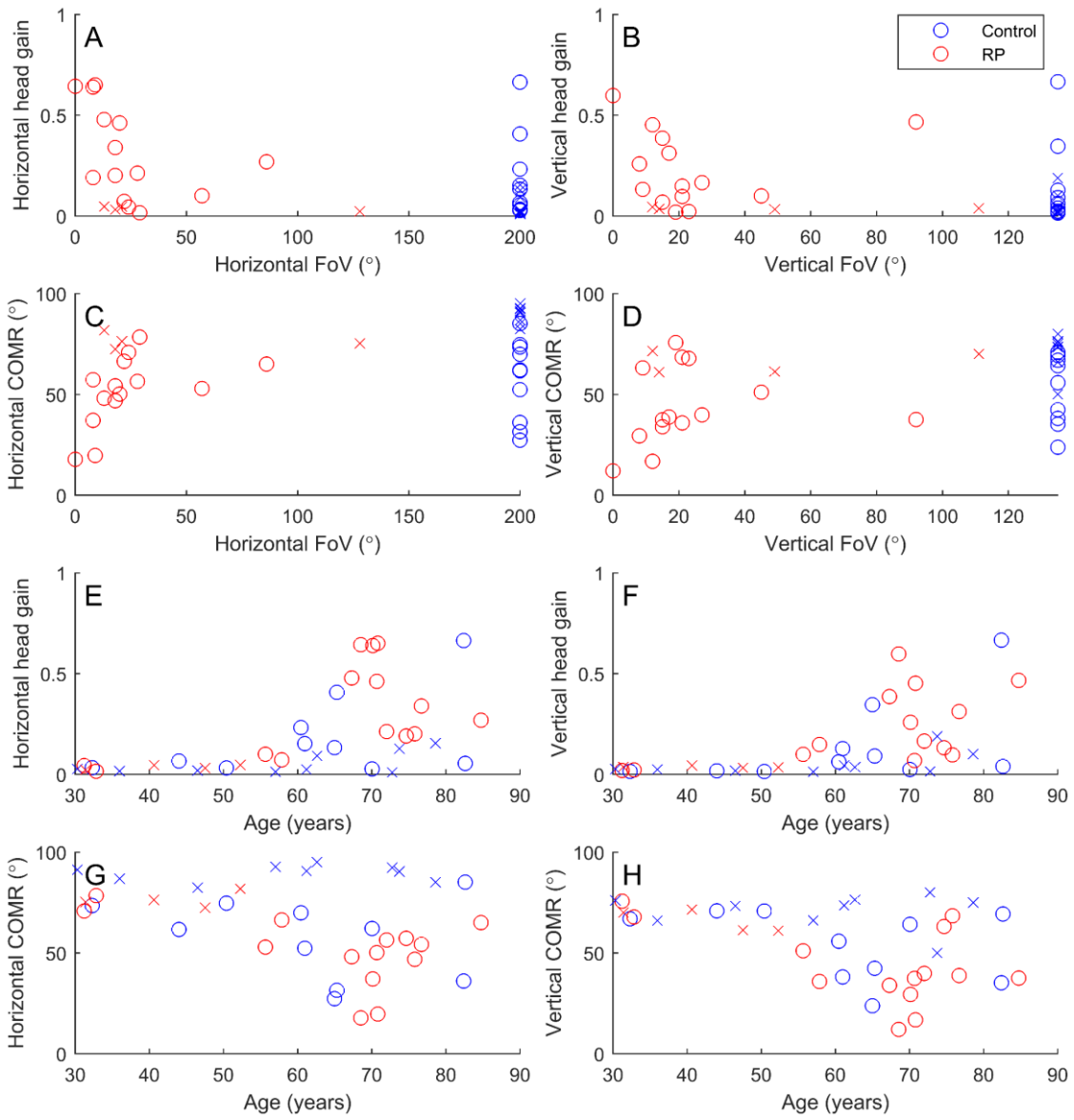

Figure 4.8: Factors affecting head movement propensity. Horizontal and vertical Head gain and COMR are plotted against age and field of view, with the early-moderate RP group in red and the control group in blue. For the control group a normal healthy field of view of 200x135° was inferred from their lack of retinal disease.[171] *Participants that were affected by a ceiling effect (see Discussion) are denoted by crosses. A great propensity for head movement is indicated by high values of head gain and low values of COMR.*

4.3.3. Minimal head movement in some participants

Some participants completed the saccade task with very little head movement even for the most eccentric targets, possibly because the saccade targets were not eccentric enough to evoke head movements in the individual. These subjects are denoted by crosses in Figure 4.8. This behaviour produces a flat $\Delta head$ vs $eye_{predicted}$ plot (Figure 4.9A) without the characteristic flanking sloped regions present in Figure 4.6, as well as an abruptly truncated $F(eye_{final})$* (Figure 4.9D). This behaviour was observed in four early-moderate RP patients (22%) and nine control subjects (47%) in both the vertical and horizontal directions.

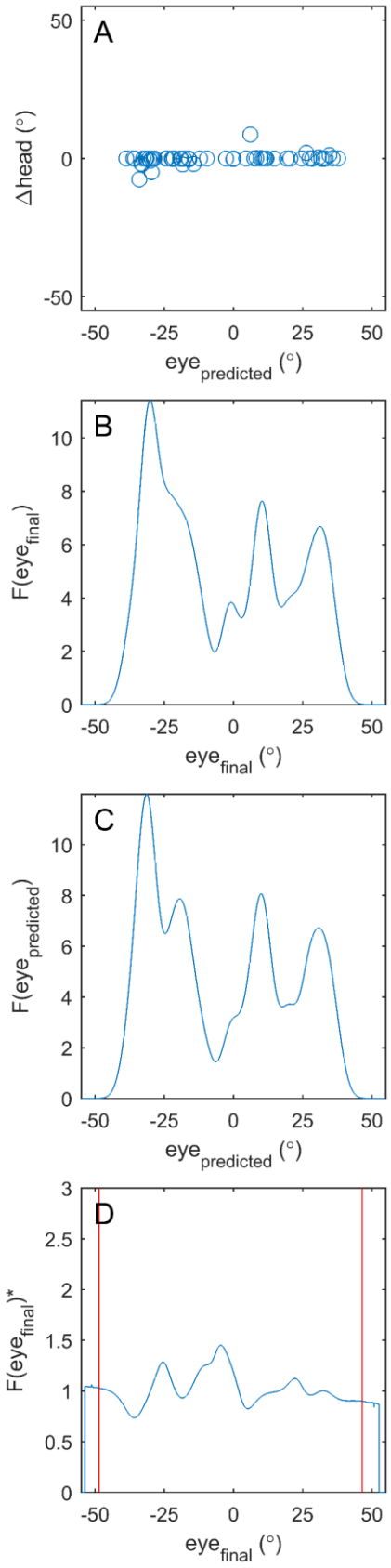

Figure 4.9: An example of COMR derivation for a participant who made very little head movement during the horizontal saccade task. (A): $\Delta head$ against $eye_{predicted}$ is flat and lacks the characteristic sloping lobes of Figure 4.6A. This is likely because the saccade targets were not eccentric enough to evoke head movements in this individual (B): Frequency of occurrence of eye_{final}. (C): Frequency of occurrence of $eye_{predicted}$. (D): Normalised frequency of occurrence of eye_{final}. The distribution is abruptly truncated and lacks the smoothly tapered edges of Figure 4.6D. The COMR (red lines) encloses 90% of the area under the curve.

4.4. Discussion

4.4.1. PVFL associated with increased head movement propensity

In the naturalistic scene task the late RP group had significantly smaller gaze dispersion than both the early-moderate RP group and the control group, which was primarily driven by a relative lack of eye movement. Considering that none of the late RP group were able to describe any features of the scene it is likely that this behaviour was caused by a lack of salient visual stimuli. Gaze dispersion was similar between the early-moderate RP and control groups, but in the early-moderate RP group the head position dispersion was greater, supporting the theory that the contribution of head movement is increased in RP.

Mean horizontal COMR in the control group (aged 30-82) was 72.7±21.3°, comparable to the value of 64.4±16.4° reported by Thumser et al (2010)[172] for a group of 60 healthy sighted participants aged 22-80. Mean horizontal head gain in the control group was 0.12±0.16, comparable to the value of approximately 0.2±0.2 (values read from figure) reported by Proudlock et al (2004)[166] for a similar smooth pursuit task in 53 healthy sighted participants aged 20-83. The early-moderate RP group had significantly greater propensity for head movement than the control group during smooth pursuit and saccade tasks. Restricted field of view due to early-moderate RP was correlated with increased propensity for head movement in the tasks. These results support the hypothesis that peripheral visual field loss is associated with a diminished range of eye movement and greater reliance on head movement. This may be driven by a habitually confined eye movement due to lack of peripheral stimulation.[158] Alternatively, it has been suggested that in PVFL head/body orientation may be more reliable than eye orientation as a cue for spatial constancy, leading patients to favour head movement more heavily,[157] although this is contradicted by the finding that exploratory saccade training improved the performance of RP patients in a mobility task.[173]

The existing literature is divided on the relationship between PVFL and eye movement. Patients with PVFL have previously been shown to: make few saccades into areas of visual defect during visual search[155]; make frequent saccades into areas of visual defect during visual search and locomotion[158]; make saccades of similar amplitude compared to healthy controls during locomotion[158]; make saccades of smaller amplitude compared to healthy controls during visual search (simulated PVFL)[156]; have more confined eye position than healthy controls in locomotion[157]; have a greater fixation area than healthy controls in locomotion[159]; and have a smaller fixation area than healthy controls in a traffic gap judgement task.[160] The wide variety of different tasks used makes it difficult to draw direct comparisons between different studies, particularly given the variable nature of tasks such as outdoor locomotion[158] and traffic gap judgement.[160] Additionally, some of these studies may be limited by small sample sizes. The lab-based tasks in the present study were highly repeatable, and the comparatively larger sizes of the early-moderate RP and control groups allowed for statistical analyses that controlled for field of view and age.

There was considerable variation in head movement propensity between individuals, even accounting for the effects of age, group, and visual field extent. This is consistent with previous studies in normal sighted participants by Thumser et al (2010)[172] and particularly Fuller (1992),[174] who classified participants as “head movers” and “non-movers”. Variation among the RP group

may also be partly explained by a greater capacity for compensatory gaze strategies in some individuals, as previously demonstrated in hemianopic patients.[175,176]

4.4.2. Age correlated with increased head movement propensity

Other studies have investigated the effect of age on head movement propensity. Our own results mirror those of Proudlock et al (2004),[166] who reported that horizontal smooth pursuit head gain was greater in over 60-year-olds compared to under 60-year-olds, with greater inter-subject variability in the older group. A later study by Thumser et al (2010)[172] found no effect of age on horizontal COMR. Thumser et al attribute this to their stimulus paradigm (originally described by Stahl (1999)[167]) which includes measures to discourage participants from modifying their behaviour to the specific task, namely their use of a wide range of target eccentricities, randomised target locations, and "perisaccadic targets". They propose that their own results reveal an "underlying mechanism" of eye-head coordination, while Proudlock's results reveal a greater capacity for modified gaze behaviour in the younger subjects, who recognised that it was more efficient to complete the specific task with eye movement only. Two findings from the same group support this argument: the expectation of future gaze shifts in any particular direction can influence eye-head coordination,[177] and COMRs measured in a lab-based saccade task correlate well with the "outdoor COMR" measured during a passive viewing task in a naturalistic setting.[178]

Considering the similarity between our result and that of Proudlock et al (2004),[166] the predictable nature of our stimuli (no peri-saccades, predictable target locations/paths), which was necessary to accommodate low-vision participants, may have encouraged modified gaze behaviour. We should interpret the results in this light and consider the measured head-gains and COMRs as task-specific. However, the "underlying" behaviour, while interesting from a vision neuroscience perspective, is not necessarily clinically useful if that behaviour is then modified to suit whatever task is at hand. We also note the similarity between the to-and-fro motion of gaze produced by both of the tasks in this study and the scanning that RP patients are encouraged to use when navigating. Our results are representative of the eye-head coordination of the participants while scanning to-and-fro and their ability to adapt their eye-head coordination to the task.

4.4.3. Implications for visual prostheses

Visual prostheses are implantable medical devices that aim to provide artificial vision to the blind.[44] Retinal implants are the predominant form of visual prosthesis, and are typically implanted in patients with end-stage RP. One of the major challenges faced by users of visual prostheses (with the exception of photodiode-based devices) is scanning of the visual environment. Eye position is decoupled from the orientation of the camera, interfering with the user's perception of space and visual constancy, and forcing them to rely entirely on head movement for visual scanning.[13] Gaze contingent systems that restore the coupling of eye position and gaze have been shown to improve hand-eye coordination in simulation[17] and in Argus II recipients[179] but have not yet reached regulatory-body-approved devices. The participants in the present study are not necessarily representative of present-day retinal implant recipients, who are typically in end-stage RP. Nevertheless, those involved in the design or psychophysical evaluation and fitting of visual prostheses should consider that the eye-head coordination strategies of their patients may have been affected by their condition, and are

likely to vary significantly between individuals. The trends observed in the present study suggest that candidates for implantation would exhibit a significantly greater propensity for head movement.

4.4.4. Limitations

Four early-moderate RP patients (22%) and nine healthy sighted controls (47%) completed the saccade task with very little head movement, leading to a ceiling effect on COMR. In these cases the true COMR is likely to be higher than the reported value. However, since the control group, which had a greater average COMR, was disproportionately affected, we find it unlikely that this would alter the main findings of the study. Repeating the analysis using the true values for those participants would most likely yield a more pronounced difference between the two groups. Future studies should include targets at greater eccentricities to ensure head movements are evoked in all participants (for example, Stahl (1999)[167] used targets at eccentricities up to ±55°).

Visual fields for the control participants were assumed within healthy limits and ascribed a representative value of 200x135° following confrontation testing and retinal examination.[171] Given that optometric testing did not reveal any signs of retinal or optic nerve disease in any control participants and only very small changes in visual field are expected with age,[180] we find it unlikely that imprecision in this visual field estimate would significantly affect our findings. This was confirmed by a Monte Carlo simulation in which the horizontal and vertical field of view of control participants were drawn from a bivariate normal distribution and the statistical analyses were repeated (n=5000, μ_x=200, μ_y=135, $3\sigma_{xy}$=14°, chosen because PVFL can be defined as HFOV<186°).[181] In 99.0% of simulations the findings of the present study were reaffirmed.

It is not clear to what extent results from the present study's highly synthetic tasks with limited field of view are generalizable to real-word conditions, but lab-based COMR has been shown to correlate well with "outdoor COMR" measured during passive viewing in a naturalistic setting.[178] In the only study to our knowledge that has commented on both eye and head movement in PVFL, Authie et al (2017)[161] showed that during locomotion head position was more variable in RP than in controls, but eye position variability was similar. This result is congruent with our results showing an increased propensity for head movement in RP.

4.4.5. Conclusion

Retinitis pigmentosa is associated with an increased propensity for head movement during gaze shifts, and the magnitude of this effect is dependent on the degree of visual field loss. Age was also associated with increased propensity for head movement; however, variation between individuals was high and dominated the effects of visual field loss and age.

Chapter 5

Oculomotor behaviour during a spatial localisation task in a 24-channel suprachoroidal retinal prosthesis

The analyses presented in this chapter are solely my own work and featured in a peer reviewed publication on which I was co-author (citation below). The written components have been changed to respect copyright.

Shivdasani M. N., Sinclair N. C., Gillespie L. N., Petoe M. A., Titchener S. A., Fallon J. B., Perara T., Pardinas-Diaz D., Barnes N. M., Blamey P. J. Identification of Characters and Localization of Images Using Direct Multiple-Electrode Stimulation With a Suprachoroidal Retinal Prosthesis. *Investig Ophthalmol Vis Sci*. 2017;58(10):3962-3974.

Purpose: Eye movements are known to interfere with perceptual localisation in retinal implants by introducing misalignments between the eyes and the head-mounted camera. This study investigated eye movements in retinal implant recipients to quantify effects on performance in a spatial localisation task.

Methods: Two participants (P1, P2) implanted with a 24-channel suprachoroidal retinal implant performed a direct-to-array variant of the BaLM location task, implemented by stimulating wedge-shaped quadrants of the electrode array. In each trial a single quadrant was stimulated for 2 seconds and the participant was required to identify which quadrant had been stimulated. Participants were instructed not to move their eyes during the experiment and stimuli were not delivered until the participant was fixating centrally. The eye position during the two second stimulation period was measured relative to the position at stimulus onset in each trial. One participant had near-perfect performance on the task, so the background distractor brightness was increased until it was 70% of the foreground target brightness, at which point performance was approximately equal to the performance of the other participant.

Results: Both participants made significant eye movements in response to the stimuli (ANOVA, $p<0.001$). Eye movement for P1 was rightwards on average, consistent with the expectation that phosphenes appear in the right visual field for subjects implanted in the left eye. Eye movement

for P2 was leftwards on average and skewed towards the direction of the stimulus. This presumed reflexive movement occurred for P2 even in cases where identification of the stimulus was incorrect. For both participants, increases in eye movement magnitudes were positively associated with correct identification of the stimulus (2-way ANOVA with Tukey test for multiple comparisons, $p<0.05$).

Conclusion: Participants implanted with a suprachoroidal retinal prosthesis did not appear capable of suppressing eye movement during a spatial localisation task. Contrary to the hypothesis, eye movements occurring after stimulus onset were associated with better, not worse, performance. This could be explained by larger eye movements occurring when the percept was clearer or more localised.

5.1. Introduction

Chapter 4 found that atypical oculomotor behaviour can be expected in subjects with peripheral visual field loss caused by retinitis pigmentosa. Eye movement and foveation are fundamental to the natural visual experience, so it is important to understand the types of eye movement that occur in prosthetic vision. Alpha IMS recipients have been shown to make 'qualitatively normal' eye movements, implying some normal functionality of oculomotor control. However, the Alpha IMS image sensor is implanted within the eye, preserving the natural relationship between eye movement and field of view. No studies investigating spontaneously occurring eye movement in camera-based visual prostheses exist to my knowledge.

Eye movements are known to cause displacement of the artificial percept, and it is thought that this can lead to localisation errors in camera-based visual prostheses. Present practice is to instruct recipients to suppress all eye movement, but this advice disregards the reality that much of our oculomotor behaviour is non-volitional. In the present study we investigated oculomotor behaviour during a spatial localisation task in two participants implanted with a suprachoroidal retinal implant. We hypothesised that the participants would make significant eye movements during the task, that the direction of eye movement would be stimulus-related, and that larger eye movements would be associated with worse performance on the task due to displacement of the percept.

5.2. Methods

5.2.1. Participants

Two participants implanted in the left eye with a 24-channel suprachoroidal retinal prosthesis (introduced in Section 3.1.1) as part of a clinical trial (NCT01603576) took part in the study. The participants were aged 52 (P1) and 49 (P2), and had advanced retinitis pigmentosa. Comprehensive details of the cohort and clinical trial outcomes are available in Ayton (2014).[88]

5.2.2. Light localisation task

Two participants were tasked with distinguishing stimuli presented as fixed patterns of electrode activation in a 'direct-to-array' implementation of the BaLM light localisation task described by Bach et al.[121] Stimuli were four spatially distinct electrode activation patterns – created by mapping the regular BaLM wedge stimuli onto the electrode layout of the implant (Figure 5.1).

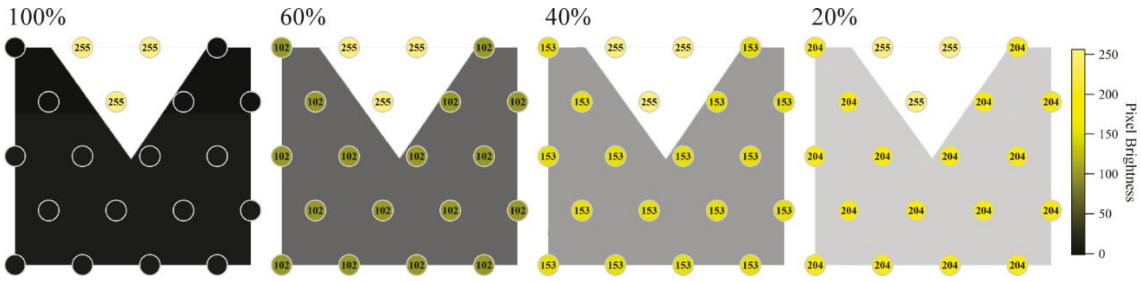

Figure 5.1: Electrode activation pattern derived by mapping the BaLM wedge stimulus onto the 24 channel electrode array at different contrast levels. Reused with permission from Shivdasani et al. (2017) [CC BY-NC-ND 4.0]. [16] Activation pattern for 'up' wedge stimulus shown. Percentages above each frame indicate the contrast level (background intensity relative to foreground intensity, with foreground intensity fixed to 100%). Circles indicate electrode sampling locations and the numbers inside the circles represent the stimulation intensity for that electrode (max 255).

The task was presented as a four-alternative forced choice. In each trial one of the four stimuli, selected at random, was presented to the participant for a period of two seconds. The participant was required to indicate the orientation of the stimulus and was instructed to keep their gaze fixed centrally throughout the task.

Data was collected over multiple sessions spanning several weeks with various customisations of the stimulation parameters. P1 had excellent recognition of individual electrodes and performed the task with 100% accuracy. Therefore, to make the task more challenging the contrast of the stimulus was reduced by raising the intensity of the background distractors in steps of 10%. In Patient 2, higher stimulation rates were found to produce fuller, more sustained phosphenes, so the task was repeated with 400pps stimulation as well as their default 50pps parameter set.

5.2.3. Eye tracking

Eye position was monitored throughout the experiment using the head mounted eye tracker described in Section 3.2. As the visual calibration was not possible with non-sighted participants the system was configured to output the raw uncalibrated pupil-in-image position (arbitrary units, a.u.) at 60Hz. Eye position data was cleaned to remove blink artefact prior to any analysis and smoothed with a moving average filter with a window width of 300ms and then down-sampled to 20 Hz.

5.2.4. Analyses

Eye movements during the light localisation task were analysed for three datasets: P1 at 70% background intensity (chosen to match the task performance of P2 with 400pps stimulation), P2 with 50pps stimulation, and P2 with 400pps stimulation. Additionally, 'sham trials', sequences of eye position data recorded during the inter-trial periods in absence of any stimulus, were used as a control for each participant. In each trial the pupil position immediately prior to stimulus onset was used as a reference point, since the participants were instructed to maintain central gaze during this period. The pupil position at 150ms prior to stimulus onset was selected as an approximation of centre for each trial as this was the last (smoothed) data point generated from measurements made entirely before stimulus onset. Eye position data was normalised to this reference on a per-trial basis prior to any statistical analyses.

Statistical analyses were performed to determine whether significant eye movements occurred, whether the magnitude of eye movement varied with the accuracy of the participant's response

in the trial, and whether the direction of eye movement was associated with the direction of the stimulus. Eye position data was limited to the time period from 150ms before stimulus onset to 2s after stimulus onset for all statistical analyses. The horizontal and vertical components of eye position were analysed separately.

5.3. Results

Figure 5.2 displays the average (± s.e.m.) eye position relative to centre over time. P1 and P2 both made significant eye movements in the two second period after stimulus onset (Separate one way ANOVAs, $p<0.001$). On average P1 made rightward eye movements, while P2 made upward eye movements initially and then leftward movements. These systematic movements, which were irrespective of stimulus orientation, were not detected during sham trials (control datasets) in the absence of any stimulus ($p>0.986$). In other words, the gaze average did not depart significantly from zero during sham trials.

Two-way ANOVAs on average eye movement were performed to test for possible effects of stimulus direction and response accuracy on eye movement. For each trial, only the eye movement along the axis congruent with the direction of the stimulus presented was analysed, i.e. horizontal eye position for left and right stimuli and vertical eye position for up and down stimuli. The interaction between stimulus direction and correctness was found to be significant ($p<0.001$). Results of multiple-comparisons (Tukey test) are presented in Table 5.1. When comparing trials with correct and incorrect responses, eye movement in the direction of the stimulus was significantly greater when the participant responded correctly (for 10 out of 12

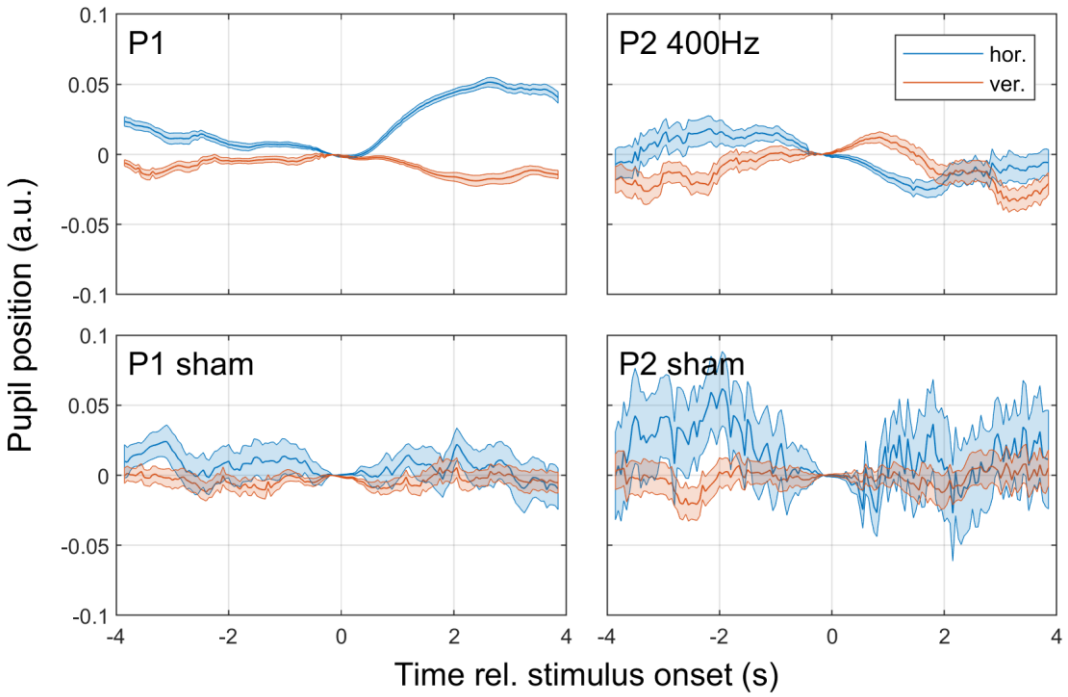

Figure 5.2: Eye movement relative to the initial eye position (mean ± s.e.m.) as a function of time relative to stimulus onset. Movements in the horizontal dimension are plotted in blue, with positive values indicating rightward movement, while movements in the vertical dimension are plotted in red, with positive values indicating upwards movements. (A) Patient 1 (n=45 trials). (B) Patient 2 with 400pps stimulation (n=84 trials). (C) Patient 1 sham trials (n=99). (D) Patient 2 sham trials (n=73). Data for Patient 2 at 50pps stimulation not shown.

Table 5.1: A summary of multiple comparisons (Tukey test) following a 2-way ANOVA on eye position with stimulus direction and response accuracy (correct/incorrect) as factors. In each trial only the eye movement along the axis congruent with the stimulus direction was analysed.

** conditions where correct trials were associated with significantly larger eye movement*

† the single condition where incorrect trials were associated with significantly larger eye movement

Patient	Gaze Direction	Stimulus	*N* Correct	*N* Incorrect	*P* Value for Correct > Incorrect
P1	x	Right	7	4	0.019†
		Left	9	3	<0.001*
	y	Up	10	2	<0.001*
		Down	7	3	<0.001*
P2 50pps	x	Right	2	17	<0.001*
		Left	12	15	<0.001*
	y	Up	19	8	<0.001*
		Down	8	20	<0.001*
P2 400pps	x	Right	9	8	0.379
		Left	17	7	<0.001*
	y	Up	14	7	0.043*
		Down	13	9	<0.001*

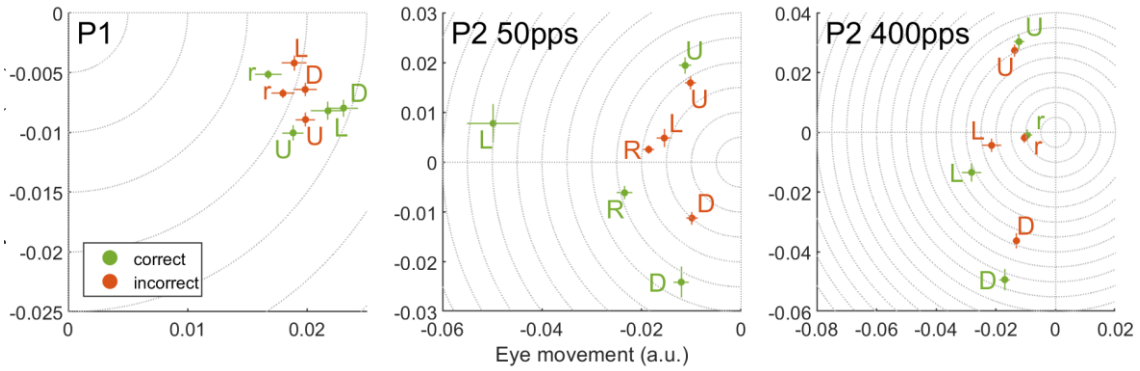

Figure 5.3: Average eye movement (±s.e.m.) relative to the initial eye position in each trial. Results are separated by response accuracy (Green: correct. Red: incorrect) and stimulus direction ('U', 'D', 'L', 'R' for up, down, left, and right respectively). Correct responses were associated with greater eye movement in the direction congruent with the stimulus (e.g. upwards eye movement for upward wedge stimulus) for 10 out of 12 conditions tested, indicated by capital letters. Lower-case letters denote the two cases in which correct responses were not associated with greater eye movement. For P1, rightward stimulus, incorrect responses were associated with greater eye movement, while for P2 400pps, rightward stimulus, there was no significant difference in eye movement between trials with correct and incorrect responses.

conditions tested). The only exceptions were for P1, rightward stimulus, in which greater eye movement was associated with incorrect responses, and P2 50pps, rightward stimulus, in which a similar degree of leftward eye movement was observed for correct and incorrect responses. Average eye movement in each condition is also plotted in Figure 5.3.

5.4. Discussion

Both participants made systematic eye movements even though they were instructed to keep their eyes fixed during the task, and it appeared that these movements were made in response to the stimuli since there were no systematic movements made during sham trials. It has been shown that eye movements in epiretinal implant recipients can cause phosphenes to move in

the visual field.[142] We expected eye movements to have a detrimental effect on performance, and that eye movements of larger magnitude would have a more severe effect. However, in both participants, larger eye movement was associated with better performance in the task. This could be explained by larger eye movements occurring when the percept was clearer or more localised. The observed eye movements may have been a reflexive response to the appearance of a percept, or may indicate compensatory habits developed by the participants to account for the surgical position of the implant on the retina.

In P2 the direction of the eye movement was generally congruent with the direction of the stimulus, suggesting the participant attempted to move their gaze towards the percept. This would be quite a normal response to a flash of light, and a similar relationship between stimulus direction and eye movement was reported in recipients of the Alpha IMS subretinal implant.[145] The association between stimulus direction and eye movement direction remained even in trials in which the participant responded incorrectly, suggesting the eye movement may have been driven by retinotopic cues of which the participant was not always cognisant. In P1 the eye movement was primarily rightwards for all stimuli and the relationship between stimulus direction and eye movement was less clear. A previously published phosphene mapping study showed that all of the phosphenes for P1 appeared in the right visual field.[9] This was expected because the electrode array covers the temporal retina of the left eye. It is therefore likely that all four stimuli all appeared in the right visual field, eliciting rightward eye movement, but were still spatially discriminable.

While the results do not demonstrate that eye movements are a cause of poor performance in a direct-to-array image localisation task it is still thought that eye movements would be detrimental in tasks using the head-mounted camera. Eye movements have been shown to affect hand-camera coordination by introducing eye-camera misalignments in target localisation tasks in simulated prosthetic vision[17] and in retinal implant recipients.[142,179] Currently, the standard practice for mitigating the effect of eye-camera misalignment is to instruct users to keep their gaze fixed centrally at all times. The present study demonstrates that users are unable to keep their gaze fixed even when instructed to do so, highlighting the importance of investigating techniques to compensate for eye movements. The findings are limited to direct-to-array stimulation and static images. The following chapter extends this study to conditions that more closely resemble normal use of the device by introducing dynamic stimuli that are sampled by the head-mounted camera with unrestrained head movement.

Chapter 6

Oculomotor responses to dynamic stimuli in a 44-channel suprachoroidal retinal prosthesis

Published as:

Titchener, S. A., Kvansakul, J., Shivdasani, M. N., Fallon, J. B., Nayagam, D. A. X., Epp, S. B., Williams, C. E., Barnes, N., Kentler, W. G., Kolic, M., Baglin, E. K., Abbott, C. J., Luu, C. D., Allen, P. J., Petoe, M. A. Oculomotor responses to dynamic stimuli in a 44-channel suprachoroidal retinal prosthesis. *Transl Vis Sci Technol.* 2020;9(13):31

Additional figures that did not appear in the publication have been included as an appendix.

Purpose: To investigate oculomotor behaviour in response to dynamic stimuli in retinal implant recipients.

Methods: Three suprachoroidal retinal implant recipients performed a 4-alternative forced-choice motion discrimination task over six sessions longitudinally. Stimuli were a single white bar ('moving bar') or a series of white bars ('moving grating') sweeping left, right, up, or down across a 42" monitor. Performance was compared with Normal video processing and Scrambled video processing (randomised image-to-electrode mapping to disrupt spatiotemporal structure). Eye and head movement was monitored throughout the task.

Results: Two subjects had diminished performance with Scrambling, suggesting retinotopic discrimination was utilised in the Normal condition, and made smooth pursuit eye movements congruent to the moving bar stimulus direction. These two subjects also made stimulus-related eye movements resembling optokinetic reflex (OKR) for moving grating stimuli, but the movement was incongruent with stimulus direction. The third subject was less adept at the task, appeared primarily reliant on head position cues (head movements were congruent to stimulus direction), and did not exhibit retinotopic discrimination and associated eye movements.

Conclusions: Our observation of smooth pursuit indicates residual functionality of cortical direction-selective circuits and implies a more naturalistic perception of motion than expected. A distorted OKR implies improper functionality of retinal direction-selective circuits, possibly due to retinal remodelling or the non-selective nature of the electrical stimulation.

Translational relevance: Retinal implant users can make naturalistic eye movements in response to moving stimuli, highlighting the potential for eye tracker feedback to improve perceptual localisation and image stabilisation in camera-based visual prostheses.

6.1. Introduction

Visual prostheses attempt to restore some visual function to the profoundly vision impaired. To date, three visual prostheses have been granted regulatory approval; the Argus II epiretinal implant (Second Sight, USA)[82], the Alpha AMS subretinal implant (Retina Implant AG, Germany)[78] and the IRIS II epiretinal implant (Pixium, France).[182] Other implants are at the clinical trial stage, such as a second generation suprachoroidal retinal implant (Bionic Vision Technologies, Australia) (Allen P.J., IOVS, 2020, 61, ARVO E-Abstract 2200; Kolic M., IOVS, 2020, 61, ARVO E-Abstract 2199; Petoe M.A., IOVS, 2019, 60, ARVO E-Abstract 4993), the PRIMA subretinal implant (Pixium Vision, France)[84], the Orion cortical implant (Second Sight, USA)[7,183], and the suprachoroidal-transretinal stimulation retinal implant (Nidek, Japan).[118] Present day visual prostheses can produce localisable and spatially distinct phosphenes that can be used to convey useful visual information to the subject[6], but the visual experience delivered is very crude; fewer than 50% of Argus II and Alpha IMS users tested had a measurable visual acuity in a grating acuity task.[61,75]

Large electrodes (necessitated by safe charge density limits), current spread, and the incidental stimulation of axonal pathways lead to large and irregularly shaped phosphenes and limited spatial discriminability.[9,16,184] Additionally, non-selective stimulation that activates both 'on' and 'off' pathways indiscriminantly is likely to have unusual perceptual effects that are not well understood.[10] Novel electrode designs and advances in targeted stimulation strategies offer some promise for future visual prostheses.[128–130,134] Despite current technical limitations, users of present-day retinal implants have demonstrated improved performance in activities of daily living and in tasks involving navigation, obstacle avoidance, and light localisation (Kolic M., IOVS, 2020, 61, ARVO E-Abstract 2199; Petoe M.A., IOVS, 2019, 60, ARVO E-Abstract 4993).[16,57,75,79]

In addition to spatial and form vision, visual prostheses should also ideally enable the perception of motion. Discrimination of direction of motion has previously been demonstrated in patients implanted with a 24-channel suprachoroidal retinal implant[16], a subretinal implant[75,79], and an epiretinal implant.[63] The subjective characteristics of the percepts experienced by participants during these tasks, as well as the particular perceptual cues used to identify motion, has received little attention. One study reported diminished performance when the image-to-electrode mapping was scrambled, demonstrating that retinotopic cues were useful for motion discrimination.[63] However, it remains unclear whether the recipients experience a naturalistic perception of motion. Given the low spatial and temporal resolution of present-day visual prostheses, they might instead perceive a series of discrete flashes that must be consciously interpreted as motion.

In natural vision, direction-selective circuits in the retina and visual cortex compute direction of motion from stimuli that move across the retina, encoding motion for the image-forming pathway, and also effecting oculomotor responses. Direction-selective circuits are important in the generation of smooth pursuit (the regulated eye movements made to maintain fixation on a moving target) and opto-kinetic reflex (a nystagmus that occurs in response to motion across the full visual field, characterised by slow-phase movements in the direction of stimulus motion punctuated by opposing fast-phase movements), both of which act to stabilise moving stimuli on the retina.[11] To our knowledge, the functionality of these circuits under electrical stimulation from a retinal implant has not been investigated.

In the present study we investigated the oculomotor behaviour in response to moving stimuli in recipients of a suprachoroidal retinal implant (Bionic Vision Technologies Ltd., Australia) with end-stage retinitis pigmentosa. The stimuli were designed to evoke smooth pursuit and optokinetic reflexive eye movements in order to determine the functionality of retinal and cortical direction-selective circuits under electrical stimulation with the implant. As a corollary, we aimed to reveal the strategies and perceptual cues used by the subjects to determine direction of motion. We categorise the observed eye movements and discuss the implications for prosthetic visual experience.

6.2. Methods

6.2.1. Participants

Three subjects (S1, S2, S3) with end-stage retinitis pigmentosa (bare light perception only) participated in the study. These subjects, along with a fourth who did not participate in the present study, were implanted with a 44-channel suprachoroidal retinal implant as part of a 2-year longitudinal clinical trial (NCT03406416, Feb. 2018- Dec. 2020). Prior to implantation, none of the participants had measurable visual field remaining (Goldmann kinetic perimetry with target sizes III and V4e). The prosthesis was implanted in the eye with poorer vision at baseline; for S1, this was the left eye while for S2 and S3 this was the right eye. Participant details are summarised in Table 6.1. Device fitting began 8 weeks post-operatively ('switch-on'), followed

Table 6.1: Participant profiles

	S1	S2	S3
Gender	Male	Male	Female
Age at implant (years)	47	63	66
Eye condition	Retinitis pigmentosa (rod cone)	Retinitis pigmentosa (rod cone)	Retinitis pigmentosa (cone rod)
Observed nystagmus	Mild	Intermittent	None
Visual acuity	Light perception OU	Light perception OU	Light perception OU
ffERG stimulus light threshold (cd.s/m2)	0.1	0.1	0.001
Age when legally blind	20	34	41
Years of useful form vision	34	43	56
Primary mobility aid	Cane	Cane	Guide dog
Implanted eye	Left	Right	Right

by lab-based training and at-home training. The subjects performed a 'moving bar' motion discrimination task periodically as part of a suite of outcome assessments, occurring at 17, 20, 32, 44, 56, and 68 weeks post switch-on. Home- and laboratory-based training continued between assessment time points but was not specific to the motion discrimination task. S1 and S2 also performed a "moving grating" motion discrimination task at a single time-point each (S1: 62 weeks post switch-on. S2: 66 weeks post switch-on). The study was approved by the Royal Victorian Eye and Ear Hospital Human Research and Ethics Committee, and was carried out in accordance with the tenets of the Declaration of Helsinki with the informed consent of all participants.

6.2.2. Suprachoroidal retinal prosthesis

The retinal implant comprised 46 platinum disc electrodes embedded in silicone implanted in the suprachoroidal space, connected via a lead-wire to a pair of subcutaneous stimulators behind the ear. Two larger diameter (2 mm) electrodes were reserved as return electrodes and 44 smaller electrodes (1 mm diameter) were available for stimulation.[5] The infrared ocular images (Spectralis, Heidelberg Engineering Gmbh, Germany) presented in Figure 6.1 show the placement of the array with respect to the fovea for each subject.

A psychophysical fitting procedure established the optimal stimulation parameters for each individual. This involved selecting the subset of electrodes that produced the optimal experience for the individual. Electrodes were excluded from the configuration if they did not yield a phosphene within safe charge limits (250nC per electrode at a rate of 50 pulses per second, biphasic pulse, 500µs phase width) (Nayagam D.A.X., IOVS, 2017, 58, ARVO E-Abstract 4204),[85] or if the phosphene was confusing, indistinct, or not easily discriminable from other phosphenes. Any two neighbouring electrodes could optionally be operated as a shorted pair to increase the effective surface area and raise the safe charge limit, yielding phosphenes in areas of the retina where single-electrode stimulation did not produce useful phosphenes. The electrodes that were selected for stimulation in each subject are circled in green in Figure 6.1. The stimulation parameters for each subject were established within the first 10 weeks post switch-on, and were then used for all training and at home use. To maintain consistency and aid in familiarising the artificial percepts the stimulation parameters for each participant were kept consistent across all tasks and settings for the duration of the clinical trial, except for minor adjustments to charge levels on individual electrodes to account for changes in perceptual thresholds.

Electrode activity was modulated by images captured by a head mounted camera. Camera images were processed using a Lanczos2 antialiasing filter as described in our previous work.[185] A "Scrambled" condition was also used, in which the same sampling locations were randomly assigned to the electrodes every five seconds to disrupt the spatial structure of the image while maintaining field of view, overall brightness, and number of phosphenes, as described in previous work.[154,186]

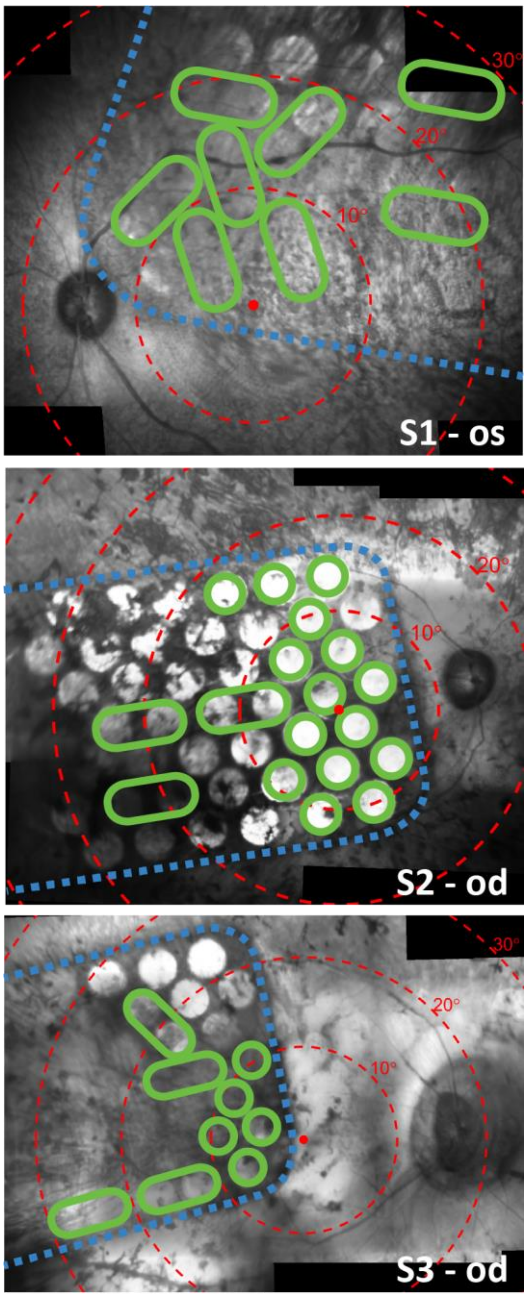

Figure 6.1: Stitched composite infrared fundus images (Spectralis, Heidelberg Engineering Gmbh, Germany) showing the placement of the array on the retina for S1 (top, 17 weeks post-operatively), S2 (middle, 8 weeks post-operatively), and S3 (bottom, 8 weeks post-operatively). Electrodes are visible in the images as bright circles. Note that some electrodes are obscured from view due to pigmentation. Dashed blue lines trace the edge of the implant. Red dots indicate the estimated location of the fovea and concentric red circles indicate 10° eccentricities of visual field according to the Drasdo and Fowler schematic eye.[125,126] *Green circles signify electrodes that were included in the subject's unique stimulus configuration, which was kept constant for all tasks and settings during the clinical trial. Larger green ovals indicate that two electrodes were operated as a shorted pair. Electrodes that are not circled in green were excluded from the stimulus configuration and were therefore not stimulated during the motion discrimination task. Some optical distortion and stitching artefact is expected.*

6.2.3. Moving bar task

Moving stimuli were presented in a four-alternative forced choice paradigm (4AFC). In each trial a single horizontal or vertical white bar of width 5° swept left, right, up, or down, across a black background on a 42" monitor viewed at approximately 40cm distance (approx. 100x67° visual arc). The subject's non-implanted eye was patched. The direction of motion was selected according to a balanced-random schedule. The orientation of the bar was always perpendicular to direction of motion. The subject's task was to identify the direction of motion and respond by pressing the corresponding key on a keypad. Audio cues signalled the appearance of the bar (trial start) and the acknowledgement of the subject's response. No other feedback was given. Initially the speed of the bar was set to 7°/s and 24 trials per condition were performed with Normal vision processing, Scrambled vision processing, and with the System Off on a balanced-random schedule. Then the speed was increased to 15°/s for a further 24 trials per condition, and finally to 30°/s for 24 trials per condition. The subjects were not informed of the Scrambled condition, anticipating that the device was either turned on or off. The task was repeated at regular intervals during the course of the clinical trial as part of a larger suite of outcome assessments (Kolic M., IOVS, 2020, 61, ARVO E-Abstract 2199; Petoe M.A., IOVS, 2019, 60, ARVO E-Abstract 4993). Subjects could move their head freely and they were not given any particular instruction regarding eye movement; however, in the course of their training they had been made aware that eye position can affect the locations of phosphenes.

6.2.4. Moving grating task

The moving grating task was identical to the moving bar task except the bar stimulus was replaced by a grating stimulus, consisting of regularly spaced parallel white bars. The white bars were 5° in width with a pitch of either 20 or 30° (corresponding to a 15 or 25° gap between neighbouring bars). This spacing was selected to be smaller than the device's visual field (Figure 6.1) such that at least one bar of the grating was within the sampling region at any given time, while being mindful of the limited visual acuity of the retinal implant. As in the moving bar task, the stimulus moved in one of the four cardinal directions at random and the subject was required to determine the direction of motion and respond by pressing a key on a keypad. The stimulus filled the entire monitor and was displayed continuously until a response was logged. Due to time constraints the task was only performed in S1 and S2 in the Normal condition.

6.2.5. Eye and head tracking

A head-mounted eye tracker (Arrington Research, AZ, USA) recorded the position of the implanted eye at 60 Hz. Eye position data was processed to remove blink artefact prior to any analysis. Calibration of the system was not possible with non-sighted participants, as the calibration sequence requires the participant to fixate on a number of visual targets. Instead, following the manufacturer guidelines for this scenario, the system was calibrated for a sighted user and this calibration was then applied during data acquisition in this study. The eye-facing cameras were positioned such that the canthi were aligned with the left and right edges of the image to ensure the size of the eye in the camera image was consistent across all sessions. Small changes in the position of the camera relative to the eye are expected when moving the headset from the sighted user to the non-sighted user and this can introduce slippage error in the calculated gaze position. However, only relative changes from stimulus onset are analysed in this study, so small changes in absolute gaze estimates are unlikely to significantly affect the results. Head azimuth and elevation was recorded in degrees at 20 Hz using a magnetic motion

tracker (Ascension trakSTAR, Ascension Technology Corporation, VT, USA). Saccadic eye movements were identified using a velocity threshold of 50°/s. A subset of the data for each subject was visually inspected to verify the robustness of the saccade detection.

The net head movement in each trial of the moving bar and moving grating task was quantified by ΔHead, the aggregate of all head movement made between stimulus onset (first electrode stimulated) and stimulus offset (last electrode activated). Likewise, $\Delta Eye_{saccadic}$ and ΔEye_{drift} respectively quantify the aggregate saccadic and drift (non-saccadic) eye movement between stimulus onset and offset. If an eye movement continued after stimulus offset (eye velocity greater 4°/s) then the sampling time was extended until either the movement ceased (velocity less than 4°/s), the direction of the movement deviated more than 30° from the original movement, or 300 ms after stimulus offset, whichever occurred first. This ensured that any eye movement that began during the period of stimulation was fully captured. The ΔEye and ΔHead vectors were then normalised by subtracting the angle of stimulus motion, such that the normalised ΔEye and ΔHead represented the direction of the eye or head movement relative to the direction of the stimulus.

6.2.6. Statistical analyses

Mean normalised ΔHead and ΔEye_{drift} were compared against zero to determine whether any significant head movements or drift eye movements congruent to the stimulus direction occurred in the moving bar task (Hotelling's one sample T-test with Bonferroni correction for multiple comparisons). Any trial in which the initial eye position was greater than two standard deviations from the mean eye position over the entire session was excluded in order to mitigate any possible effect of an eccentric initial eye position. Nystagmus was identified by comparing the mean $\Delta Eye_{saccadic}$ and ΔEye_{drift} over many trials – whereby drift and saccadic movements with opposing polarities indicated nystagmic eye movement. Behavioural responses from the keypad were compared for significance against chance (25%) using a binomial test with an alpha level of 0.05.

6.3. Results

6.3.1. Moving bar task performance

S1 and S2 completed the moving bar task for all three stimulus speeds. S3 attempted the 7°/s stimulus on all assessment dates, the 15°/s stimulus at 20, 30, and 68 weeks post switch-on, and did not attempt the 30°/s stimulus at all due to time constraints. Accuracy on the task is presented for all subjects in Figure 6.2. Accuracy was very consistent between sessions, so data from all sessions was pooled together. For S1 accuracy in the Normal condition was good (61-67%) and accuracy in the Scrambled condition was worse (47-23%) but still significantly above chance for 7°/s and 15°/s stimuli ($p<0.001$). For S2 accuracy in the Normal condition was excellent (83-87%) but accuracy in the Scrambled condition was not significantly above chance for any stimulus speed. For S3 accuracy was significantly above chance for in the Normal and Scrambled conditions for 7°/s stimuli but not for 15°/s stimuli. Accuracy was not significantly above chance in the System Off condition for any participants.

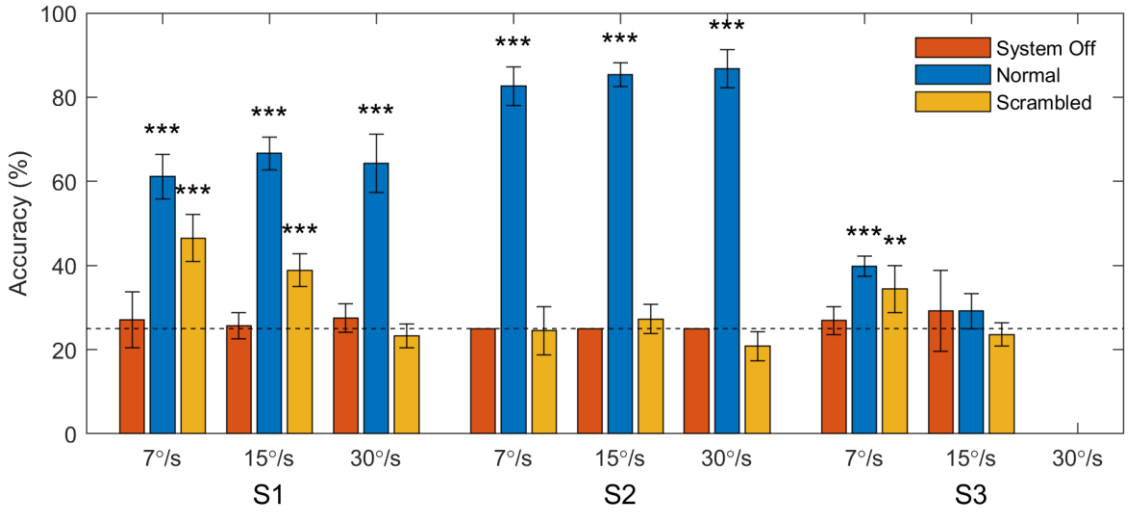

*Figure 6.2: Response accuracy for each subject in the moving bar task. Bars represent accuracy pooled across all sessions. Error bars represent the standard error of the mean of accuracy per session. Data are separated by the speed at which the stimulus moved and by the image processing condition (Normal, Scrambled, System Off). The horizontal dotted line specifies the chance rate of 25%. Asterisks denote above-chance performance for data pooled across sessions (Binomial test, **p<0.01, ***p<0.001).*

6.3.2. Stimulus-related smooth pursuit eye movements

Stimulus-related drift eye movements were observed for two subjects. Figure 6.3A and 3B respectively show an exemplar eye and head response for a single trial with S1 in which a 30°/s left-moving stimulus was presented. Figure 6.3C and 3D respectively show the mean (± standard deviation) eye and head response for S1 for all trials in which 30°/s left-moving stimuli were presented. Similar data were obtained for S2 and S3, and summarised as vectors of maximal eye and head motion with respect to normalised stimulus direction (Figure 6.4).

Figure 6.4 summarises the drift eye movements, head motion, and inferred strategy on the task for all participants. Normalised ΔHead and ΔEye_{drift} vectors and are plotted for each stimulus speed, showing the head movement and drift eye movement relative to the direction of stimulus movement. Vector angles near 0° indicate eye or head movement congruent to the stimulus movement, i.e. systematic and repeatable eye and head movements aligned with the stimulus were observed. Circular markers without vector lines denote cases where the mean normalised ΔHead or ΔEye_{drift} was not significantly different to zero, indicating that either minimal movement occurred or the direction of the movement was not correlated with the direction of stimulus movement. Responses for 15°/s stimuli were not included for S3 as these stimuli were not discriminable by the subject (Figure 6.2).

Head movements congruent to the stimulus motion were observed for S1 for 7°/s and 15°/s stimuli, and for S3 for 7°/s stimuli, implying a strategy that utilised head scanning (Figure 6.4G, I). No significant head movements were observed for S2 (all stimulus speeds) or S1 for 30°/s stimuli, implying a strategy that utilised retinotopic information and not head scanning.

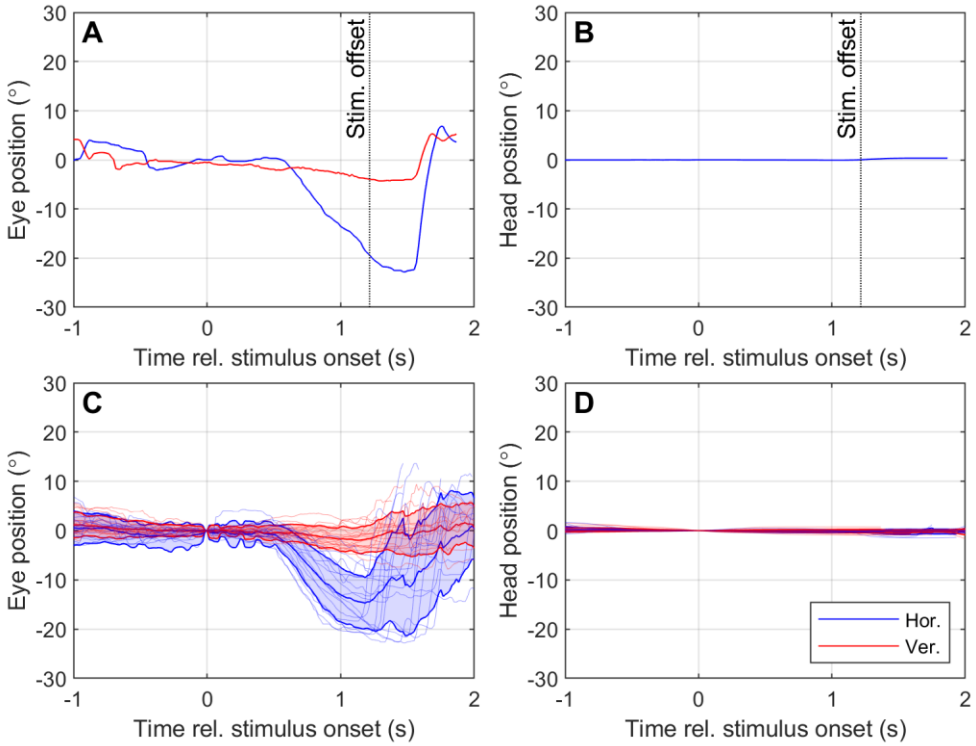

Figure 6.3: Example of eye and head responses to moving stimuli. Panels A and B respectively display the eye and head movement during a single trial in which a 30°/s left-moving stimulus was presented. Panels C and D respectively display the average (± standard deviation) eye and head movement over all trials in which a 30°/s left-moving stimulus was presented and correctly identified. Eye and head position are measured relative to the position at stimulus onset (t=0). Positive values on the y-axis indicate rightwards horizontal movement (blue lines) or upwards vertical movement (red lines).

S1 and S2 both had significant drift eye movements congruent to the stimulus direction in the Normal condition (Figure 6.4A, B), but these eye movements did not occur when the retinotopic information was scrambled (Figure 6.4D, E). These drift eye movements are unlikely to represent the slow phase of nystagmus because of their dependence on the task stimuli. Nor are they likely to represent vestibulo-ocular reflex, because the head movement was either minimal or was in the same direction as the eye movement. It is therefore probable that these drift eye movements are smooth pursuit. An example of a supposed smooth pursuit waveform (S1, 30°/s left-moving stimulus) is presented in Figure 6.3A. The eye movement occurring between approximately t=0.5-1.5s bears the primary characteristics of a smooth pursuit: a prolonged eye movement at sub-saccadic velocities in a direction congruent with a moving stimulus. This response was highly repeatable (average extent of 14.7 ± 5.1°, Figure 6.3C).

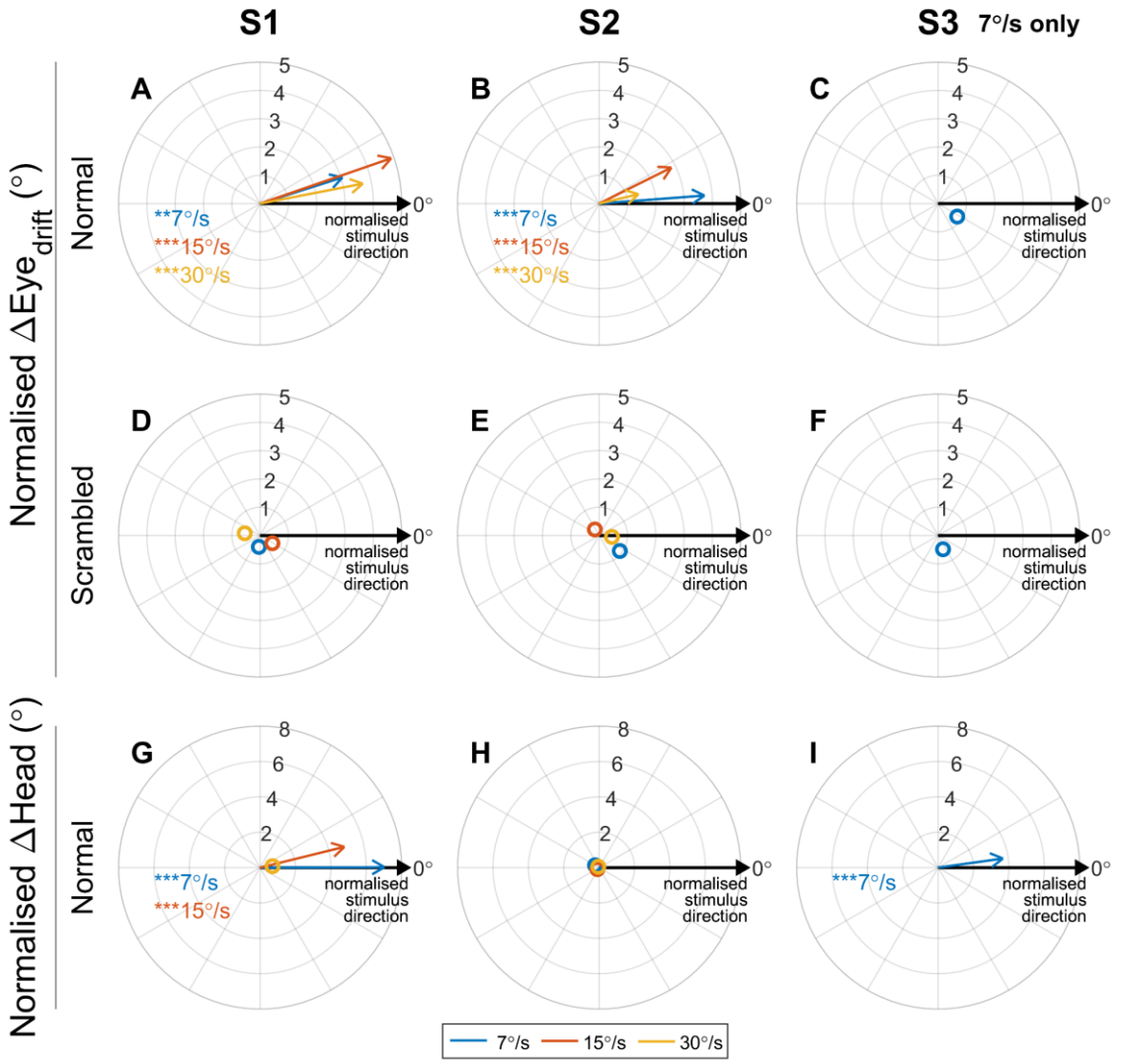

*Figure 6.4: Polar plots displaying the angular error between the direction of motion of the stimulus and the average ΔEye_{drift} and ΔHead for all subjects in the Normal and Scrambled conditions for 7°/s (blue), 15°/s (red) and 30°/s (yellow) stimuli. Each vector represents the mean direction and magnitude of the eye or head movement relative to the direction of motion of the stimulus. Vectors pointing approximately rightward (0°) indicate that on average the eye or head movement was in the same direction as the stimulus (for all stimulus directions). Asterisks indicate mean eye or head movement was significantly different to zero (Hotelling's one sample T-test with Bonferroni correction for multiple comparisons; *p<0.05, **p<0.01, ***p<0.001). Hollow markers denote mean eye/head movements that were not significantly different to zero, indicating little movement or non-systematic movement.*

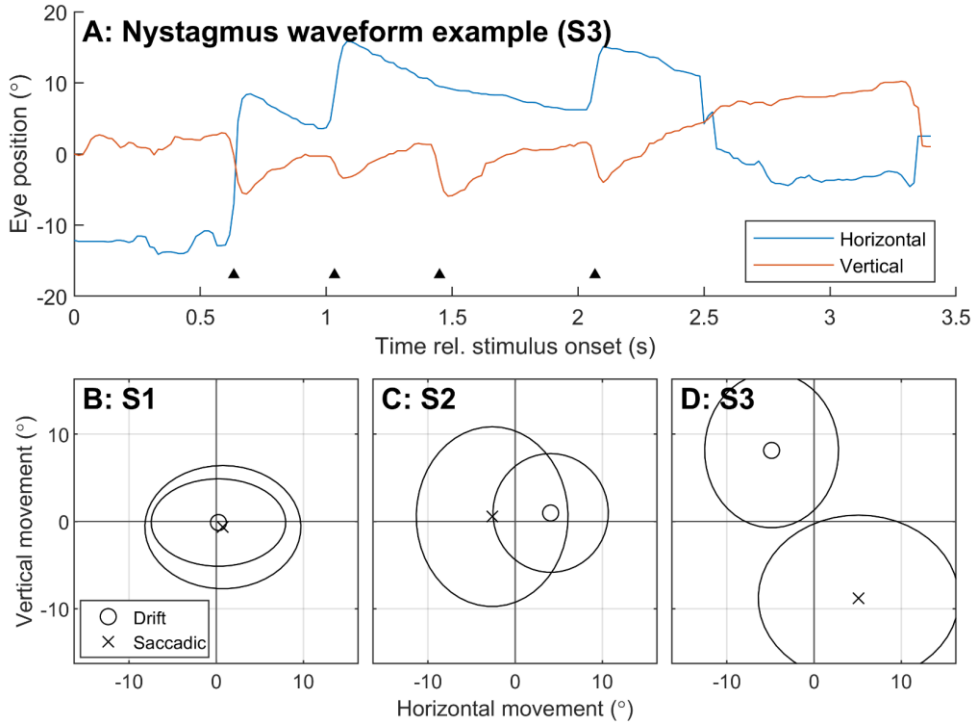

Figure 6.5: Characterisation of baseline acquired nystagmus for each subject using eye movement during the moving bar task in the System Off condition. Data was pooled across all stimulus speeds. A) Example of a nystagmic waveform in S3. Black triangles indicate the beat (saccadic component) of the nystagmus. B-D) Mean ΔEye_{drift} (circle markers) is compared to mean $\Delta Eye_{saccadic}$ (crosses) for each participant. Ellipses indicate standard deviation. Slow and fast phase movements with opposing polarity indicate a beating nystagmus. S1 had no notable nystagmus, S2 exhibited a left-beat nystagmus, and S3 exhibited a down-beat nystagmus.

6.3.3. Characterisation of baseline acquired nystagmus

To characterise any baseline acquired nystagmus, ΔEye_{drift} and $\Delta Eye_{saccadic}$ during the System Off condition were compared (Figure 6.5). Data from all stimulus speeds and directions were pooled under the assumption that the subjects received no visual input during the task (bare-light perception only, no electrical stimulation, and resultant accuracy not significantly greater than chance). No normalisation for stimulus direction was performed. Nystagmus is characterised by slow-phase (drift) eye movements punctuated by 'beating' fast-phase (saccadic) eye movements in the opposite direction[11], so ΔEye_{drift} and $\Delta Eye_{saccadic}$ movements with opposite polarity would indicate a nystagmus. Figure 6.5 shows no notable nystagmus for S1, a left-beating nystagmus for S2, and a down-beating nystagmus for S3.

6.3.4. Optokinetic reflex

Response accuracy using the keypad for the moving grating task for S1 was 50% (30°/s, 20° pitch) and for S2 was 63% (15°/s, 20° pitch), 83% (30°/s, 20° pitch) and 92% (30°/s, 30° pitch). Sawtooth-like waveforms that resembled optokinetic reflex appeared intermittently in the recorded eye position signal during the moving grating task. An example of one such movement is shown in Figure 6.6A, while the mean ΔEye_{drift} and $\Delta Eye_{saccadic}$ are normalised against trial duration and plotted for each subject in Figure 6.6B-C. In healthy vision, the beat (saccadic component) of optokinetic reflex is expected to oppose the direction of stimulus movement.[11] Nystagmic eye movements were identified, but for both subjects the beat was always upwards – regardless of stimulus direction. For S2 the severity of nystagmus varied with stimulus direction, but up-beat nystagmus was observed for all moving grating stimuli tested (Figure 6.6,

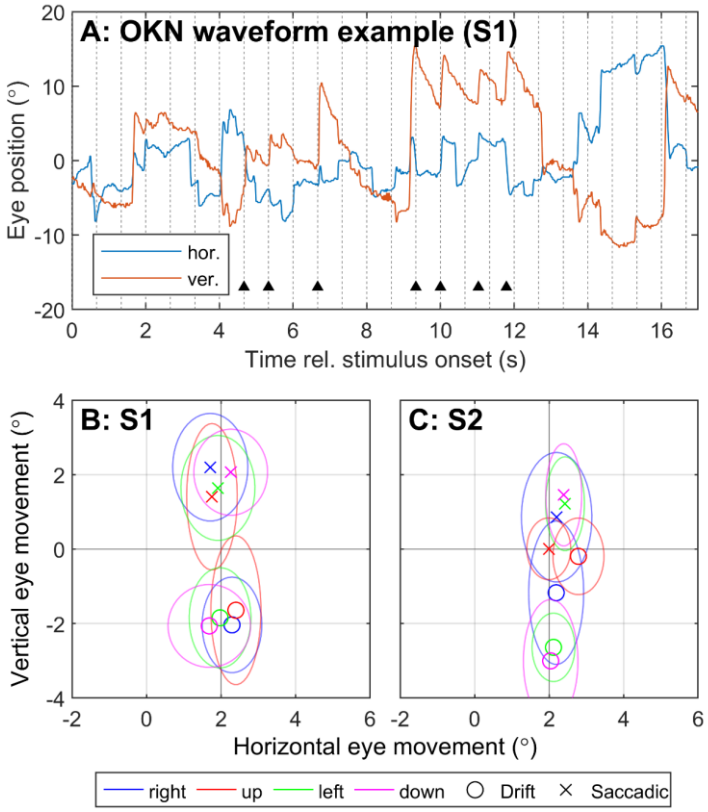

Figure 6.6: Characterisation of nystagmus for S1 and S2 in the moving grating task. A) Example of a nystagmic waveform observed in S1 during the moving grating task. B-C) Mean ΔEye_{drift} (circle markers) is compared to mean $\Delta Eye_{saccadic}$ (crosses) for each stimulus direction for each participant. Colour represents the direction of motion of the stimulus. Ellipses indicate standard deviation. Slow and fast phase movements with opposing polarity indicate a beating nystagmus. Both participants exhibited up-beat nystagmus in response to the moving grating stimuli, regardless of stimulus direction. Only data for 30°/s, 20° pitch are shown.

only data for 30°/s, 20° pitch are shown). Up-beat nystagmus is inconsistent with either subject's baseline nystagmus (Figure 6.5) – S1 exhibited no notable nystagmus with System Off and S2 exhibited a left-beating nystagmus.

6.4. Discussion

6.4.1. Smooth pursuit and nystagmus

In this study we examined the contributions of fast (saccadic) and slow (drift/pursuit) eye movements to overall eye movement in a motion discrimination task using prosthetic vision. Our observation that two subjects made smooth pursuit eye movements in the direction of stimulus motion is particularly significant because smooth pursuit generally only occurs in response to a moving visual target. Direction- and orientation- selective circuits in V1, which integrate spatiotemporal patterns of excitation within their receptive fields to encode motion, are necessary for the generation of smooth pursuit in primates and also provide a direction selective input to the image forming pathway.[11,187] A series of discrete flashes could be interpreted as motion in the context of the task, but this would not be expected to elicit a smooth pursuit. Therefore, the observation of smooth pursuit in two subjects might suggest the experience of motion was more naturalistic than expected. Both these two subjects described their experience of motion during the task as "normal".

In the moving grating task two subjects made eye movements that resembled an optokinetic reflex, however, the movement was always up-beat regardless of the direction of stimulus motion. The observed movements are likely to be stimulus-related, rather than acquired nystagmus, because they did not match the earlier characterisation of each subject's baseline acquired nystagmus, the degree of nystagmus varied with stimulus direction in one subject, and the subjects were screened before enrolment for neurological conditions known to cause up-beat nystagmus.

In mammals the optokinetic reflex is modulated by direction-selective retinal ganglion cells that project to the accessory optic system, though the actual direction-selective computation is performed by starburst amacrine cells in the inner retina.[188,189] Given the limited spatial resolution of electrical stimulation with the suprachoroidal retinal implant (1.5mm electrode pitch), and the fact that suprachoroidal stimulation activates neurons in all retinal layers (likely activating direction-selective retinal ganglion cells directly, regardless of any activation and subsequent computation occurring in the inner retina)[88,190], it is unsurprising that a normal optokinetic reflex was not observed. It is possible that the video processing and electrode sequencing algorithms, which are constrained by the video processing rate (12.5 Hz) and safe stimulation protocols, produced artefact that led to up-beat nystagmus. Alternatively, the significant neural remodelling that occurs in retinal degeneration may have affected the function of the retinal direction-selective circuits and interfered with the generation of the optokinetic reflex.[191] It is unclear what the perceptual effects of such remodelling might be; direction selective retinal ganglion cells are most strongly implicated in optokinetic control and their role in image-forming remains under debate.[192] Further understanding of retinal remodelling and its perceptual and oculomotor effects will be important in establishing a naturalistic integration of retinal implants in late-stage retinal degeneration.

It should also be noted that foveation and image stabilisation, the primary purpose of smooth pursuit and optokinetic reflex, is not possible with the present 44-channel suprachoroidal retinal implant. This is due to the decoupling of eye position and camera orientation. The observed smooth pursuit eye movements would not have had the effect of stabilising the percept, and would in fact have caused further movement of the percept, as eye movements cause movement of phosphenes within the visual field.[17,98,142,179] This is also likely to have interfered with the generation of an optokinetic reflex. Nevertheless, the observation of smooth pursuit movements is an encouraging result for photovoltaic retinal implants or future visual prostheses that incorporate eye position feedback.

6.4.2. The contribution of retinotopic information

Analyses of eye and head movement revealed a range of strategies employed in the task. S3 appeared to be the most dependent on head scanning, exhibiting head movements congruent to the stimulus direction and a relatively small decrease in performance when the retinotopic information was scrambled. In contrast, S2 was highly proficient at retinotopic discrimination and made almost no head movement, resulting in excellent performance in the Normal condition and chance performance in the Scrambled condition. S1 employed a mixture of head scanning and retinotopic discrimination – scrambling the retinotopic information diminished performance, but performance remained above chance in cases where head movements were observed (7°/s and 15°/s stimuli). Taken together, these results suggest head position cues were

useful when available but that the task was also possible using retinotopic cues only. These results are consistent with published results showing decreased performance in Scrambled versus Normal for subjects implanted with the Argus II epiretinal implant performing a moving bar task,[63] and for subjects implanted with a 24-channel suprachoroidal retinal implant performing acuity and localisation tasks.[16,154]

6.4.3. Array placement and stimulation parameters

Some aspects of the oculomotor response may be explained by the placement of the array on the retina (Figure 6.1). In S3, the electrodes that were selected for stimulation span a relatively small area of the retina, which may explain S3's relatively low accuracy on the task and apparent reliance on head movement cues. In S1, the stimulating electrodes lie superior to the fovea, such that phosphenes are expected to appear in the lower hemisphere of the visual field on both the left and right sides. S1 consistently performed worse for up-moving stimuli than any other direction (see response matrix in Supplementary Figure S6.1), and this was the only stimulus for which smooth eye movements were incongruent with stimulus direction. This may be related to the absence of any electrodes inferior to the fovea and much better coverage of active electrodes horizontally than vertically. In S2, with a sparse electrode mapping in the temporal superior region (Figure 6.1), left-moving and down-moving stimuli were the most commonly confused stimuli (Supplementary Figure S1), and the direction of smooth eye movements for those stimuli appeared mostly downwards. This was corroborated by the subject, saying the two directions were difficult to distinguish because the lower left of his visual field was unclear.

The results suggest that placing the array squarely over the fovea is optimal, as it provides phosphenes in all quadrants of the visual field. Overall accuracy in the task also appears to be correlated to the number of active electrodes included in the subject's individual stimulation configuration, which depends on the response of the neurons surrounding each electrode to electrical stimulation within safe limits. Presumably one of the key predictors of performance on the task would therefore be the integrity of the degenerate retina. The finding that all subjects made significant eye movements, despite understanding that eye movement could be detrimental to their performance, further underscores the need for eye position feedback and image stabilisation in camera-based visual prostheses.

6.4.4. Conclusion

Subjects implanted with a 44-channel suprachoroidal retinal implant use a variety of strategies to discriminate direction of motion, with some subjects making use of head position cues and others relying entirely on retinotopic cues. The observation of smooth pursuit eye movements in two subjects indicates some influence of cortical direction-selective circuits under stimulation from the implant, and implies a more naturalistic experience of motion than previously expected. The finding that naturalistic oculomotor responses to moving stimuli can occur even in low resolution prosthetic vision highlights the potential for eye tracker feedback to improve perceptual localisation and image stabilisation in camera-based visual prostheses.

6.5. Supplementary material

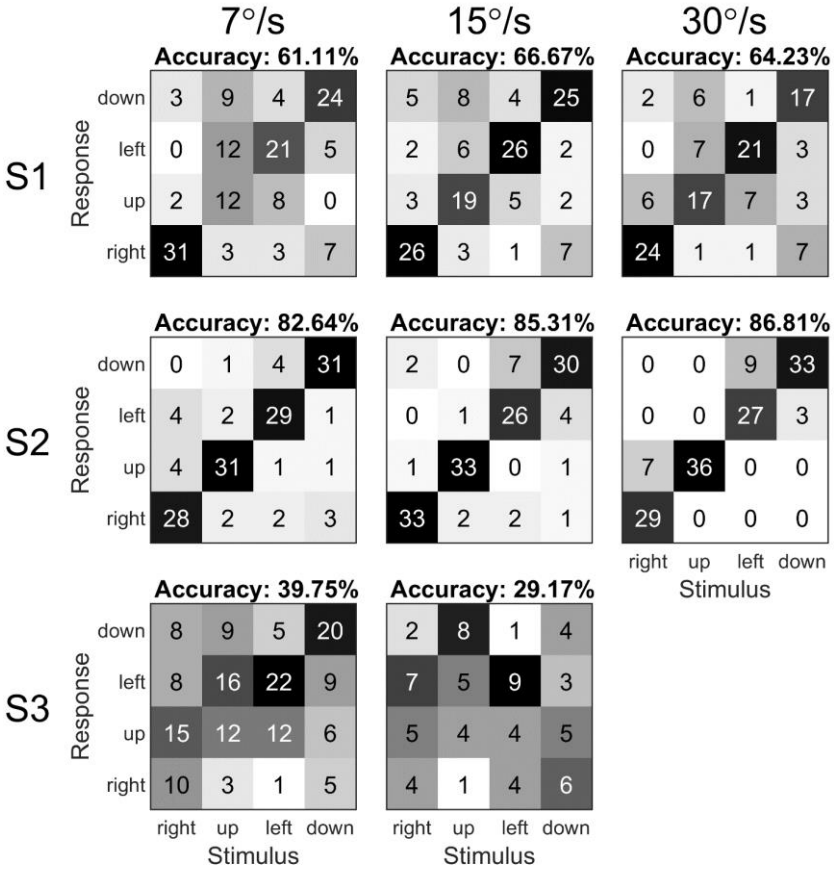

Supplementary Figure S6.1: Response matrices for accuracy in the moving bar task in the Normal condition. Data is pooled across all sessions. Results for each stimulus speed are presented separately. Numbers inside squares indicate number of trials, and darker coloured squares indicate a higher proportion of responses. S3 did not attempt the task for 30°/s stimuli. Overall accuracy on the task is displayed above each matrix.

6.6. Appendices

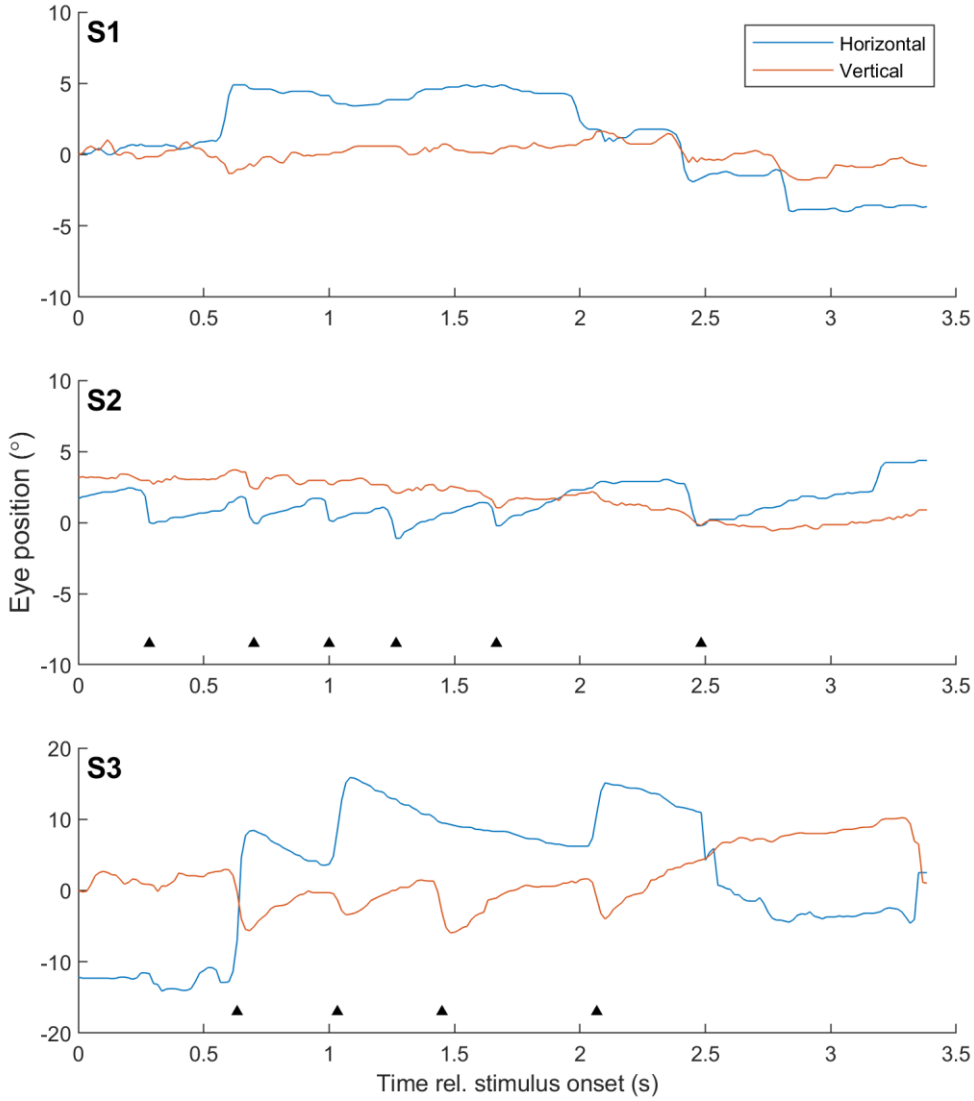

Appendix 1: Examples of nystagmic waveforms observed in each participant during the moving bar task in the System Off condition. Blue lines represent horizontal eye position (with positive y axis values indicating rightward displacement) and red lines represent vertical eye position (with positive y values indicating upwards displacement). Black triangles indicate the beat (saccadic component) of the nystagmus. No nystagmus is observed for S1 (top), a left-beating nystagmus is observed for S2 (middle), and an down- and right-beating nystagmus is observed for S3 (bottom).

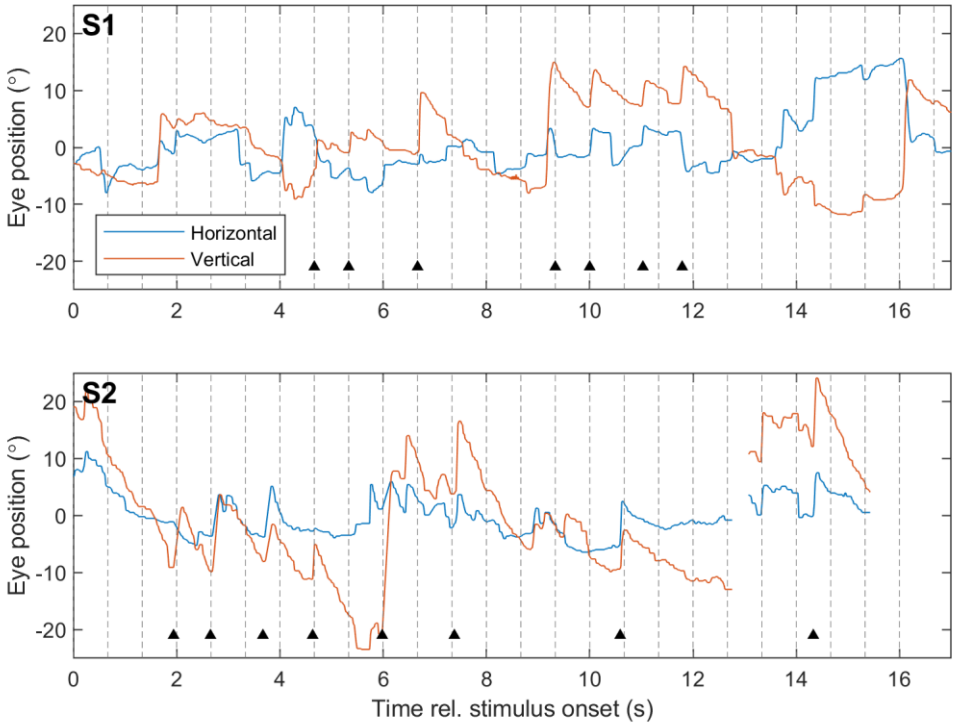

Appendix 2: Examples of nystagmic waveforms observed in each participant during the moving grating task. Blue lines represent horizontal eye position (with positive y axis values indicating rightward displacement) and red lines represent vertical eye position (with positive y values indicating upwards displacement). Black triangles indicate the beat (saccadic component) of the nystagmus. Up-beating nystagmus was observed in S1 and S2. S3 did not participate the moving grating task.

Chapter 7

Gaze Compensation as a Technique for Improving Hand-Eye Coordination in Prosthetic Vision

Published as:

Titchener S. A., Shivdasani M. N., Fallon J. B., Petoe M.A. Gaze Compensation as a Technique for Improving Hand–Eye Coordination in Prosthetic Vision. *Transl Vis Sci Technol*. 2018;7(1):2.

Purpose: Shifting the region-of-interest within the input image to compensate for gaze shifts ("*gaze compensation*") may improve hand-eye coordination in visual prostheses that incorporate an external camera. The present study investigated the effects of eye movement on hand-eye coordination under simulated prosthetic vision (SPV), and measured the coordination benefits of gaze compensation.

Methods: Seven normal-sighted subjects performed a target localisation pointing task under SPV. Three conditions were tested, modelling: retinally stabilised phosphenes (uncompensated); gaze compensation; no phosphene movement (centre-fixed). The error in pointing was quantified for each condition.

Results: Gaze compensation yielded a significantly smaller pointing error than the uncompensated condition for six out of seven subjects, and a similar or smaller pointing error than the centre-fixed condition for all subjects (Two-way ANOVA, $p<0.05$). Pointing error eccentricity and gaze eccentricity were moderately correlated in the uncompensated condition (azimuth: $R^2=0.47$; elevation: $R^2=0.51$) but not in the gaze-compensated condition (azimuth: $R^2=0.01$; elevation: $R^2=0.00$). Increased variability in gaze at the time of pointing was correlated with greater reduction in pointing error in the centre-fixed condition compared to the uncompensated condition ($R^2=0.64$).

Conclusions: Eccentric eye position impedes hand-eye coordination in SPV. While errors can be reduced by limiting eye eccentricity in uncompensated viewing, gaze compensation is effective in improving coordination for subjects unable to maintain fixation.

Translational Relevance: The results highlight the present necessity for suppressing eye movement and support the use of gaze compensation to improve hand-eye coordination and localization performance in prosthetic vision.

7.1. Introduction

Visual prostheses aim to provide artificial vision to blind patients by using implanted electrodes to electrically stimulate the retina,[75,82,88,193] optic nerve,[101] thalamus,[107] or visual cortex,[49] evoking localised visual percepts. The location of the percept within the patient's egocentric spatial map is known to move in parity with the orientation of the eyes.[49,82,142] This apparent movement is because eye position plays an important role in the integration of retinotopic visual signals into a consistent spatial map,[12] even after blindness.[194]

For tasks of coordination it is important that the percept location properly reflects the real world. This requires the orientation of the image sensor to be directly coupled with eye position; however, most present devices use an external camera of fixed orientation, divorcing the camera axis from the pupillary axis.[82,88,193] Recipients of these devices must rely exclusively on head movements to direct their field of view. While retinal implants have been shown to assist in hand-eye coordination tasks[193,195–197] it is likely that the decoupling of the camera and pupillary axes negatively affects performance on the tasks.

Currently, patients are trained to suppress eye movements at all times in order to maintain alignment between the camera and pupillary axes[64,143] but the accessibility of this technique is questionable. Patients have little intuition of the orientation of their eyes[142] and have difficulty suppressing eye movements, particularly those associated with nystagmus. We have previously found that suprachoroidal implant recipients made significant eye movements in response to stimuli during a static image localisation task despite being instructed not to.[16] A separate study in Argus II recipients found that camera-gaze misalignments occurred frequently during a visual search task, often due to the vestibulo-ocular reflexive movements that occur naturally during head scanning, and that patients rely on a series of complex head movements to properly localise objects in daily life.[142] Some have suggested that percept localisation is so difficult that many patients simply use their devices as light detectors, ignoring any retinotopic information and instead relying solely on head and neck orientation.[82,154,195]

Other visual prostheses forego the external camera and instead use implanted photodiode arrays, such as the Alpha IMS/AMS subretinal implant.[75] In these devices, electrode activity is modulated by the light that is naturally incident to the eye, enabling naturalistic eye scanning. Studies with Alpha IMS recipients have shown that patients exhibit "qualitatively normal" oculomotor behaviour when the hardware permits eye scanning.[145] Restoring naturalistic eye scanning in camera-based retinal and cortical implants is desirable as it has implications for perceptual localisation and hand-eye coordination, and would reduce the cognitive burden on the recipient by facilitating more intuitive interaction with the technology. Implantable intraocular cameras have been proposed as one way of achieving this,[147,198,199] but to our

knowledge the clinical feasibility of this approach has not been established. Others have proposed tracking the eye position and dynamically shifting the region-of-interest (ROI) inside a wide field of view image to compensate for eye movements as they occur.[146,200] This technique, which we term "gaze compensation", is the more immediately applicable and clinically relevant technique.

Existing studies have examined the benefits of gaze compensation in prosthetic vision. In a previous study on suprachoroidal retinal implant recipients we showed that gaze compensation improved performance in a static image localisation task but we did not assess hand-eye coordination specifically.[148] Similarly, McIntosh (2015)[146] showed that subjects under simulated prosthetic vision performed better in a reach-and-grasp task and a visual search task when foveation was restored; however, significant results were found only at high phosphene densities, possibly because the tasks were too difficult to perform at low resolution even with gaze compensation.

Other studies have reported eye position as a confounding factor in hand-eye coordination. Sabbah et al (2014)[142] tested the accuracy of epiretinal Argus II patients in a target localisation task when the eyes were purposefully held in an eccentric position. They reported that pointing was skewed towards the direction of eye displacement; however, the analysis was limited to directionality and did not quantify the effect of eye displacement magnitude. In a separate study, Argus II patients indicated the location of percepts generated by direct-to-array stimulation during forced eccentric eye movements. After estimating the effect of eye movement, the authors inferred the retinotopic placement of electrodes from the pointed location.[98] A simulated prosthetic vision study in a visually impaired subject found that nystagmus adversely affected performance on a hand-eye coordination task when phosphenes moved in parity with the eyes.[200] Two preliminary reports regarding experiments in Argus II recipients (Caspi et al. IOVS 2017; ARVO E-Abstract 4192)[149] and simulated prosthetic vision (Hozumi et al. IOVS 2016; ARVO E-Abstract 1958)[201] respectively have demonstrated reduced pointing error in a target localisation task when gaze compensation was used. Finally, changes in the optimal camera alignment in Argus II patients have been shown to correlate with long-term changes in eye orientation (Barry et al. IOVS 2017; ARVO E-Abstract 4687).[202] It is clear that a relationship between eye position and hand-eye coordination exists, but to our knowledge the specific effect of gaze eccentricity on coordination has not been characterised in any of the existing literature.

The present study aimed to test the effectiveness of gaze compensation for improving hand-eye coordination in visual prosthetic recipients. We used a prosthetic vision simulator, based on the classic scoreboard model of phosphene vision, with built-in eye tracking to simulate prosthetic vision with and without gaze compensation. Further, we aimed to characterise the relationship between eye position and pointing error in a target localisation task under simulated prosthetic vision in order to better understand the effect of eye movements on hand-eye coordination. In contrast to the studies by Caspi et al (2017)[98] and Sabbah et al (2014),[142] any pupil eccentricity was spontaneously occurring rather than experimenter-controlled. We hypothesised that pointing error in the gaze-compensated condition would be significantly smaller than in the uncompensated condition and comparable to an idealised condition in which phosphenes never moved and camera-gaze misalignments did not arise from eye movement. We further

hypothesised that the magnitude and directionality of pointing error would be correlated to eye position, but that these correlations would diminish with gaze compensation.

7.2. Methods

7.2.1. Subject Selection

Seven volunteers aged 22-31 participated in the experiment. All subjects had normal or corrected-to-normal vision and had no relevant medical history, and informed consent was obtained for all subjects. The research adhered to the tenets of the Declaration of Helsinki and was approved by The University of Melbourne School of Health Sciences Human Ethics Advisory Group (HREC 1647240).

7.2.2. Phosphene Rendering for Simulated Prosthetic Vision

Real-time phosphene rendering for simulated prosthetic vision was achieved using an abstract model of phosphene vision previously described by McCarthy et al (2014).[137] Briefly, phosphenes appeared in a predefined layout as white spots whose intensity was greatest in the centre and decayed with radial distance according to a Gaussian profile with standard deviation proportional to the peak intensity. Phosphene intensities were calculated according to the minimal vision processing scheme described by Barnes et al (2016),[185] whereby each phosphene intensity was calculated using a projection of 42 electrodes onto the input image and the peak intensity of each phosphene was set to a quantised value (eight levels) of the underlying pixel in the input image. The phosphene layout was modelled after the electrode layout of Bionic Vision Australia's second-generation 44-channel retinal implant,[203] with 42 phosphenes arranged in a hexagonal grid (Figure 7.1).

7.2.3. Simulated Prosthetic Vision Apparatus

Subjects wore a virtual reality headset (Rift DK2, Oculus Inc., Irvine, CA, USA) with a wide field of view camera (Logitech c390e, FoV: 80.7x50°, 30 fps) mounted to the headset in front of the left eye (Figure 7.2). Images from the camera were pre-warped to eliminate lens distortion. A 15x15° region-of-interest (ROI) (based on a conservative retinal projection of the electrode array[9]) was sampled from each frame to be rendered as a phosphene image and presented on the headset display to the left eye only. The subject could redirect the camera axis by moving their head. Phosphene rendering latency was 50ms and the display refresh rate was 90 Hz, yielding latencies between 50-61 ms for the display to reflect a change in camera image.

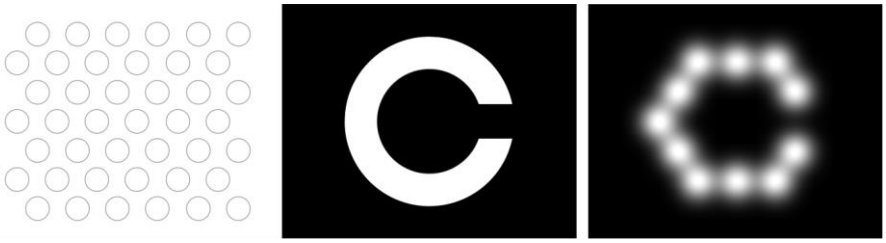

Figure 7.1: Phosphene rendering for simulated prosthetic vision using the abstract model described by McCarthy et al (2014).[137] (Left): electrode layout. (Centre): input image. (Right): phosphene rendering produced by sampling the input image at the electrode locations.

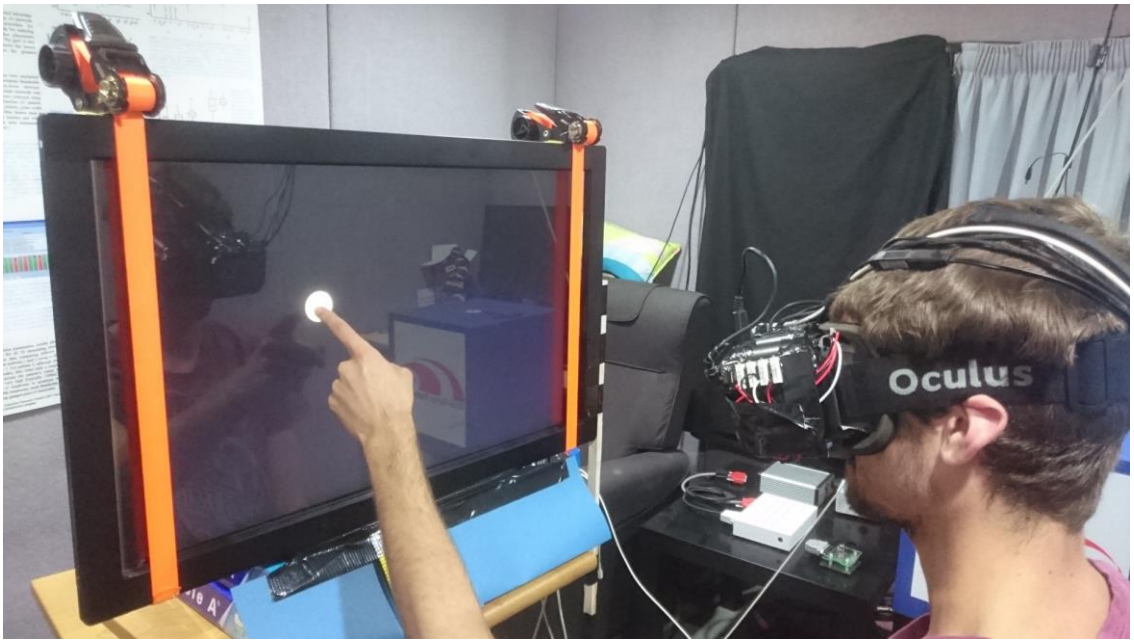

Figure 7.2: Experiment set-up. Targets were displayed on a 30-inch touchscreen at a viewing distance of 40cm. Subjects wore a simulated prosthetic vision headset that included a front-facing camera, head motion tracker, and eye tracker.

7.2.4. Tracking Eye and Head Position

An infrared eye tracker (Arrington Research, Scottsdale, AZ, USA) mounted inside the headset recorded the position of the left pupil at 60 Hz, to an accuracy of ±0.5°. Blinks and poor quality data points were identified and discarded based on a pupil size and shape criterion reported by the eye tracker software. A 16-point fixation target calibration procedure mapped pupil locations within the eye tracker camera image to pixel locations on the headset display. The location of the natural gaze origin relative to the headset display was estimated post-hoc for each subject from the distributions of measured eye azimuths and elevations during the stimulus-absent periods between experiment trials. Gaussian curves were fitted to the two distributions, and the gaze angles at the peak of each curve were taken as the natural gaze origin. Then, using the known geometry of the headset, gaze locations in pixel coordinates were transformed to degrees of visual arc relative to the natural gaze origin in a head-centred coordinate system. The combined eye azimuth (θ) and elevation (ϕ) are referred to as the "gaze angle". Figure 7.3 illustrates the calibration process.

A motion tracker (trackSTAR, Ascension Technology Corp, Shelburne, VT, USA) on the headset recorded head position and bearing at 20 Hz. By accounting for the instantaneously measured head position the locations of real-world objects were also expressed in the head-centred coordinate system, allowing for direct comparison between eye position and world locations.

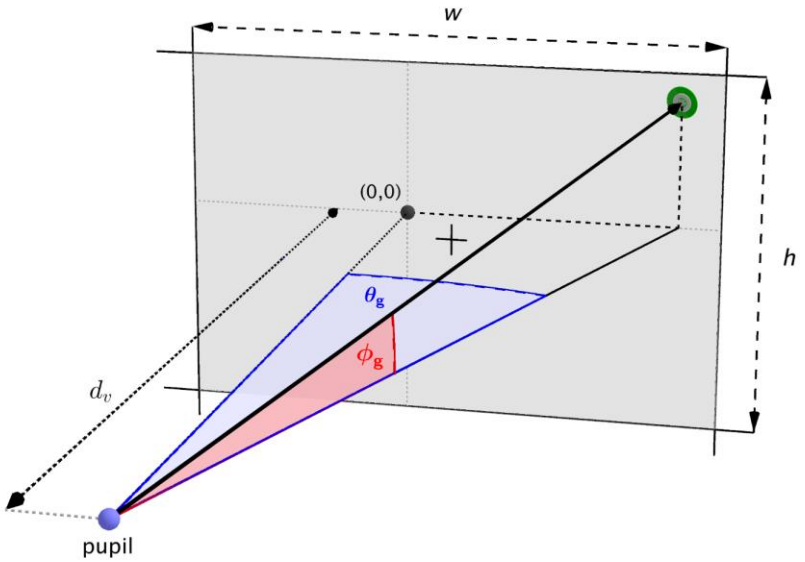

Figure 7.3: Eye tracker calibration. The subject was required to fixate on a series of calibration targets (green) on the headset display. The heavy black line shows the direction of gaze. The eye tracker software produced a calibration that mapped the pupil location to headset display pixel coordinates. Then, by using the known screen geometry (display width, w; display height, h; viewing distance, dv) and estimated gaze origin (0,0), gaze locations in pixel coordinates were transformed to azimuth (ϑ_g) and elevation (φ_g) angles in a head head-centred coordinate system relative to the natural gaze origin. The black plus indicates the centre of the display, which was not necessarily aligned with the natural gaze origin. Real-world locations were expressed in the same head-centred coordinate system by accounting for the instantaneous measured head position.

7.2.5. Phosphene Movement Conditions

The simulator could optionally use eye position measurements in a closed loop configuration to retinally stabilise the phosphenes. Additionally, the input image sampling region-of-interest (ROI) could be shifted in parity with the measured gaze angle (gaze compensation). Three conditions were tested:

1) **Uncompensated:** modelled a retinal implant without gaze compensation. Phosphenes were retinally stabilised and the camera image ROI remained fixed in the centre of the image. Head scanning was the only means of directing the field of view, and eye movements could introduce camera-gaze misalignments.
2) **Gaze-compensated:** modelled a retinal implant with gaze compensation. Phosphenes were retinally stabilised and gaze compensation was applied to continuously transpose the input image sampling ROI. The camera image was mapped to the headset display such that the centre of the image corresponded to the centre of the display. Head scanning and eye scanning could both be used to direct the field of view.
3) **Centre-fixed:** a control condition is which the phosphenes never moved. The phosphene array and input image sampling ROI remained fixed in the centres of the headset display and the camera image respectively, regardless of any eye movement. Subjects were able to foveate on any part of the field of view; however, eye movements did not cause the phosphene array shift relative to the camera image. Head scanning was the only method of directing the field of view.

The latency for the phosphene display to respond to an eye movement ranged from 52-80ms (60Hz eye tracker acquisition + 2ms eye tracker processing latency + 50ms phosphene rendering + 90Hz display refresh), which may have been perceptible as a slight lag in response.

7.2.6. Target Localisation Task

Subjects wore the prosthetic vision simulator and sat 40 cm in front of a touchscreen monitor in a darkened room. The monitor (Dell U3011) measured 30 inches diagonally with a 16:10 aspect ratio, equating to a field of view of 78°x54°. Subjects were free to move their heads but were encouraged not to move their upper bodies so as to maintain a constant distance to the monitor. In each trial of the task, a single stationary white circular target with a diameter of 5° appeared in a random location on the monitor, restricted to the central 52°x34° region, against a black background. The appearance of the target was accompanied by an audio tone that signalled the start of the trial. Subjects were instructed to search for the target and touch it with a finger of their dominant hand to the best of their ability with no restriction on time, and were permitted to rest their non-dominant hand on the table to orient themselves throughout the task. A different audio tone signalled when a touch had been successfully registered by the touchscreen monitor, ending the trial. Figure 7.2 shows the experiment set up.

One of the three simulator conditions (uncompensated, gaze-compensated, or centre-fixed) was selected at random for each trial. Subjects were not briefed on the parameters of the different conditions. Trials were executed in blocks of 10, and before each block an eye tracker slip-correction sequence, in which the subject briefly fixated a single calibration target, was executed to account for any relative movement between the eye tracker camera and the subject's eye. The touch location, target location, response time, and the eye and head positions during the trial were recorded. Subjects could stop or request a break at any time and breaks were enforced after each 100 trials. Prior to beginning the experiment, subjects performed 3-10 trials using normal vision to familiarise themselves with the task. The primary stopping condition was 240 trials in total and at least 50 trials in each condition. In a debriefing session following the experiment, subjects were asked to describe any strategies they had used in the task.

7.2.7. Data Analysis

The primary measure of performance on the task was the pointing error, which characterised hand-eye coordination. Pointing error was measured in degrees of visual arc between the centre of the circular target and the location touched by the subject. This enabled direct comparisons between the gaze angle, target, and touch in a common head-centred coordinate system relative to the natural gaze origin (Figure 7.3). The gaze angle at the time that the subject touched the screen is referred to as the "response gaze".

Task performance, measured in terms of pointing error and response time, was compared between simulator conditions using two-way ANOVAs with subject and condition as factors. We then examined the relationship between response gaze and pointing error in terms of magnitude and directionality to determine whether eccentric gaze was correlated with poor performance in the gaze-compensated and uncompensated conditions. Finally, the distribution of eye positions recorded during the experiment was examined to quantify the typical range of eye movements during the localisation task.

The centre-fixed condition was used as a control for any systematic biases in pointing error, since phosphenes were stationary and eye position was not expected to affect pointing error in this condition. Two sources of bias were considered:

1) Gaze offset bias: Any offset between the natural gaze origin and the centre of the headset display, which was mapped to the centre of the camera image, introduced a constant displacement between the percept (as seen by the subject) and the target. The gaze offset bias existed only in the centre-fixed and gaze-compensated conditions, because in the uncompensated condition the centre of the camera image was mapped to the fovea rather than to any particular area of the headset display.
2) Open-loop pointing bias: arises from the lack of visual feedback with which to guide the pointing motion,[204] as well as from the spatial separation between the image sensor and the headset display. This bias is likely to be present equally in all three conditions as it is intrinsic to the individual subject and to the physical dimensions of the simulator apparatus.

Assuming a 1:1 correlation between gaze offset and pointing error, the gaze offset bias is equal to the visual arc between the natural gaze origin and the display centre. This value was subtracted from the recorded touch location for each trial in the centre-fixed and gaze-compensated conditions only. The remaining systematic bias in the centre-fixed condition is attributed to open-loop pointing bias and was subtracted from the recorded touch locations in all conditions. All pointing errors presented have been treated in this way unless otherwise stated.

7.3. Results

All subjects were able to complete the task, and each subject performed between 57 and 89 trials under each condition. Figure 7.4 shows an example result from a single trial for subject S6 in the uncompensated condition.

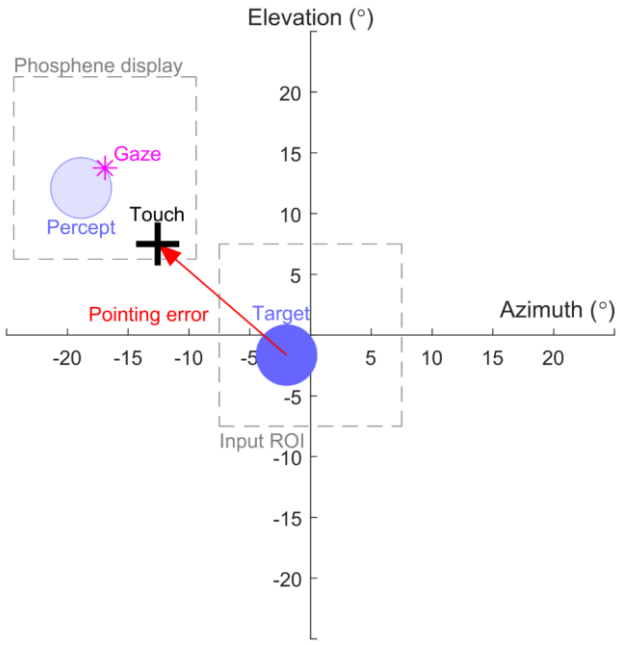

Figure 7.4: Results from a single trial for subject S6 in the uncompensated condition. The input image region-of-interest is sampled from a central location while the phosphene display appears at the gaze location. The location of the 5 degree target (dark blue circle), the location touched by the subject (black plus symbol), the gaze location (magenta star), and the location of the percept representing the target (transparent blue circle) are all expressed in degrees of visual arc in the head-centred coordinate system. The pointing error (red arrow) is measured between the target location and the touch location. Note the percept of the target has moved in parity with the subject's gaze resulting in a pointing error in the direction of the percept despite the camera being pointed towards target.

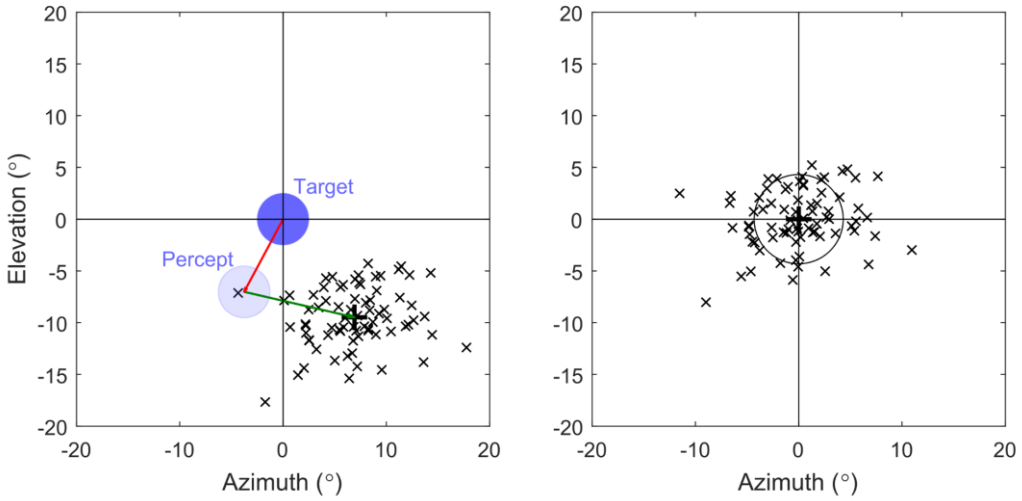

Figure 7.5: Systematic bias in pointing error for subject S3 in the centre-fixed condition. (Left): touch locations relative to the target location (black crosses, with centroid indicated by the black plus symbol) are biased downward and rightward of the target. The bias is composed of gaze-offset bias (red arrow), caused by the misalignment between the fixed phosphene array and the gaze origin, and open-loop pointing bias (green arrow). (Right): Pointing error for the same subject with bias subtracted.

7.3.1. Systematic bias in pointing error

Figure 7.5 demonstrates systematic bias in pointing error for subject S3 in the centre-fixed condition, showing the separate contributions of gaze offset bias and open loop pointing bias. Among the cohort, gaze offset magnitudes ranged 3.3-15.9° degrees, open-loop pointing bias magnitudes ranged 9.6-14.7° degrees, and total bias magnitudes ranged 4.9-17.6°.

7.3.2. Performance Measures

The data for pointing error across conditions and subjects were heteroscedastic and had non-normally distributed residuals. For analysis of pointing error we performed a rank transform in conjunction with Welch's ANOVA, which does not assume homoscedasticity and is insensitive to non-normality for large sample sizes.[205] A separate Welch's ANOVA was performed for each subject using a Bonferroni-adjusted alpha level (α=0.05/7, or 0.007) and the Games-Howell procedure for multiple comparisons. For six out of seven subjects, pointing error magnitude (Figure 7.6) was significantly greater in the uncompensated condition than the gaze-compensated and centre-fixed conditions (S1 $p<0.05$; S2, S3, S5, S6, S7 $p<0.001$). No significant difference was detected between the gaze-compensated and centre-fixed conditions for any subject except S6, for whom the centre-fixed condition resulted in a larger pointing error ($p<0.003$).

The mean pointing error across all subjects after correcting for systematic bias was 6.6±0.2° in the gaze-compensated condition, 6.7±0.2° in the centre-fixed condition, comparable to 5.0±1.6° for simulated ultra-low vision subjects reported by Endo et al (2016).[204] Mean pointing error in the uncompensated condition across all subjects was 12.1±0.3°. A previous study in simulated prosthetic vision reported higher mean pointing error for gaze-compensated and uncompensated viewing, possibly because they had not corrected for bias in pointing (Hozumi et al. IOVS 2016; ARVO E-Abstract 1958).[201]

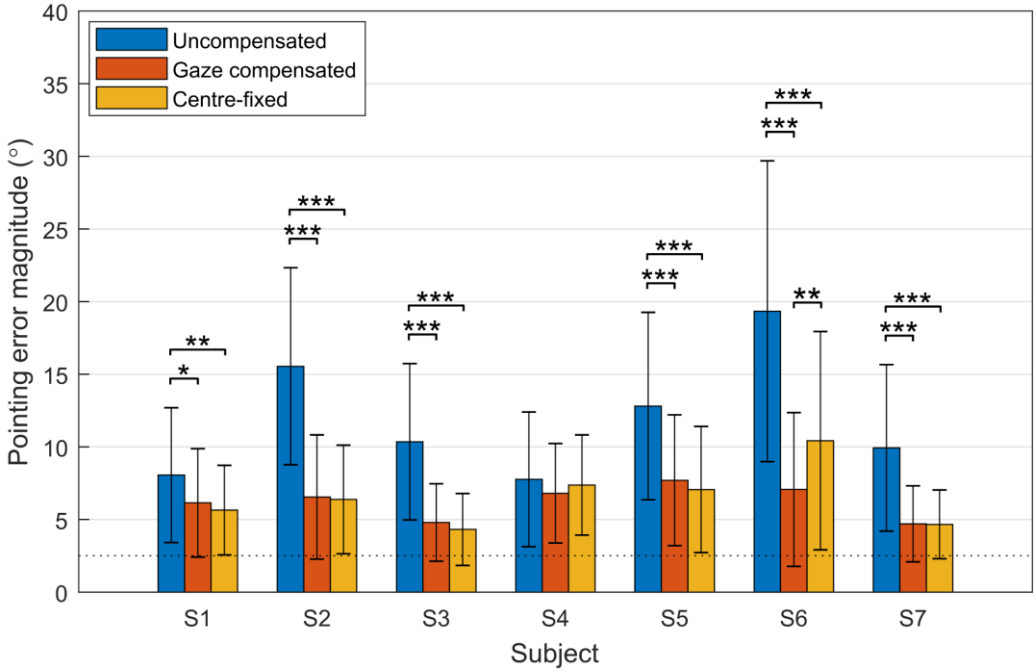

Figure 7.6: Mean pointing error magnitude in each condition for each subject. Error bars show standard deviations, asterisks denote a significant difference between two conditions (single asterisk: p<0.05; double asterisk: p<0.01; triple asterisk: p<0.001), and the dashed line indicates the radius of the target. Pointing error was significantly greater in the uncompensated condition than in the gaze-compensated and centre-fixed conditions for six out of seven subjects. A significant difference between the gaze-compensated and centre-fixed conditions was observed only for S6.

Response times varied from 0.85-109.05 seconds. There was a significant effect of condition on response time for subject S1 only (Separate Welch's ANOVAs on ranks for each subject with Bonferroni correction and Games-Howell's multiple comparisons procedure); S1 had significantly shorter response times in the centre-fixed condition than in the gaze-compensated ($p<0.001$) and uncompensated ($p<0.001$) conditions. Welch's ANOVA was selected because the data were heteroscedastic and has non-normally distributed.

7.3.3. Eccentric Gaze as a Confounding Factor

Our second hypothesis stated that the larger pointing error in the uncompensated condition was specifically attributed to non-central gaze. We investigated this by testing correlation between pointing error and response gaze for the gaze-compensated and uncompensated conditions using least-squares linear regression analysis (Figure 7.7). Data from all subjects were analysed collectively. The azimuth and elevation were analysed separately to preserve both the magnitude and directionality of the pointing error vector. Although the residuals were found to be non-normally distributed in all four cases, linear regression is robust against non-normality, particularly with large sample sizes.

In the uncompensated condition, there was a moderate correlation between gaze and pointing error in both dimensions (Figure 7.7A, azimuth: $R2=0.47$, slope=0.79, $p<0.001$; Figure 7.7B, elevation: $R2=0.51$, slope=0.67, $p<0.001$), with the pointing error smallest when gaze was central and largest when gaze was eccentric. In the gaze-compensated condition, there was a statistically significant but extremely weak correlation between the response gaze azimuth and pointing error azimuth (Figure 7.7C, azimuth: $R2=0.01$, slope=0.08 $p<0.05$), and no significant correlation in the elevation dimension (Figure 7.7D, elevation: $R2=0.00$, slope=0.01, $p=0.72$).

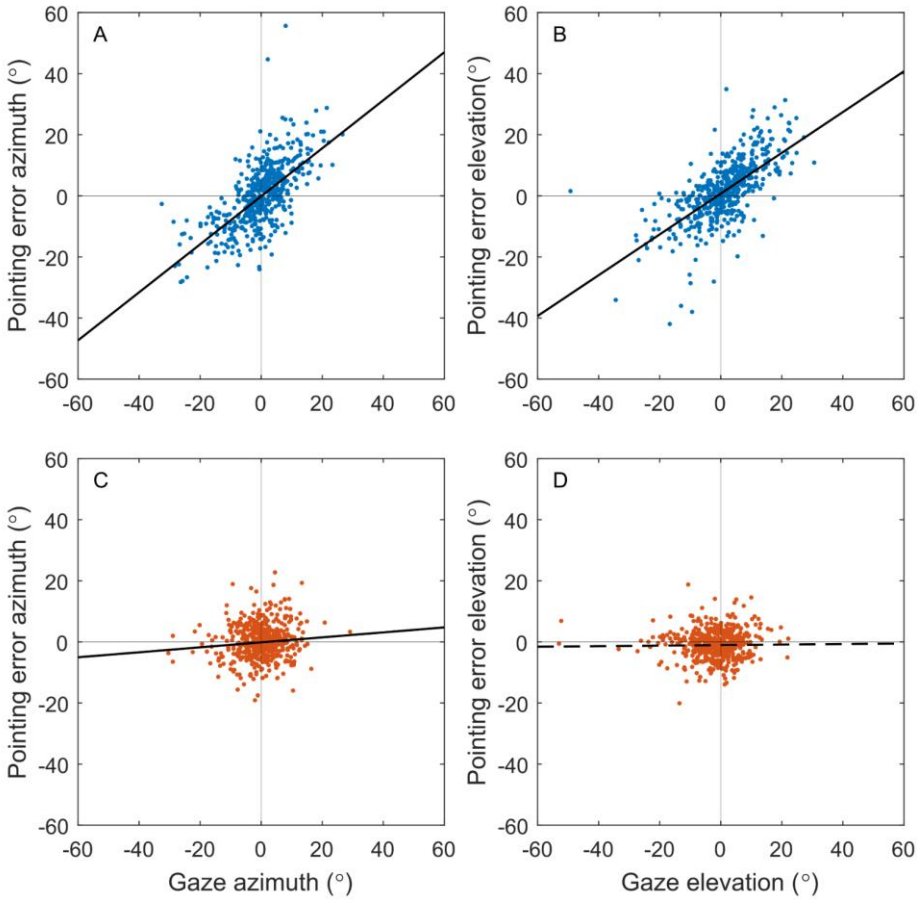

Figure 7.7: Pointing error against response gaze for the uncompensated condition (top row) and the gaze-compensated condition (bottom row). The azimuth dimension (left column) is analysed separately from the elevation dimension (right column). Data are aggregated across all subjects. Solid black lines indicate significant linear trends (p<0.05), and dashed black lines indicate insignificant trends.

As a secondary measure, the correlation between the vector angles of response gaze and pointing error was tested using circular correlation analysis as described by Jammalamadaka et al (2001)[206] and implemented in the CircStat toolbox for Matlab.[207] This method purely examines directional information, discarding magnitude. All error-free trials (i.e. touch point within target boundary, 2.5° from target centre) were excluded. A significant correlation between the directionalities of gaze and pointing error was observed in the uncompensated condition (Jammalamadaka's r=0.58, p<0.001) but not the gaze-compensated condition (r=-0.00, p=0.93).

7.3.4. Scanning Strategies

After completing the task, four subjects, S1, S2, S4, and S5, reported that they primarily used head-scanning while attempting to keep their eyes fixed centrally. For S1, S2, and S4 this was because they had noticed that the percept was moving in response to their eye movements, while S5 could not articulate a reason. S3, S6, and S7 reported using head and eye scanning in conjunction. The distribution of response gazes in the uncompensated condition is plotted for each subject in Figure 7.8. Each point represents the gaze at the time of response for a single trial, and the variability of the distribution is characterised by the mean distance from the centroid, V. Greater variability was correlated with greater difference in average pointing error between the centre-fixed and uncompensated conditions (R2=0.64).

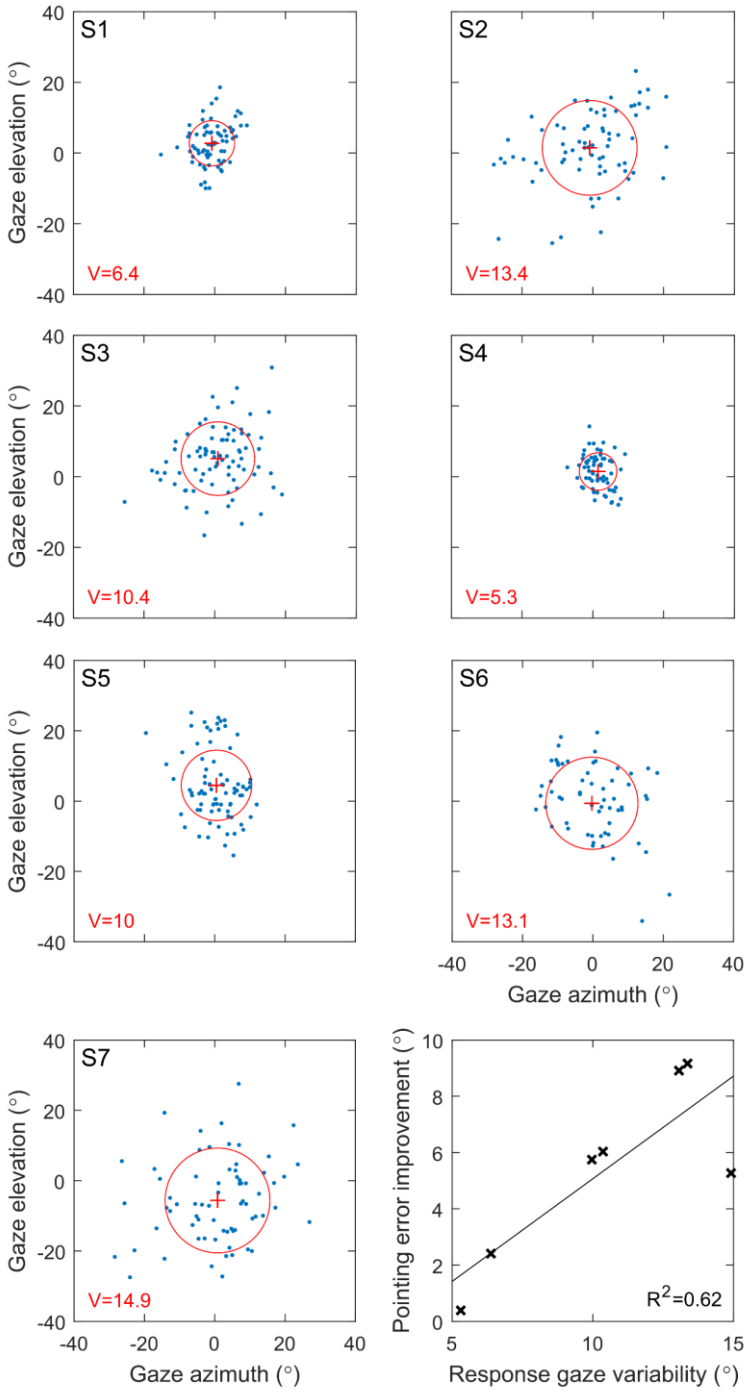

Figure 7.8: Greater variability in uncompensated response gaze is correlated with larger reduction in mean pointing error when comparing the centre-fixed condition to the uncompensated condition. Panels S1-S7 show the gaze position at time of response for trials in the uncompensated condition for each subject, with the centroids denoted by red plus symbols. The variability of the distribution (red circle) is characterised by V, the mean distance from the centroid. Bottom right: Difference in mean pointing error between the centre-fixed and uncompensated conditions versus the response gaze variability in the uncompensated condition for each subject.

7.3.5. Range of Eye Movements Required During Gaze Compensation

A gamma function was fitted to the distribution of eye position magnitudes for all eye position recordings made during trials in the gaze-compensated condition. Data from all subjects was analysed collectively. Based on the CDF of the fitted distribution, ninety five percent of the measured eye positions were within 24.44° of the natural gaze origin.

7.4. Discussion

The present study tested the effectiveness of gaze compensation in improving hand-eye coordination in a target localisation task under simulated prosthetic vision. Gaze compensation significantly reduced pointing error in six of the seven subjects when compared to the uncompensated condition. Further, pointing error in the gaze-compensated condition was similar or better for all subjects when compared to that in the centre-fixed condition in which phosphenes did not move. The gaze at the response time was found to be predictive of the direction of pointing error, and more eccentric gaze was predictive of higher magnitude pointing error. These results strongly suggest that non-central gaze impeded coordination in the uncompensated condition by misrepresenting the location of the target and biasing pointing direction towards the gaze point.

Four of the seven subjects reported that they primarily relied on head scanning and attempted to confine their gaze to the central region. This strategy is the same as the standard instruction given to Argus II recipients to minimise the incidence of camera-gaze misalignments. Interestingly, the subject with the least variability in response gaze (S4, Figure 7.8) was the same subject for whom the pointing error did not depend on the condition tested. This can be attributed to a floor effect; eye movements were suppressed sufficiently well that any negative effect of gaze on coordination was beneath the noise floor. The remaining six subjects were less successful in suppressing eye movement and all benefited from gaze compensation. Further, greater variability in response gaze was correlated with greater reduction in pointing error in the gaze-compensated condition compared to the uncompensated condition. This result highlights the importance of suppressing eye movements in prosthetic vision; however, it is notable that the majority of subjects were unsuccessful in supressing eye movement. This observation is in agreement with the existing literature, which reports that even experienced retinal implant recipients have difficulty supressing eye movement.[142,208] In contrast, gaze compensation provided coordination comparable to the centre-fixed condition for all subjects with no training or suppression of eye movement required. The findings provide motivation for the integration of eye trackers into visual prosthesis devices for gaze compensation.

7.4.1. Response Time

McIntosh (2015) reported that subjects were faster at a visual search task when gaze compensation was used,[146] while Sabbah et al (2014) reported that patients implanted with the Argus II often made a series of time-consuming compensatory head and neck movements to resolve camera-gaze misalignments before reaching for an object.[142] In contrast, the present study showed significantly decreased response times in the gaze-compensated condition for only one of seven subjects. Two aspects of the experiment design may have contributed to this. First, subjects were not briefed on the simulator conditions or told which condition was active at any time. Second, there was no visual or tactile feedback with which the subject could gauge

their pointing accuracy. Thus the subjects had no opportunity to develop compensatory techniques for any specific condition.

7.4.2. Gaze Correlated with Pointing Error

Previous studies have revealed that a relationship between eye movement and pointing error exists,[98,142] but to our knowledge the present study is the first time that relationship has been quantified. Interestingly, the linear correlations that were observed between gaze and pointing error in the uncompensated condition had gradients less than one (Figure 7.7). In other words, pointing error was on average less eccentric than gaze, even though the percept was displaced by an amount equal to the gaze angle. This is in agreement with Endo et al (2016), who reported that "low vision subjects tended to touch more toward the central side of the target".[204]

7.4.3. Limitations of Simulated Prosthetic Vision

The prosthetic vision simulation paradigm used in this study was idealised compared to present visual prostheses. In particular, the simulated phosphenes were uniform in shape and layout, unlike the phosphenes elicited by stimulation of the retina which are known to be irregular in size, shape, and layout.[9] It is therefore likely that the resolution of the simulated prosthetic vision was higher than that of present devices. However, the optotypes used in the task were relatively large and simple, and subjects were not required to resolve any particular detail of the optotype, only to detect its presence and location. We should also consider that practised implantees might possess a certain level of intuition in interpreting phosphenated vision that was not available to the normal-sighted subjects in this study, and that additional confounding factors (such as irregular phosphenes) might have obscured the result while being only tangential to the hypothesis. The results are consistent with findings in actual prosthesis recipients (Caspi et al. IOVS 2017; ARVO E-Abstract 4192)[149] and simulated prosthetic vision (Hozumi et al. IOVS 2016; ARVO E-Abstract 1958),[201] and we therefore find it unlikely that the uniform phosphenes of the simulator imparted any significant advantage. The findings of this simulation study are also likely to extend to future high resolution devices.

7.4.4. Implementation of Gaze Compensation in Visual Prostheses

Selecting the correct region of the image to display to the patient requires accurate calibration of the eye tracker and consideration of the surgical placement of the electrode array, which may be eccentric from the fovea. Typical fixation target eye tracker calibration routines are inaccessible to visual prosthesis patients, who lack foveation, so unconventional calibration techniques are necessary. Caspi et al (2017)[98] demonstrated a calibration routine for retinal implants whereby patients repeatedly placed a visual marker at arm's length to indicate the location of a percept. The authors solved for the calibration coefficients and the retinotopic placement of the electrodes by assuming a 1:1 correlation between gaze displacement and the eccentricity of the marked location.

The notion that pointing tasks can be a useful tool for eye tracker calibration is supported by the linear relationship between gaze and pointing error presented in this study; however, pointing error was on average smaller than gaze eccentricity (Figure 7.7, uncompensated condition: gradients < 1). It follows that a calibration dependent upon patients pointing to a percept may underestimate gaze angles. Other biases in pointing direction may also affect the calibration, such as the downward and lateral bias in open-loop pointing that exists in normal vision[204] and

in artificial vision.[142] The role of pointing in calibration could be minimised by instead requiring patients to move their eyes so as to align the percept with a tactile target, though the accuracy of such eye movements and the ease with which they can be executed has, to our knowledge, not been addressed in the literature. Passive calibration procedures that determine the geometry of the eye without requiring cooperation from the patient may also be useful.[209]

A second consideration for the clinical implementation of gaze compensation is that the range of measurement of the eye tracker should sufficiently encompass the normal range of movement of the eye. Gaze was found to be within 24.44° of the natural gaze origin 95% of the time during gaze-compensated viewing. Therefore, a range of measurement of ±25° would be a reasonable minimum specification for an eye tracker for retinal implants. This is within the specifications of modern video based eye trackers.[210] Kanda et al have demonstrated tracking the rotation of the eye by measuring stimulus artefact through electrodes implanted in the canthus, but did not report the range of measurement of their system (Kanda et al. IOVS 2017; ARVO E-Abstract 4188).[211] It should be noted that eye movements are known to be partly driven by visual stimulus,[14,212] and patients with RP are known to exhibit different oculomotor behaviour in certain tasks when compared to normal sighted subjects.[155,157,158] Therefore, in practice the range of eye movement of a visual prosthesis recipient may differ from that observed here. It may also be possible that horizontal range of measurement is more valuable than vertical range of measurement in realistic scenarios in which horizontally arranged visual information and horizontally moving objects are prevalent. Other considerations that may be important are the increased weight, power consumption, and processing latency that eye tracking apparatus would add to a visual prosthesis.

7.4.5. Conclusion

In conclusion, gaze compensation was effective in improving hand-eye coordination in a target localisation task. Eccentric gaze was found to be correlated with poor coordination under prosthetic vision simulation that modelled retinally stabilised phosphenes. The results emphasise the potential for eye trackers to improve patient outcomes in prosthetic vision.

Chapter 8

A preliminary investigation of gaze compensation in a 44-channel suprachoroidal retinal prosthesis

Purpose: The preceding chapter demonstrated a confounding effect of eye movement on pointing accuracy and a benefit of eye tracker feedback (gaze compensation) in a target localisation task using simulated prosthetic vision. Two recently published studies have demonstrated a similar effect in epiretinal implant users. This pilot study aimed to extend those findings to subjects implanted with our 44-channel suprachoroidal retinal implant.

Methods: Four participants (P1-4) implanted with a 44-channel suprachoroidal retinal implant performed a target localisation task. A 10° square white target was presented at random locations on a 42" touchscreen, and participants were required to find it touch it with their index finger. Eye position of the implanted eye was tracked throughout the experiment. Pointing precision – defined as the spread of touch locations relative to the target after subtracting the mean – was compared between three conditions: System On (no eye tracker feedback), System Off, and Gaze Compensation. System On and System Off data was collected over several sessions between 17 and 96 weeks post-device-activation. Gaze Compensation data was collected in a single session for P2, P3, and P4, and is not available for P1. The correlation between pointing error and eye position was tested for eye position sampled at the touch time onset of electrical stimulation, and a third time-point selected for each patient based on the observed head scanning behaviours.

Results: Pointing precision was significantly improved (reduced) for System On versus System Off in all four participants ($p<0.001$), indicating the device was useful for localisation. Contrary to expectations, the correlation between pointing error and eye position was not statistically significant and extremely weak for all four participants (least-squares linear regression, highest $R^2=0.18$) regardless of the time-point at which the eye position was sampled. Gaze Compensation did not lead to improved performance in any of the participants. Significant methodological differences were identified between this study and the existing literature that may explain this result.

Conclusion: In this preliminary investigation, eye position was not correlated with pointing error, which was unexpected based on previous reports from an epiretinal implant. Several methodological issues were identified and further investigation is required to properly determine a possible effect of eye position on localisation in the suprachoroidal retinal prosthesis.

8.1. Introduction

The study presented in Chapter 7 investigated the effects of eye-camera misalignments in simulated prosthetic vision in a target localisation task. It was found that eye position was correlated with pointing error, with more eccentric eye positions associated with worse accuracy. Using eye tracker feedback to update the sampling region of the head mounted camera ("Gaze compensation") was shown to improve performance on the task by eliminating the misalignment between eye position and camera angle. Following the publication of the study in Chapter 7, similar findings were twice reported in Argus II recipients[179,213], and a separate study in Argus II recipients provided further evidence for the relationship between eye movement and percept movement.[98]

This chapter describes a preliminary study in which we took a first step towards extending the findings of Chapter 7 (and similar studies in Argus II recipients) to subjects implanted with a 44-channel suprachoroidal retinal prosthesis. Using similar analyses to Chapter 7, we investigate the relationship between pointing error and eye position at the time of pointing. However, we also investigate the effect of eye position at other points during the task, as a recent phosphene mapping study in Argus II recipients demonstrated that eye position at stimulus onset, rather than at the time of pointing, was more important in determining the percept location in that particular task.[98] Additionally, an implementation of gaze compensation was tested and its effect on performance in the target localisation task was studied.

8.2. Methods

8.2.1. Participants

Four participants (P1-4) with end-stage retinitis pigmentosa took part in the study. The participants were each unilaterally implanted with a 44-channel suprachoroidal retinal implant (described in Section 3.1.2) in the eye with least residual vision (P1, P2, P4: right eye; P3: left eye) as part of a longitudinal clinical trial (NCT01603576). Device 'switch-on' and lab-based training began approximately eight weeks after post-operative recovery. The participants performed a target localisation task as part of a suite of lab- and home-based assessments at 17, 20, 32, 44, 56, 68, 80, and 92 weeks post switch-on. Data is not available for P1 beyond week 56, or for P3 and P4 beyond week 68. In addition to these regular outcome measures, P2, P3, and P4 also participated in an additional session to test the effect of eye tracker feedback on performance on the task (P2: week 17; P3: week 16; P4: week 15).

8.2.2. Target localisation task

Square white targets (width 10°) were presented against a black background on a 42" touchscreen monitor viewed at a distance of approximately 45cm. In each trial a single target appeared at a random location on the monitor, confined to a central square region measuring

19” diagonally, accompanied by an auditory tone at presentation onset. The participant was required to search for the target and attempt to touch it with their finger. A second auditory tone signalled the successful detection of the participant’s finger on the touchscreen, ending the trial. No other feedback was given. Eye and head movement were monitored throughout the task.

Participants performed the task with the retinal implant in normal operation (‘System On’ condition), with stimulation disabled (‘System Off’ condition), and in a third condition in which the spatial information of the stimulation was scrambled (’Scrambled condition’, described in previous work[154]). The Scrambled condition was excluded from all analyses as it is not relevant to the present study. In each session 3 blocks of 8 trials were completed in each of the three conditions on a balanced-random schedule. P2, P3, and P4 also participated in an additional session comparing System On performance to a fourth condition in which eye tracker feedback was used to adjust the camera field-of-view in real time (’Gaze compensation’ condition). The participants were instructed that there would sometimes be no phosphene input (System Off condition), but were not alerted to the inclusion of the Gaze Compensation condition.

Several practice runs of the task were executed at the beginning of each session in order to optimise the camera alignment, as previous studies have demonstrated that camera misalignment can introduce bias in localisation tasks.[123] If any systematic bias in the indicated versus actual target location was observed then the sampling region within the camera field of view was adjusted to minimise the observed bias. Data collected during this process was not included in any analyses.

Pointing error, the distance between the centre of the target and the point touched by the participant, was expressed in degrees of visual arc using the measured position of the head relative to the monitor at the moment the subject touched the screen. Camera misalignment can introduce pointing error bias,[17,98,123,179] therefore to enable comparison between different sessions and video processing strategies the mean pointing error was subtracted from all pointing error measures within each session and condition. The primary measure of performance on the task was the pointing precision – the mean vector magnitude of each pointing error measure after subtracting the session mean.

8.2.3. Eye and head tracking

Eye position was monitored using a head-mounted video-oculography system (Arrington Research, AZ, USA). As it was not possible for blind subjects to perform the calibration routine (see section 3.2) the system was configured to output the raw uncalibrated position of the pupil within the camera image at 60Hz, with (0, 0) representing the bottom left corner and (1, 1) representing the top-right corner of the image. However, a calibrated eye position measurement was necessary for gaze compensation, therefore, in one session per participant a proprioceptive calibration technique was employed. The visual calibration targets were replaced by tactile markers, which the subject attempted to foveate using their sense of proprioception. As this procedure was time-consuming, the calibration procedure was only carried out when gaze compensation was to be used. To account for possible differences in the position of the eye-facing cameras between sessions the pupil-in-image position was normalised by subtracting the median pupil position during the session. If the eye-facing camera position was knocked or

adjusted during a session then the data before and after the adjustment were treated separately. Head position and bearing relative to the monitor was measured at 20Hz using a magnetic motion tracker (Ascension Technology Corporation, VT, USA).

8.2.4. Gaze compensation

Gaze compensation was implemented by translating a sampling region around the scene-camera image in parity with the recorded angular eye position. This approach was only used during the single session per participant in which the proprioceptive calibration was attempted. The width of the scene camera field-of-view was 70° and the width of the sampling region was determined by the surgical positioning of the array and the projection on the retina of the subject's electrode configuration (e.g. Figure 3.3). Prior to commencing the task the sampling region within the scene camera field-of-view was aligned with the participant's estimated natural gaze origin by asking them to touch a tactile marker with their finger and fixate on their finger-tip with their eyes in a central position. The sampling region was then shifted so that the most foveal electrodes were aligned with the location of the finger within the camera image.

8.3. Results

8.3.1. Task performance

Touch locations relative to target locations per trial are presented for System On and System Off for each subject in Figure 8.1A-D, with the radius of the enclosing circles indicating the radius of pointing precision. Circles with centres offset from the origin signify systematic bias in pointing error due to camera alignment or open loop pointing error (no visual feedback of hand position during pointing). For example, in the System On condition P2 consistently pointed left of the target. Pointing locations for P4 System Off are strongly biased downward and rightward because this participant simply pointed to the lower right corner of the screen whenever he assumed there was no phosphene input.

Figure 8.1E compares pointing precision between System Off and System On for each participant. All four subjects had significantly more precise pointing in System On versus System Off (Kruskal-Wallis with Dunn's test for multiple comparisons, $p<0.001$). Mean pointing precision for P3 and P4 in System On was only slightly greater than the target radius of 5°. Figure 8.2 presents a similar analysis comparing System On and Gaze Compensation for the single additional session for P2-P4. For P2, pointing was significantly less precise in Gaze Compensation versus System On (Kruskal-Wallis with Dunn's method for multiple comparisons, $p=0.005$). For P3 and P4 there was no significant difference in pointing precision between System On and Gaze Compensation. There was no significant difference in response time between System On and Gaze Compensation for any subjects (Kruskal-Wallis with Dunn's test for multiple comparisons).

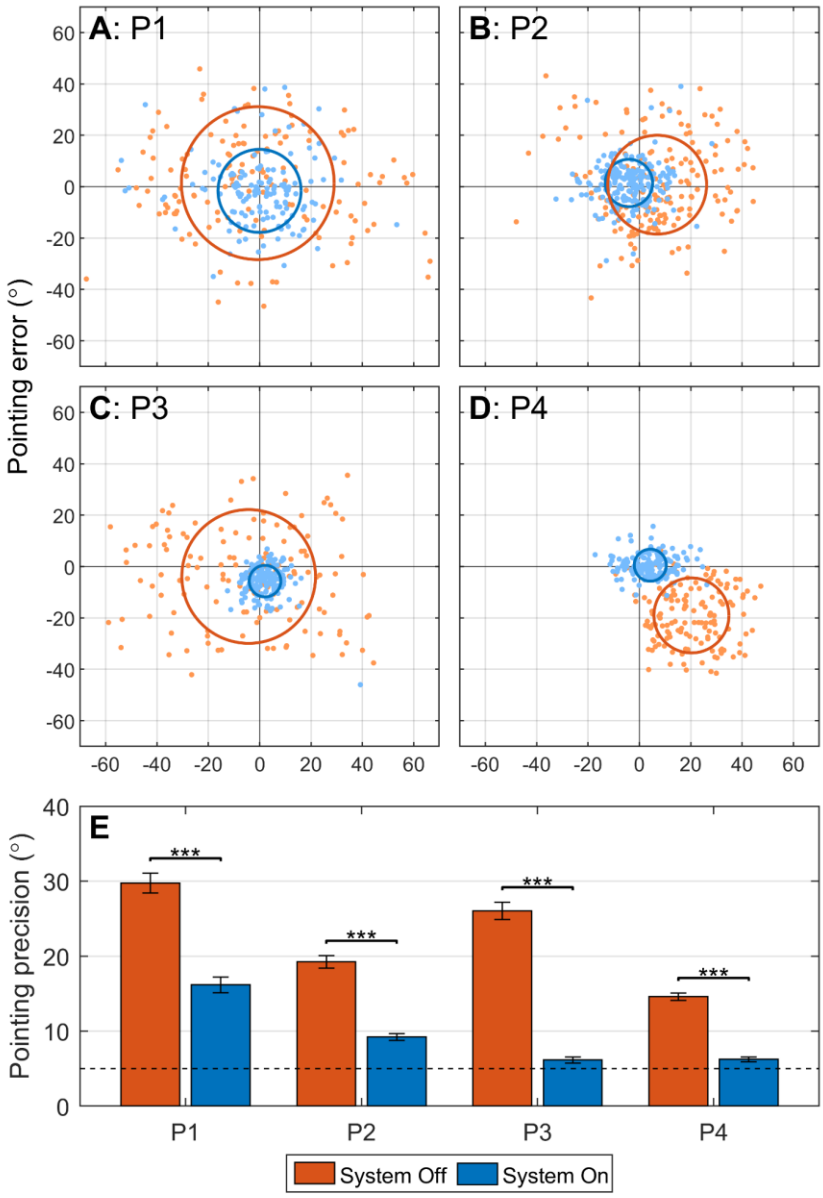

Figure 8.1: Comparison of pointing error in System Off (red) vs. System On (blue) in the target localisation task. Data was pooled across all sessions. (A-D): touch location relative to target centre for each participant. Dots represent raw pointing measurements (prior to subtraction of mean). Large circles are centred on the mean pointing error and have radii equal to the pointing precision. (E): Mean pointing precision (±s.e.m) in System Off and System On per subject. The dashed line at 5° indicates half the width of the target. Pointing precision smaller than 5° would indicate that the subject touched within the target on average (after subtracting bias). Pointing was significantly more precise in System On compared to System Off for all subjects (Kruskal-Wallis with Dunn's test for multiple comparisons, p<0.001).

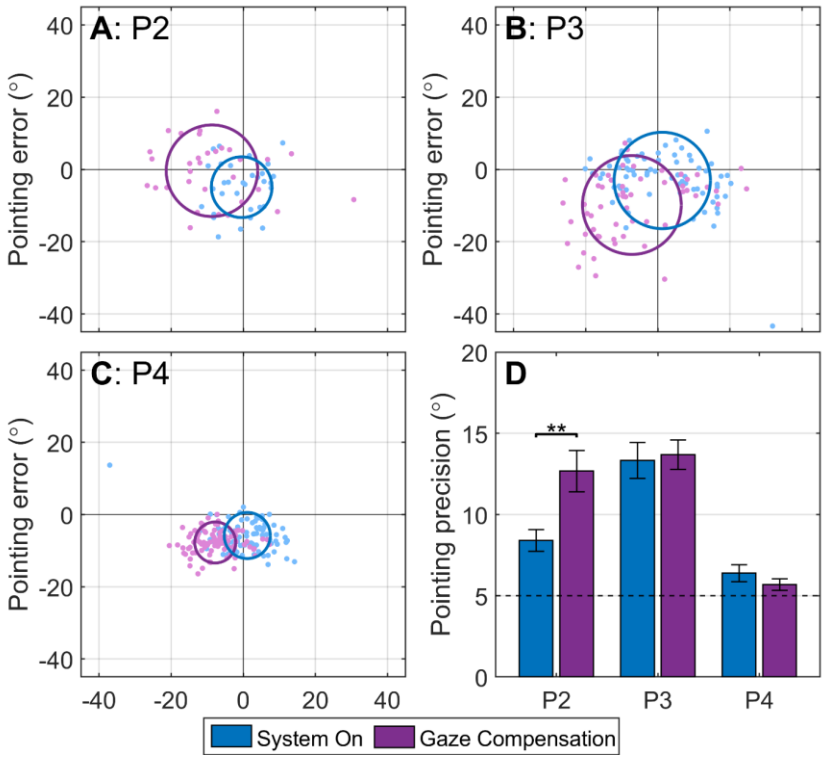

Figure 8.2: Comparison of pointing error in System On (blue) vs. Gaze Compensation (purple) in the target localisation task during a single session for each of P2, P3, and P4. (A-C): touch location relative to target centre for each participant. Dots represent raw pointing error measurements (prior to subtraction of mean). Large circles are centred on the mean pointing error and have radius equal to the pointing precision. (D): Comparison of pointing precision in System On versus Gaze Compensation for each subject. The dashed line at 5° signifies half the width of the target. Pointing precision smaller than 5° would indicate that the subject touched within the target on average (after subtracting bias). For P2 pointing precision was significantly less precise in Gaze Compensation versus System On (Kruskal-Wallis with Dunn's method for multiple comparisons, p=0.005). For P3 and P4 there was no significant difference in pointing precision between System On and Gaze Compensation.

8.3.2. Eye and head scanning strategies

In order to identify head scanning strategies, rotational head velocity (the change in azimuthal and elevational head bearing) over the course of each trial was calculated. Average rotational head velocity over all trials is plotted against time (relative to the time that the participant touched the display) for each participant in Figure 8.3. Systematic patterns of head movement behaviour were observed in all four participants. Generally, average rotational head velocity was constant until the final seconds of the trial, at which point average velocity began to decrease ('knee point' determined by a broken-stick fit and indicated by black dashed line). Figure 8.3 also displays a histogram of the time of the first stimulation in the trial for each participant. If there were multiple periods of stimulation during the trial (delineated by a gap of more than 500ms between consecutive pulses) then only the final period of stimulation was considered so as to exclude any errant stimulation that was not related to the target. In P3 and P4, the knee-point at which average rotational head velocity began to decrease is within 200ms of the most commonly occurring stimulation onset time. We took this 'knee point' to be synonymous with 'target detection', meaning that the participant had recognised the presence of the target and was terminating their search strategy prior to pointing.

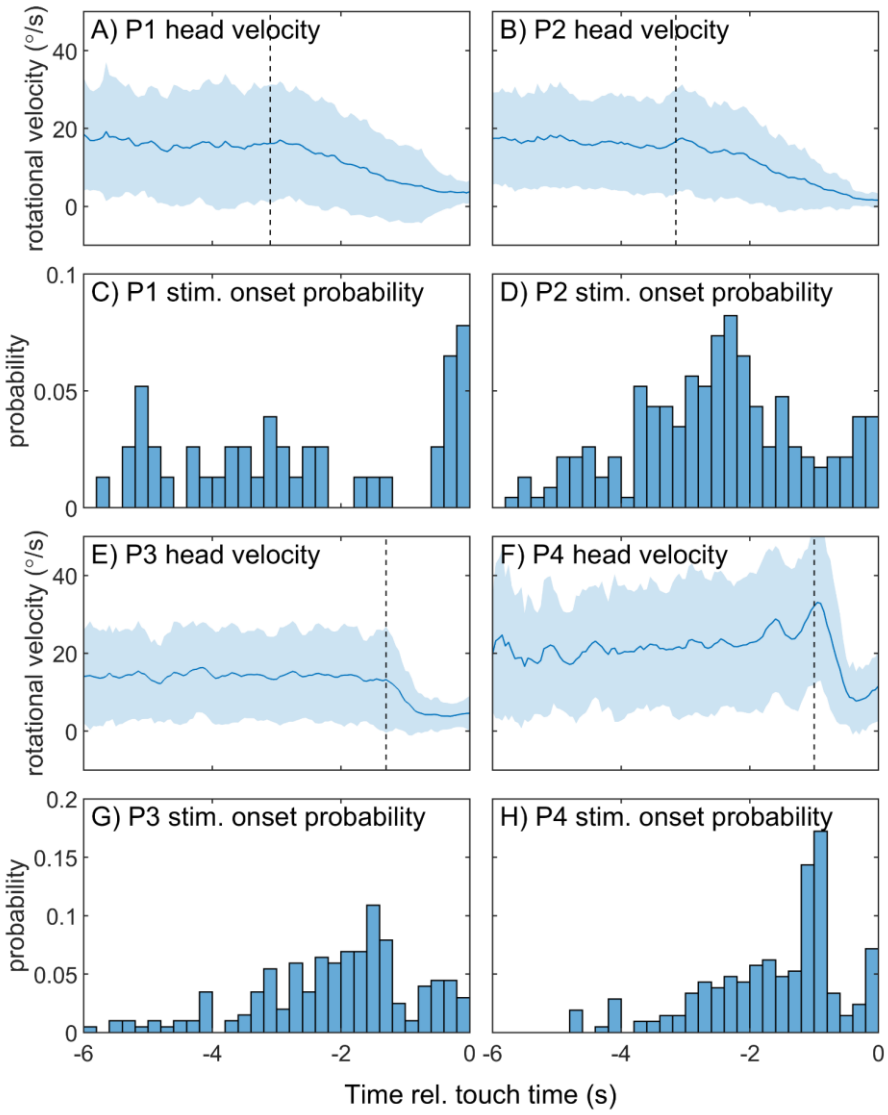

Figure 8.3: (A, B, E, F) Mean rotational head velocity (±s.d.) relative to the touch time for each participant. Only the six seconds immediately prior to the touch are plotted. For all four participants average rotational head velocity was constant throughout the trial until target detection (black dashed line, determined by a broken-stick fit). After target detection, average head velocity began to decrease. (C, D, G, H) Histograms showing the distribution of the time of onset of stimulation relative to the touch time for each participant.

All pupil positions recorded during trials in the Device On and Gaze Compensation conditions are shown for each participant in Figure 8.4. The solid line defines the confidence ellipse containing 95% of eye position samples. The area of the ellipse, specified in each panel, measures the variability in eye position for each condition, with a larger ellipse area indicating more variable pupil position, i.e. more eye movement. Variability in pupil position was similar (<20% difference) between System On and Gaze Compensation for P2, P3, and P4.

To determine whether the participants favoured foveal electrodes for localisation, the number of stimulation pulses delivered to each electrode was plotted against the electrode eccentricity relative to the fovea (Figure 8.5). In the System On condition, for all three participants the electrodes closest to the fovea received the highest proportion of stimulation pulses, and electrodes in the periphery received relatively few stimulation pulses. This indicates the

participants favoured the foveal phosphenes for localisation. This behaviour was also observed in Gaze Compensation for P3 and P4. In the case of P2, stimulation in the Gaze Compensation condition was evenly distributed across the entire electrode array, suggesting the absence of a foveation behaviour for this participant.

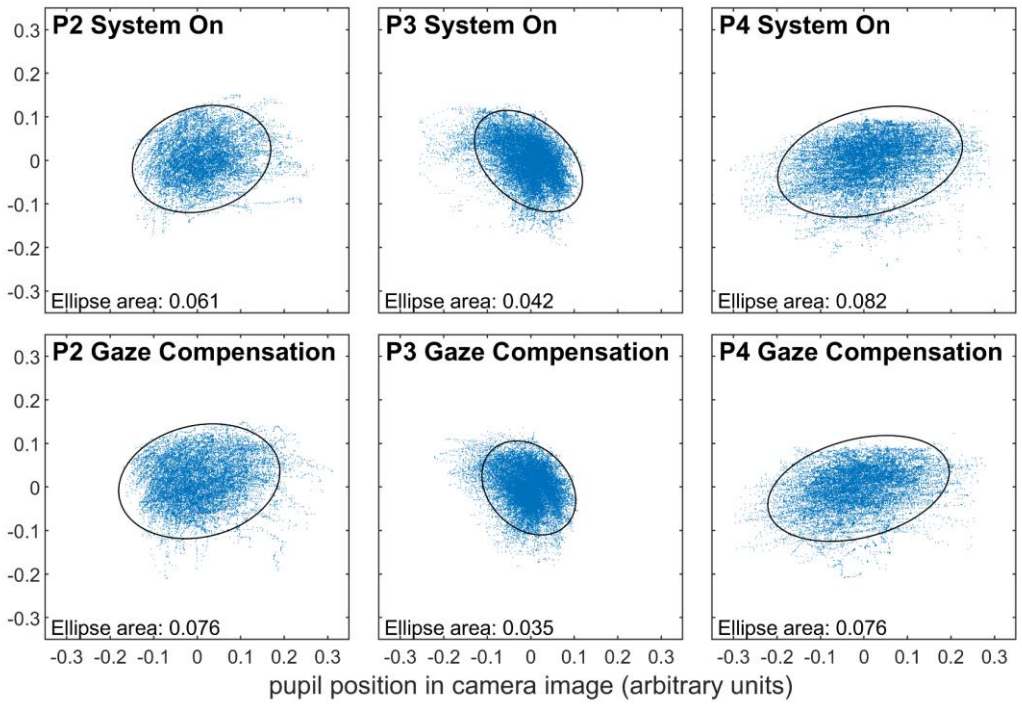

Figure 8.4: Pupil position samples in all trials during a single session for each participant for the System On and Gaze Compensation conditions. Black ellipses define the confidence ellipse enclosing 95% of recorded eye positions. The variability in eye position is quantified by the area of the ellipse, stated in the lower left corner of each panel.

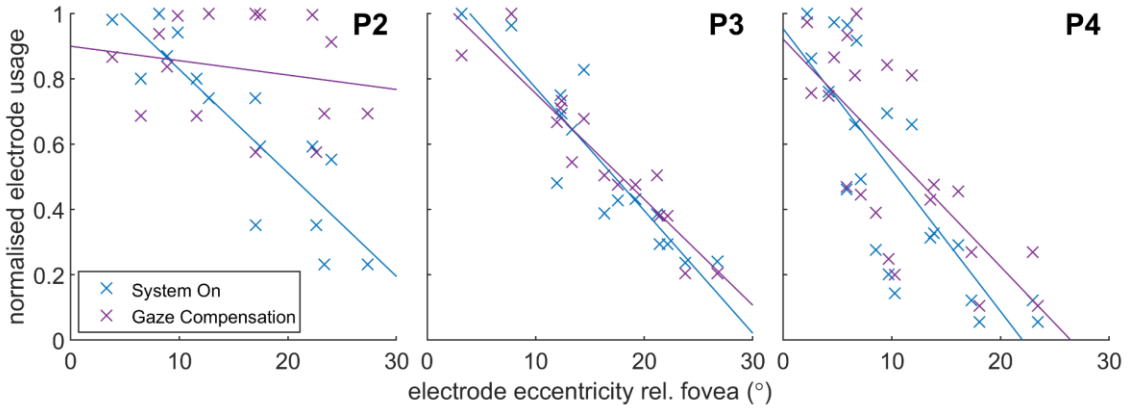

Figure 8.5: Number of stimulation pulses delivered to each electrode in the System On (blue) and Gaze Compensation (purple) conditions, normalised relative to the electrode that received the most stimulation overall. The horizontal axis shows the eccentricity of the electrode relative to the fovea. Solid lines indicate linear fits calculated by least-squares linear regression.

8.3.3. Effect of eye position on pointing error

The eye positions at four time-points during the trial were identified as potentially being influential in localisation of the target:

- the touch time (t=0)
- Target detection, defined by the knee point in the plot of average rotational head velocity (Figure 8.3, P1: t=-3.10s; P2: t=--3.15s; P3: t=-1.30s; P4: t=-1.00s)
- the onset of electrical stimulation in the trial (excluding stimulation unrelated to the target, as described above)

The correlation between pointing error and eye position at each of these four time-points was tested for each participant using least-squares linear regression. A Bonferroni correction factor of 6 (α=0.0083) was used to determine the significance of the correlation to account for two directions (horizontal and vertical) and three time-points tested per subject. The correlation was weak regardless of when the eye position was sampled. For eye position at the touch time (Figure 8.6, top two rows) the correlation was statistically significant in five out of eight cases and the highest R^2 value was only 0.14 (for P4, horizontal). The results were similar when the eye position at other time-points was considered. The strongest correlation observed was for the eye position at the time of target detection (Figure 8.6, bottom two rows) for P3 with R^2=0.18.

8.4. Discussion

That eye movement causes phosphene movement is well established in the literature. This phenomenon has been demonstrated behaviourally in retinal and cortical implants[49,98,142] and can be explained by current models of the oculomotor and spatial updating systems.[13] Additionally, previously reports have demonstrated that eye movement can lead to localisation errors in simulated prosthetic vision and in retinal implant recipients, and that gaze compensation can improve localisation.[17,146,179,213] However, in this pilot study eye movement had no significant effect on localisation and Gaze Compensation therefore did not improve performance in the task. For two participants there was no significant difference in pointing precision between System On and Gaze Compensation, while a third participant performed significantly worse with Gaze Compensation. This unexpected result can be attributed to the subject's localisation strategies and to important methodological differences between this pilot study and previously published works.

The absence of an effect of eye position suggests that the subjects had developed strategies to compensate for phosphene movement. This is supported by the excellent performance of P3 and P4 in System On (pointing precision only marginally greater than the target radius of 5°). A 'knee-point' in rotational head velocity was observed for all four participants, delineating an initial period of higher velocity head movement from a subsequent period of lower velocity head movements occurring in the several seconds prior to the touch time. The knee point approximately coincided with the onset of electrical stimulation, suggesting a 'searching' phase of coarse head movements to detect the general location of the target, followed by a 'localisation' phase of fine head movement to more precisely localise the target. It is possible that during this 'localisation' phase the subjects consciously ignored the location of the percept

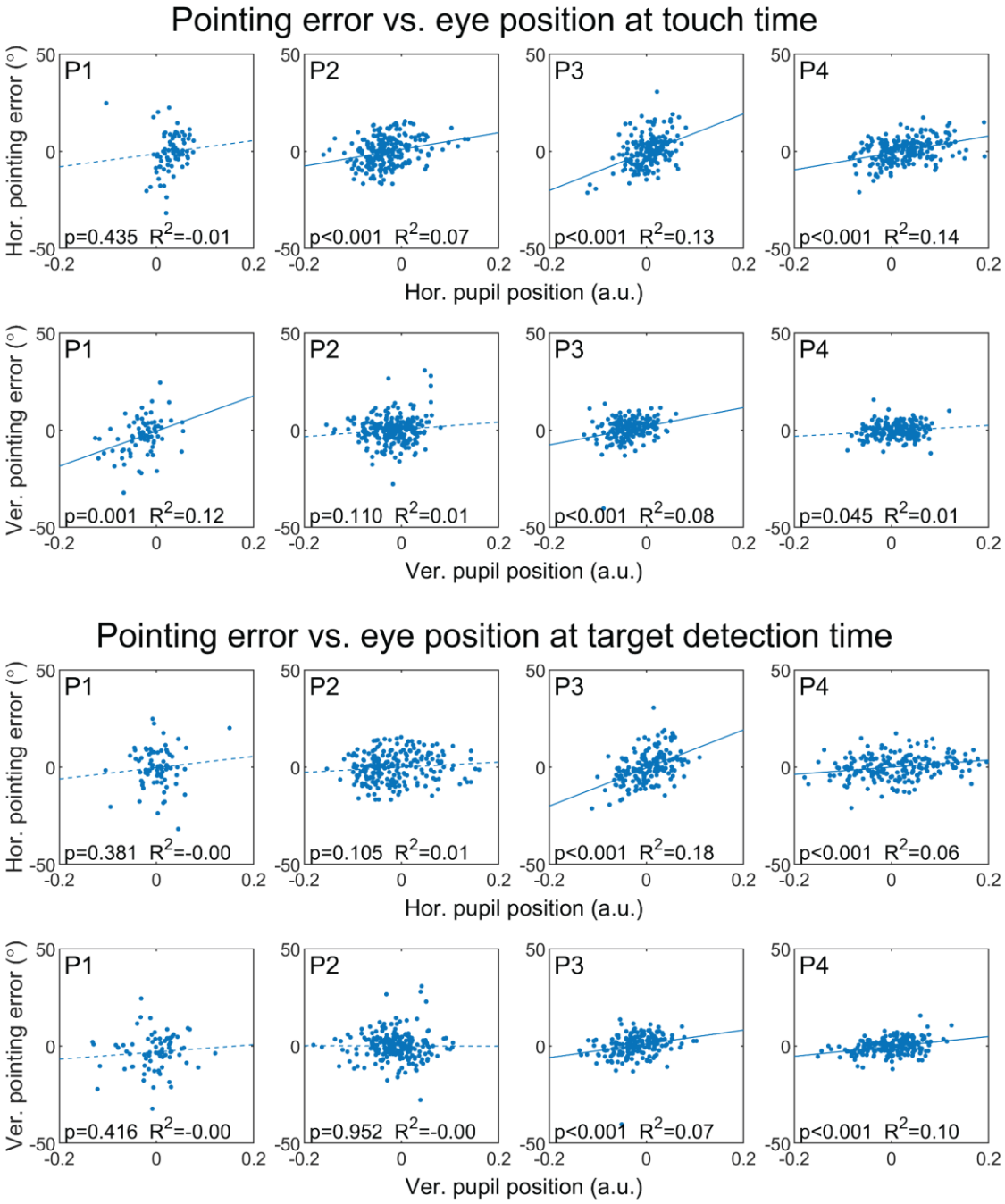

Figure 8.6: Pointing error versus pupil position at the moment the subject touched the screen in each trial (top two rows) and at the target detection time, defined as the 'knee-point' at which average head velocity began to decrease (bottom two rows). Horizontal pointing error is plotted against horizontal pupil position, and vertical pointing error is plotted against vertical pupil position. A linear fit (least-squares regression) is shown for each dataset along with p and R^2 values for the model. A Bonferroni-corrected alpha level of 0.025 is used to determine significance because two correlations are calculated per subject per time-point. Solid lines indicate fits that were statistically significant and dashed lines indicate fits that were not statistically significant.

in their visual field and instead pointed to an imagined projection of the camera axis. Argus II users may be less likely to develop this strategy because eccentric eye positions cause the wireless power link to decouple, and that system provides an auditory beep to cue the subject to return their gaze to centre.[179] This constrain on eye movement in the Argus II device is a profoundly different scenario to the unrestricted eye movement in this pilot study.

Another major difference between this pilot study and other similar studies is that here the subjects were naïve to the Gaze Compensation condition, anticipating only System On and System Off. When Argus II users were instructed which condition to expect they adapted their strategies accordingly – all subjects tested made less head movement and more eye movement when gaze compensation was enabled.[179] No such change in eye movement was observed in the present study (Figure 8.4). Gaze compensation may even have interfered with established strategies. For example, if the subject assumed a static sampling region (System On condition) and used a projection of the camera axis for localisation, as hypothesised earlier, then unexpectedly shifting the sampling region could cause less accurate localisation. This could explain P2's worse performance in the Gaze Compensation condition. In the System On condition P2 favoured the foveal electrodes, which produce the most spatially distinct phosphenes. However, when gaze compensation was introduced, electrode activity was equally distributed over the electrode array (Figure 8.5). It is possible this subject had difficulty aligning the foveal electrodes with the stimulus because they did not anticipate that their eye movement could affect the sampling region. In order to more fairly assess the effect of gaze compensation on localisation, participants should be told which condition to expect so that they may adopt an appropriate strategy.

An additional contribution to the lack of a Gaze Compensation effect is likely to have been the low fidelity of the proprioceptive eye tracker calibration, as no calibration validation could be performed. Incorrect mapping of pupil movement to camera sampling-region movement could cause Gaze Compensation to instead have a confounding effect on pointing error. A possible ceiling effect was also identified – two subjects had excellent performance with System On pointing precision only marginally greater than the target radius, indicating they touched within or very near the target on average. Any possible benefit of gaze compensation might become more apparent if the task were made more difficult, for example by reducing the target size or introducing time limits and cognitive loading.

That retinal implant users can learn compensatory strategies to achieve accurate localisation without gaze compensation is encouraging for present-day camera-based visual prostheses. However, gaze compensation may provide benefits beyond simply improving perceptual localisation. As eye movement is a more naturalistic behaviour for visual search than head scanning, users are likely to require much less localisation training with gaze compensation; experienced Argus II users had similar or better localisation ability with Gaze Compensation compared to System On despite having never been exposed to Gaze Compensation previously.[179,213] Other potential benefits of controlling the visual field using eye movement include reduced percept fading,[145] improved visual acuity through effective eye scanning techniques (so-called 'hyper-acuity'),[56] and enabling any preserved oculomotor reflexes to redirect the visual field naturalistically (see Chapter 5 and Chapter 6).

8.4.1. Conclusion

In this pilot study, eye movement did not cause localisation errors in the target localisation task, probably because the subjects had developed strategies to compensate for the phosphene movement induced by eye movement. Gaze compensation did not deliver the expected improvement in localisation accuracy, however, significant methodological problems were identified, and further investigation is required to conclusively determine any effect of gaze

compensation on localisation in the suprachoroidal retinal implant. Future studies will require robust eye tracker calibration or self-calibrating eye trackers suitable for use with non-sighted participants,[214] a more difficult task to avoid a possible ceiling effect on localisation ability, and the participants should be advised when gaze compensation is to be used so they may adapt their strategy accordingly.

Chapter 9

General Discussion

The studies presented in the preceding chapters investigated oculomotor behaviour in prosthetic vision. Chapter 4 investigated the relative contributions of eye and head movement to overall gaze behaviour in retinitis pigmentosa and constitutes a characterisation of the target patient population for retinal implants. A high degree of variation was observed between individuals, but, on average, retinitis pigmentosa was associated with a restricted range of eye movement and a corresponding greater dependence on head movement compared to healthy sighted individuals. The strength of this effect was correlated with the degree of peripheral visual field loss. Chapter 5 and Chapter 6 describe analyses of eye movements made in response to static and moving stimuli in recipients of a suprachoroidal retinal implant. The results demonstrated that the subjects were capable of retinotopic discrimination, and they made systematic eye movements in response to the stimuli despite instructions that eye movement was not an effective way to perform a visual search with their prosthesis. Some of the observed eye movements appeared naturalistic and suggest preserved oculomotor response, however, with current camera-based systems they were not an effective way to redirect the field of view.

Having demonstrated that naturalistic eye movement is preserved in prosthetic vision, and suppression of this eye movement is difficult, the thesis then investigated the effect of eye movement on hand-eye coordination. The study presented in Chapter 7 used simulated prosthetic vision to demonstrate that eye movement can lead to localisation errors and that gaze compensation using eye tracker feedback is effective in reducing these errors. Chapter 8 presented a pilot study in which we attempted to extend these findings to a suprachoroidal retinal implant but found no effect of eye movement on hand-eye coordination, possibly because the subjects had developed strategies to compensate for phosphene movement. However, some methodological issues were identified. Similar studies in Argus II epiretinal implant recipients have reported a correlation between eye movement and pointing error, and accordingly a positive benefit of gaze compensation. Considering the existing literature and the limitations of the study in Chapter 8, further investigation to determine the effect of gaze compensation on hand-eye coordination in the suprachoroidal implant is recommended. Regardless of whether accurate localisation is possible without gaze compensation, I argue that gaze compensation could offer other benefits such as reduced rehabilitation time, reduced percept fading, and the naturalistic integration of eye movement into prosthetic vision.

9.1. Altered oculomotor behaviour in RP

The study presented in Chapter 4 found abnormal oculomotor behaviour in participants with retinitis pigmentosa compared to normal sighted controls. The retinitis pigmentosa group had a habitually smaller range of eye movement compared to the control group, and the size of this effect was correlated with the degree of visual field loss. We speculated that this effect arose from a lack of salient stimuli in the peripheral visual field due to peripheral visual field loss, disrupting "bottom-up" saccade generation. However, a wide degree of variation in behaviour was observed, with some retinitis pigmentosa individuals having a wide range of habitual eye movement.

As end-stage retinitis pigmentosa is currently the predominant indication for visual prostheses, it is likely that the atypical gaze behaviour observed would also be present in visual prostheses recipients, particularly if implants begin to be prescribed earlier in vision loss. It is also notable that the suspected mechanism behind the altered gaze behaviour, namely reduced visual field disrupting bottom-up saccade generation, is also expected to be present in prosthetic vision (regardless of the specific blindness indication) as all present-day visual prostheses provide only a very limited visual field extent. Increasing the visual field coverage might promote more naturalistic oculomotor behaviour in visual prostheses.

Presently, in camera-based visual prostheses, users are instructed to suppress eye movement and maintain central fixation in order to mitigate the effect of camera-gaze misalignment. In this instance a habitually constrained range of eye movement would be beneficial, but in eye tracking-enabled visual prostheses there would be no reason to suppress eye movement. Moreover, maintaining central fixation is difficult during ambulation. Some evidence suggests that specific training to encourage conscious exploratory eye movement can be beneficial for navigation in retinitis pigmentosa,[173] and similar benefits might be realised in visual prosthesis users. Head movements are less efficient and less responsive than eye movements, hence oculomotor planning in foveate mammals acts to minimise unnecessary head movement.[167,177,215] For this reason it is desirable to promote eye scanning over head scanning where possible.

9.2. Eye movements in response to phosphene activity

In Chapter 5 we found that retinal implant recipients made eye movements in response to static stimuli. The direction and magnitude of the eye movements varied systematically depending on the particular stimulus delivered, whereas no systematic eye movements were observed during periods of no electrode activity, indicating that the observed eye movements were stimulus related. Based on the data we could not determine whether these were reflexive or volitional eye movements, however, there was some indication that larger eye movements were correlated with better performance. This could be explained by larger eye movements occurring when the percept was clearer or more localised.

In Chapter 6 similar behaviour was observed in response to moving stimuli – significant eye movements occurred, and the direction of the movements varied with the direction of stimulus movement. Notably, smooth pursuit movements in the direction of the stimulus motion were observed in two subjects. This was interpreted as an indication that direction-selective circuits

in the primary visual cortex were being usefully engaged, suggesting that the experience of motion was possibly more naturalistic than had been expected. Optokinetic nystagmus (OKN) was not conclusively identified during presentation of a moving grating stimulus, however, the extent to which OKN should be expected for retinally stabilised stimuli is not clear. Nevertheless, it was considered unlikely that retinal direction-selective circuits, which are important in the generation of OKN (as opposed to cortical direction-selective circuits, which are important to the generation of smooth pursuit), would function normally with the suprachoroidal retinal implant. Stimulation from suprachoroidal electrodes indiscriminately stimulates many cell types across all layers of the retina. The likely effect is that direction selective-ganglion cells encoding opposing directions of motion would be simultaneously and indiscriminately activated, resulting in an incoherent output. Note that this would not necessarily affect other types of eye movements with different neural origins.

Oculomotor behaviour is modulated by bottom-up and top-down flows of information. Bottom-up information comprises cues relating to visual saliency and motion, encoded in the output of retinal ganglion cells, while top-down information relates to contextual and goal oriented factors originating in many different brain areas.[14] In this way the visual system achieves a balance between reflexive and cognitive guidance of gaze. It is conceivable that retinal or optic nerve implants would stimulate retinal ganglion cells in such a way as to elicit bottom up eye movement (with the aforementioned exception of OKN), and this might have contributed to the stimulus-related eye movements observed in Chapter 5 and Chapter 6. This, in theory, permits an interaction between bottom-up and top-down streams in a similar manner to normal vision. This is supported by the finding that Alpha IMS recipients reported 'qualitatively normal' oculomotor behaviour, including fixational micro-saccades, and eye movements that reflected the location and size of stimuli.[145] Thalamic and cortical implants presumably cannot exploit the normal bottom-up pathways to the same degree because some eye movement commands originate in the retina and the electrical stimulation occurs later in the visual pathway. In this case we might expect the generation of bottom-up eye movements to be disrupted and top-down information to play a relatively greater role in oculomotor planning.

Against expectations, eye movement was not associated with diminished performance in the spatial localisation (Chapter 5) or motion discrimination (Chapter 6) tasks. In fact, certain systematic eye movements were associated with correct identification of the stimuli. These are presumed to be reflexive movements made in response to visual stimuli, as would be expected in normal vision. This is a promising indication for the naturalistic integration of artificially evoked percepts into the visual system, but the primary purpose of these eye movements, namely fixation and image stabilisation, cannot be fulfilled without gaze compensation.

9.3. The case for eye tracking in visual prostheses

Chapter 7 showed that gaze compensation can improve localisation in simulated prosthetic vision. This was followed by a pilot study in Chapter 8 attempting to extend these findings to retinal implant recipients. Unfortunately, methodological problems were identified and further study will be required to properly establish any possible benefit of gaze compensation for localisation in the suprachoroidal retinal prosthesis. However, one notable outcome of the study was that some subjects were very proficient at localisation without gaze compensation, and eye

movement did not appear to have any effect on this. Since it is well established that eye movement causes phosphene movement,[49,98,142] this result indicates that these subjects had developed strategies to cope with this phosphene movement, for example by ignoring percept location within the visual field and instead pointing along the camera axis. Although such strategies could be effective, they presumably require a certain degree of training, familiarisation, and cognitive engagement. Two studies have shown experienced Argus II users achieved similar or better localisation accuracy when gaze compensation was enabled, despite having no prior experience with gaze compensation.[179,213] This suggests that gaze compensation reduces the time and effort for a subject to become proficient at localisation by enabling more naturalistic interpretation of artificial percepts.

Other less invasive visual aids can enable useful localisation. For example, experienced users of the Brain Port sensory substitution device can localise light sources by interpreting electrical stimulation of the tongue.[216] One of the primary advantages of visual prostheses compared to sensory substitution devices is that they interface directly with the visual system, exploiting existing structures specifically tuned for visual tasks such as localisation, detection of motion, and visual search. For both visual prostheses and sensory substitution devices, localisation with respect to a fixed camera can only be as accurate as the subject's estimation of the camera bearing. Gaze compensation would enable localisation with respect to the visual field, exploiting the existing capacity of the visual system for this task to provide a naturalistic and intuitive interaction with the technology.

Aside from perceptual localisation, gaze compensation could provide other benefits such as more efficient visual search, naturalistic control of visual attention and fixation, and reduced percept fading. Chapter 5 and Chapter 6 showed that some normal oculomotor reflexes are preserved in prosthetic vision – subjects made eye movements towards static stimuli appearing in the peripheral visual field and made smooth pursuit eye movements that followed moving stimuli. Similarly, subjects implanted with the photovoltaic Alpha IMS made eye movements that accurately reflected the location and shape of the stimuli presented, providing evidence that naturalistic control of visual attention is possible in visual prostheses when eye movement control is enabled.[145] While head scanning could be used to compensate for these functionalities to some extent in camera-based visual prostheses, this requires training and familiarisation, and is unlikely to be as efficient or effective as naturalistic eye movement control. For example, in Chapter 6 S1 used head scanning to maintain fixation on the moving bar stimulus but this was not viable for fast-moving (30°/s) stimuli, whereas smooth pursuit eye movements were observed for all stimulus speeds.

Gaze compensation may also help to reduce the fading of percepts evoked by electrical stimulation. In healthy vision, percepts that are stabilised with respect to the retina fade into invisibility after only a few seconds due to neural adaption to an unchanging stimulus.[217] Small ocular drifts and micro-saccades that occur constantly, even during fixation, act to counter this by ensuring constant motion of the image across the retina.[218,219] In camera-based visual prostheses eye movement does not cause any change in the input image, leading to rapidly fading percepts.[220] Alpha IMS recipients have been observed making fixational eye movements that are 'qualitatively similar' to those made by healthy controls, and these eye movements

were associated with more persistent percepts.[145] Gaze compensation might enable similar behaviour in camera-based visual prostheses, reducing the severity of phosphene fading.

Recent years have seen a number of photovoltaic retinal implants emerge that incorporate an implanted image sensor that captures ambient light that naturally enters the eye.[75,79,221,222] However, the photovoltaic approach is not feasible for suprachoroidal retinal implants because the intervening retinal layers attenuate incidental light, nor is it suitable for visual prostheses that target the optic nerve, thalamus, or visual cortex, because incidental light will not reach the implant. For these devices an external image sensor of some kind is necessary. Although the research in this thesis was primarily concerned with retinal implants, most of the findings are also relevant to other types of visual prosthesis, and the implementation and benefits of gaze compensation are likely to be similar. Cortical implants in particular have been the subject of growing attention due to their relatively wide range of indications.[112,116] If photovoltaic retinal implants eventually displace conventional camera-based devices, then gaze compensation may come to be primarily applied in cortical implants.

Anecdotally, the subjects implanted with the Bionic Vision Technologies suprachoroidal retinal implant do not seem particularly concerned about, or routinely aware of, the effects of eye movement on their perception. A similar lack of spatial awareness was reported in Argus II users whereby the study cohort were unable to recognise or adapt to camera misalignments over a 12 month period.[123] The authors argued that the vision provided by present devices was too poor for any meaningful visual feedback with which to recognise camera misalignment, let alone rectify or compensate for it, as without form vision users cannot recognise objects or even their own hands. For example, if a user finds that an object is not where they had perceived it to be they might assume that they had actually been looking at something else entirely, or that the percept was not anything meaningful. However, if future visual prostheses confer a quality of vision sufficient for recognition of objects and one's own body, and appreciation of the spatial structure of a scene, then camera-gaze misalignments would be readily apparent to the user and eye movement might even cause the dizzying experience of motion across the entire visual field.[123,223]

9.4. Implementation of eye tracking in visual prostheses

Eye tracking has been used in research laboratories for decades, but only recently has any attempt been made to produce eye tracking for consumer applications. Among the few examples are eye trackers for virtual reality gaming, consumer research[224,225], and monitoring driver distraction in freight trucks.[226] The requirements and constraints vary depending on the specific application. In Chapter 8 a video oculography system was used in a proof-of-concept study for gaze compensation in simulated prosthetic vision. However, a considerable development effort would be required before this concept could be integrated into a visual prosthesis for unsupervised use in daily life. Considerations such as portability, power usage, measurement accuracy and precision, ease of calibration (particularly in non-sighted users), and latency of updating the camera input, will be important in this process.

Video oculography is currently the most widespread form of eye tracking. The eye is illuminated with infrared light and an eye-facing camera monitors the location of the pupil and the glints of

the IR light sources on the cornea. The system may be placed on a benchtop or head mounted.[227,228] Conventionally, calibration of these systems requires the user to fixate on a series of predefined targets, a procedure which is not accessible to blind users. However, modern calibration-less devices use stereo cameras, multiple light sources, and models of eye curvature to determine gaze angle without manual calibration.[214] Video oculography carries with it a relatively high computational and power footprint and is susceptible to interference in uncontrolled lighting conditions. The use of blackout lenses or even a fully enclosed system may improve the tracking robustness.

Scleral search coil eye tracking was widely used before advances in computing and video processing enabled the less-invasive method of video oculography.[210,229] In this method, a small search coil contained within a contact lens is placed on the eye. Two or three large external coils generate orthogonal frequency-encoded magnetic fields, and the current induced in the search coil is measured via two wires that exit the contact lens. The angle of the eye is determined by frequency domain analysis of the measured current. Eye angle is measured in real-world coordinates, so typically head movement is restricted.[230,231] However, a recent proof-of-concept study successfully demonstrated a miniaturised head-mounted scleral search coil system for eye tracking in virtual reality, allowing free head rotation and measurement of gaze angle in head-centred coordinates.[232] Such a system could conceivably be mounted on a pair of spectacles. The primary disadvantage of scleral search coils in visual prostheses is that the recording cable connecting to the search coil is prone to breaking and causes irritation of the eye and is therefore unlikely to be tolerated for extended use on a daily basis.

Double magnetic induction offers the possibility of less invasive scleral search by eliminating the recording wire and instead placing a second set of recording coils near the eye. The currents induced in the search coil in turn induce secondary currents in the external recording coils, and these secondary currents are measured. Double magnetic induction suffers from a weak signal to noise ratio compared to conventional scleral search but would be much more tolerable for regular prolonged use.[233–235] More recently a resonant scleral search coil has been proposed as a method to improve signal-to-noise ratio in double magnetic induction. In this method the contact lens contains multiple coils resonant at different frequencies. The external transmitting coils are pulsed periodically and the induced resonant currents in the search coils are sustained between pulses. The secondary currents induced in the recording coils can then be measured without interference from the primary coils.[230,236]

Alternatively, the concept of scleral search could be reversed. The primary coil could be implanted within the eye, perhaps on the same substrate as the stimulating electrodes, and driven by the implanted stimulator. This signal could then be detected by external receiver coils. This would eliminate the need for a contact lens at the expense of added componentry on the implant. A similar effect might be achieved using an implanted permanent magnet and external magnetic field sensors,[237] or by measuring stimulation artefact with electrodes external to the eye.[211]

It remains to be seen which method will prove to be the most effective for eye trackers in visual prostheses. Regardless of the specific implementation, the basic requirements are the same:

- **Portability**: the added size and weight of the eye tracking instrumentation should not make the externally worn components overly encumbering or uncomfortable during extended use.
- **Power footprint**: battery life should not impede normal usage of the system. No published data exist for typical usage patterns, but a minimum requirement of three hours of continuous use on a single charge would seem reasonable.
- **Robustness** under a range of lighting conditions, e.g. indoors and outdoors.
- **Measurement precision**: ideally, eye position measurements should be precise enough that any error is imperceptible to the user, however, precision beyond the spatial resolution of vision is unlikely to have any additional benefit. Therefore, measurement resolution near the theoretical minimum angle of resolution is desirable. Some examples of approximate minimum angle of resolution for existing devices, calculated from the electrode pitch, are Argus II: 2°, Alpha AMS: 0.25°, BVT suprachoroidal: 4°.
- **Measurement range**: the normal horizontal oculomotor range is approximately ±45°[238]. However, very eccentric eye positions are unlikely to occur often or for any extended period. In Chapter 4, average customary oculomotor range (COMR) for the RP group was 57.1±4.2°, indicating that eye position remained within this range 90% of the time. Therefore, accurate measurement across the entire range of possible eye movement may not be necessary. No published data regarding COMR in users of any visual prosthesis are available.
- **Temporal resolution**: High sampling rates enable more sophisticated noise reduction, artefact removal, and prediction of future eye position. The stimulation rate is usually limited in visual prostheses to prevent percept fading.[220] For example, 10-50 pps (pulses per second) for the BVT 2nd generation suprachoroidal retinal implant, and 2-20 pps for the Argus II epiretinal implant.[56] This limits the frequency at which a change in the video input can affect the subject's perception, diminishing the utility of high frequency eye position sampling. However, cortical implants may have higher stimulation rate requirements to retinal implants, necessitating a higher eye tracker sampling rate. For example, Beauchamp 2020 demonstrated a dynamic stimulation paradigm using 200 pps stimulation that would require a much higher update rate of eye position. In either case, lower eye tracker sampling rates would reduce the computational overhead of eye tracking but may compromise the benefit of gaze compensation.
- **Processor**: The eye position signal must be processed in real-time by a mobile processor integrated into the prosthesis. This was achieved using a field-programmable gate array in a recent study Argus II.[239]
- **Calibration**: the eye tracking apparatus should not require calibration by the user. One-off or periodic calibration by a clinician might be acceptable.
- **Scene camera field of view**: should accommodate region of interest (ROI) movement across the entire range of measurable eye movement.

9.5. Final conclusion

Visual prostheses are still an emerging technology, but clinical results over the last ten years have been promising. Some of the present generation of devices have in general proven to be stable and well tolerated for many years and provide meaningful assistance to users in certain

activities of daily living. However, the quality of vision is still very poor, patient outcomes can be variable, and some safety and stability concerns persist. Interpreting artificial vision can be a highly unintuitive and cognitive task. In present-day camera-based visual prostheses the camera does not move in response to eye movement, causing percept locations to become dissociated from the real world. Shifting the camera in parity with eye movement, termed 'gaze compensation', has been proposed as a method to solve this.

The research presented in the thesis explored oculomotor behaviour in prosthetic vision. Retinal implant recipients were found to make naturalistic eye movements in response to artificial percepts, indicating preserved oculomotor capacity. Eye movement was found to cause localisation errors in simulated prosthetic vision but not in experienced retinal implant users, suggesting the retinal implant users had learned strategies to compensate for phosphene movement. The thesis demonstrates that gaze compensation would facilitate more naturalistic interaction with the technology by enabling naturalistic control of the field of view using preserved oculomotor capacity, and reducing the requirement to learn compensatory strategies for localisation. As developments in the field improve spatial resolution, localisation errors are likely to become more apparent to the user, adding further motivation for eye tracker feedback. Visual prostheses featuring integrated eye tracking do not currently exist but are anticipated in the near future.

Bibliography

1. 2020 V. Clear Focus: The Economic Impact and Cost of Vision Loss in Australia 2009. 2010.
2. Taylor HR, Keeffe JE, Hein TVV, et al. Vision loss in Australia. *Med J Aust*. 2005;182:565-568. doi:10.1136/bjo.2005.080986
3. Taylor HR, Pezzullo ML, Keeffe JE. The economic impact and cost of visual impairment in Australia. *Br J Ophthalmol*. 2006;90(3):272-275. doi:10.1136/bjo.2005.080986
4. Foreman J, Keel S, Xie J, et al. *National Eye Health Survey*.; 2016.
5. Ayton LN, Barnes N, Dagnelie G, et al. An update on retinal prostheses. *Clin Neurophysiol*. 2019. doi:https://doi.org/10.1016/j.clinph.2019.11.029
6. Bloch E, Luo Y, da Cruz L. Advances in retinal prosthesis systems. *Ther Adv Ophthalmol*. 2019;11:2515841418817501. doi:10.1177/2515841418817501
7. Mirochnik RM, Pezaris JS. Contemporary approaches to visual prostheses. *Mil Med Res*. 2019;6(1):1.
8. Geruschat DR, Richards TP, Arditi A, et al. An analysis of observer-rated functional vision in patients implanted with the Argus II Retinal Prosthesis System at three years. *Clin Exp Optom*. 2016;99(3):227-232.
9. Sinclair NC, Shivdasani MN, Perera T, et al. The Appearance of Phosphenes Elicited Using a Suprachoroidal Retinal Prosthesis. *Investig Ophthalmol Vis Sci*. 2016;57(11):4948-4961. doi:10.1167/iovs.15-18991
10. Fine I, Boynton GM. Pulse trains to percepts: the challenge of creating a perceptually intelligible world with sight recovery technologies. *Philos Trans R Soc B Biol Sci*. 2015;370(1677):20140208.
11. Purves D, Augustine G, Fitzpatrick D, Hall WC, Lamantia AS, Mcnamara JO. Eye Movements and Sensory Motor Integration. In: *Neuroscience*. Sinauer Associates, Sunderland, MA; 2001:453-468.
12. Klier EM, Angelaki DE. Spatial updating and the maintenance of visual constancy. *Neuroscience*. 2008;156(4):801-818.
13. Paraskevoudi N, Pezaris JS. Eye movement compensation and spatial updating in visual prosthetics: Mechanisms, limitations and future directions. *Front Syst Neurosci*. 2018;12:73.
14. Theeuwes J. Top-down and bottom-up control of visual selection. *Acta Psychol (Amst)*. 2010;135(2):77-99. doi:https://doi.org/10.1016/j.actpsy.2010.02.006
15. Titchener SA, Ayton LN, Abbott CJ, et al. Head and Gaze Behavior in Retinitis Pigmentosa. *Invest Ophthalmol Vis Sci*. 2019;60(6):2263-2273.

16. Shivdasani MN, Sinclair NC, Gillespie LN, et al. Identification of Characters and Localization of Images Using Direct Multiple-Electrode Stimulation With a Suprachoroidal Retinal Prosthesis. *Investig Ophthalmol Vis Sci*. 2017;58(10):3962-3974.

17. Titchener SA, Shivdasani MN, Fallon JB, Petoe MA. Gaze Compensation as a Technique for Improving Hand–Eye Coordination in Prosthetic Vision. *Transl Vis Sci Technol*. 2018;7(1):2. doi:10.1167/tvst.7.1.2

18. Purves D, Augustine G, Fitzpatrick D, Hall WC, Lamantia AS, Mcnamara JO. Vision: the eye. In: *Neuroscience*. Sinauer Associates, Sunderland, MA; 2001:223-250.

19. Kolb H. How the retina works. *Am Sci*. 2003;91(1):28-35.

20. Kaneda M. Signal processing in the mammalian retina. *J Nippon Med Sch*. 2013;80(1):16-24.

21. MacNeil MA, Masland RH. Extreme diversity among amacrine cells: implications for function. *Neuron*. 1998;20(5):971-982.

22. Sanes JR, Masland RH. The types of retinal ganglion cells: current status and implications for neuronal classification. *Annu Rev Neurosci*. 2015;38:221-246.

23. Schiller PH, Malpeli JG. Functional specificity of lateral geniculate nucleus laminae of the rhesus monkey. *J Neurophysiol*. 1978;41(3):788-797.

24. Covington BP, Al Khalili Y. Neuroanatomy, Nucleus Lateral Geniculate. In: *StatPearls*. StatPearls Publishing; 2019.

25. Martinez-Conde S, Macknik SL, Hubel DH. The role of fixational eye movements in visual perception. *Nat Rev Neurosci*. 2004;5(3):229-240. http://dx.doi.org/10.1038/nrn1348.

26. McCamy MB, Macknik SL, Martinez-Conde S. Different fixational eye movements mediate the prevention and the reversal of visual fading. *J Physiol*. 2014;592(19):4381-4394.

27. Moschovakis A. Neural Control of Eye Movements BT - Encyclopedia of Neuroscience. In: Binder MD, Hirokawa N, Windhorst U, eds. Berlin, Heidelberg: Springer Berlin Heidelberg; 2009:2558-2564. doi:10.1007/978-3-540-29678-2_3781

28. Burr DC, Morrone MC, Ross J. Selective suppression of the magnocellular visual pathway during saccadic eye movements. *Nature*. 1994;371(6497):511-513. doi:10.1038/371511a0

29. Gandhi NJ, Katnani HA. Motor functions of the superior colliculus. *Annu Rev Neurosci*. 2011;34:205-231.

30. Lamy D, Leber AB, Egeth HE. Selective attention. *Handb Psychol Second Ed*. 2012;4.

31. Theeuwes J, Olivers CNL, Belopolsky A. Stimulus-driven capture and contingent capture. *Wiley Interdiscip Rev Cogn Sci*. 2010;1(6):872-881.

32. Büttner-Ennever JA. *Neuroanatomy of the Oculomotor System*. Vol 151. Elsevier; 2005.

33. Gauthier GM, Nommay D, Vercher J. Ocular muscle proprioception and visual localization of targets in man. *Brain*. 1990;113(6):1857-1871.

34. Bridgeman B. A review of the role of efference copy in sensory and oculomotor control systems. *Ann Biomed Eng*. 1995;23(4):409-422.

35. Shintani K, Shechtman DL, Gurwood AS. Review and update: current treatment trends for patients with retinitis pigmentosa. *Optom Am Optom Assoc*. 2009;80(7):384-401.

36. Pagon RA. Retinitis pigmentosa. *Surv Ophthalmol*. 1988;33(3):137-177.

37. Hartong DT, Berson EL, Dryja TP. Retinitis pigmentosa. *Lancet*. 2006;368(9549):1795-1809.

38. Russell S, Bennett J, Wellman JA, et al. Efficacy and safety of voretigene neparvovec (AAV2-hRPE65v2) in patients with RPE65-mediated inherited retinal dystrophy: a randomised, controlled, open-label, phase 3 trial. *Lancet*. 2017;390(10097):849-860.

39. Darrow JJ. Luxturna: FDA documents reveal the value of a costly gene therapy. *Drug Discov Today*. 2019.

40. Ferrari S, Di Iorio E, Barbaro V, Ponzin D, S Sorrentino F, Parmeggiani F. Retinitis pigmentosa: genes and disease mechanisms. *Curr Genomics*. 2011;12(4):238-249.

41. Berson EL, Weigel-DiFranco C, Rosner B, Gaudio AR, Sandberg MA. Association of Vitamin A Supplementation With Disease Course in Children With Retinitis Pigmentosa. *JAMA Ophthalmol*. 2018;136(5):490-495. doi:10.1001/jamaophthalmol.2018.0590

42. Grant CA, Berson EL. Treatable forms of retinitis pigmentosa associated with systemic neurological disorders. *Int Ophthalmol Clin*. 2001;41(1):103-110.

43. Santos A, Humayun MS, de Juan Jr E, et al. Preservation of the Inner Retina in Retinitis Pigmentosa: A Morphometric Analysis. *JAMA Ophthalmol*. 1997;115(4):511-515. doi:10.1001/archopht.1997.01100150513011

44. Shepherd RK, Shivdasani MN, Nayagam DAX, Williams CE, Blamey PJ. Visual prostheses for the blind. *Trends Biotechnol*. 2013;31(10):562-571. doi:https://doi.org/10.1016/j.tibtech.2013.07.001

45. Pascual-Leone A, Wagner T. A brief summary of the history of noninvasive brain stimulation. *Annu Rev Biomed Eng*. 2007;9(1):527-565.

46. Volta A, Banks J. I. On the electricity excited by the mere contact of conducting substances of different kinds. *Philos Mag*. 1800;7(28):289-311.

47. Fernandez E. Development of visual Neuroprostheses: trends and challenges. *Bioelectron Med*. 2018;4(1):12.

48. Tassicker GE. Retinal stimulator. August 1956.

49. Brindley GS, Lewin WS. The sensations produced by electrical stimulation of the visual cortex. *J Physiol*. 1968;196(2):479.

50. Dobelle WH, Mladejovsky MG. Phosphenes produced by electrical stimulation of human occipital cortex, and their application to the development of a prosthesis for the blind. *J Physiol*. 1974;243(2):553-576.

51. Dobelle WH, Mladejovsky MG, Girvin JP. Artificial vision for the blind: electrical stimulation of visual cortex offers hope for a functional prosthesis. *Science (80-)*. 1974;183(4123):440-444.

52. Dobelle WH, Mladejovsky MG, Evans JR, Roberts TS, Girvin JP. 'Braille'reading by a blind volunteer by visual cortex stimulation. *Nature*. 1976;259(5539):111-112.

53. Dobelle WH, Dobelle WH, Quest DO, Antunes JL, Roberts TS, Girvin JP. Artificial vision for the blind by electrical stimulation of the visual cortex. *Neurosurgery*. 1979;5(4):521-527.

54. Dobelle WH, Turkel J, Henderson DC, Evans JR. Mapping the representation of the visual field by electrical stimulation of human visual cortex. *Am J Ophthalmol*. 1979;88(4):727-735.

55. Naumann J. *Search for Paradise: A Patient's Account of the Artificial Vision Experiment*. Xlibris corporation; 2012.

56. Stronks HC, Dagnelie G. The functional performance of the Argus II retinal prosthesis. *Expert Rev Med Devices*. 2014;11(1):23-30.

57. Bloch E, da Cruz L. The Argus II Retinal Prosthesis System. In: *Prosthesis*. IntechOpen; 2019.

58. Humayun MS, Dorn JD, da Cruz L, et al. Interim results from the international trial of Second Sight's visual prosthesis. *Ophthalmology*. 2012;119(4):779-788.

59. da Cruz L, Dorn JD, Humayun MS, et al. Five-year safety and performance results from the Argus II retinal prosthesis system clinical trial. *Ophthalmology*. 2016;123(10):2248-2254.

60. Rizzo S, Cinelli L, Finocchio L, Tartaro R, Santoro F, Gregori NZ. Assessment of Postoperative Morphologic Retinal Changes by Optical Coherence Tomography in Recipients of an Electronic Retinal Prosthesis Implant. *JAMA Ophthalmol*. 2019;137(3):272-278.

61. Ho AC, Humayun MS, Dorn JD, et al. Long-term results from an epiretinal prosthesis to restore sight to the blind. *Ophthalmology*. 2015;122(8):1547-1554.

62. Delyfer M-N, Gaucher D, Govare M, et al. Adapted Surgical Procedure for Argus II Retinal Implantation: Feasibility, Safety, Efficiency, and Postoperative Anatomic Findings. *Ophthalmol Retin*. 2018;2(4):276-287. doi:https://doi.org/10.1016/j.oret.2017.08.010

63. Dorn JD, Ahuja AK, Caspi A, et al. The detection of motion by blind subjects with the epiretinal 60-electrode (Argus II) retinal prosthesis. *JAMA Ophthalmol*. 2013;131(2):183-189.

64. Ahuja AK, Dorn JD, Caspi A, et al. Blind subjects implanted with the Argus II retinal

prosthesis are able to improve performance in a spatial-motor task. *Br J Ophthalmol*. 2011;95(4):539-543.

65. Geruschat DR, Flax M, Tanna N, et al. FLORA^{TM}: Phase I development of a functional vision assessment for prosthetic vision users. *Clin Exp Optom*. 2015;98(4):342-347.

66. Second Sight to Accelerate Development of Orion® Visual Cortical Prosthesis System. *Bloomberg*. https://www.bloomberg.com/press-releases/2019-05-15/second-sight-to-accelerate-development-of-orion-visual-cortical-prosthesis-system. Published May 16, 2019.

67. Eckmiller R, Neumann D, Baruth O. Tunable retina encoders for retina implants: why and how. *J Neural Eng*. 2005;2:S91.

68. Hornig R, Dapper M, Le Joliff E, et al. Pixium vision: first clinical results and innovative developments. In: *Artificial Vision*. Springer; 2017:99-113.

69. Pixium Vision announces updates on its Epi-retinal IRIS®II Bionic Vision System. *Pixium Vision*. https://www.pixium-vision.com/file_bdd/dynamic_content/file_pdf_pdf_en/1506445353_Pixium-IRISupdateENGfinal.pdf. Published September 27, 2017. Accessed October 22, 2019.

70. Klauke S, Goertz M, Rein S, et al. Stimulation with a Wireless Intraocular Epiretinal Implant Elicits Visual Percepts in Blind Humans. *Invest Ophthalmol Vis Sci*. 2011;52(1):449-455. doi:10.1167/iovs.09-4410

71. Menzel-Severing J, Laube T, Brockmann C, et al. Implantation and explantation of an active epiretinal visual prosthesis: 2-year follow-up data from the EPIRET3 prospective clinical trial. *Eye*. 2012;26(4):501-509.

72. Nano Retina Ltd. Nano Retina Announces Preliminary Results for First-in-Human Implantation of Its NR600 Artificial Retina Device. *Press release*. http://www.nano-retina.com/nano-retina-announces-preliminary-results-for-first-in-human-implantation-of-its-nr600-artificial-retina-device/. Published March 30, 2020.

73. Stelzle M, Stett A, Brunner B, Graf M, Nisch W. Electrical properties of micro-photodiode arrays for use as artificial retina implant. *Biomed Microdevices*. 2001;3(2):133-142.

74. Stingl K, Bartz-Schmidt KU, Besch D, et al. Artificial vision with wirelessly powered subretinal electronic implant alpha-IMS. *Proc R Soc B Biol Sci*. 2013;280(1757):20130077.

75. Stingl K, Bartz-Schmidt KU, Besch D, et al. Subretinal visual implant alpha IMS–clinical trial interim report. *Vision Res*. 2015;111:149-160.

76. Kitiratschky VBD, Stingl K, Wilhelm B, et al. Safety evaluation of "retina implant alpha IMS"—a prospective clinical trial. *Graefe's Arch Clin Exp Ophthalmol*. 2015;253(3):381-387.

77. Daschner R, Greppmaier U, Kokelmann M, et al. Laboratory and clinical reliability of conformally coated subretinal implants. *Biomed Microdevices*. 2017;19(1):7.

78. Edwards TL, Cottriall CL, Xue K, et al. Assessment of the electronic retinal implant alpha AMS in restoring vision to blind patients with end-stage retinitis pigmentosa. *Ophthalmology*. 2018;125(3):432-443.

79. Stingl K, Schippert R, Bartz-Schmidt KU, et al. Interim results of a multicenter trial with the new electronic subretinal implant Alpha AMS in 15 patients blind from inherited retinal degenerations. *Front Neurosci*. 2017;11:445.

80. Daschner R, Rothermel A, Rudorf R, Rudorf S, Stett A. Functionality and performance of the subretinal implant chip alpha AMS. *Sens Mater*. 2018;30:179-192.

81. Krader CG. Lessons learned from subretinal implant. *Euro Times*. https://www.eurotimes.org/lessons-learned-from-subretinal-implant/. Published April 29, 2019.

82. Luo YH-L, da Cruz L. The Argus® II Retinal Prosthesis System. *Prog Retin Eye Res*. 2016;50:89-107. doi:https://doi.org/10.1016/j.preteyeres.2015.09.003

83. Pixium Vision receives approval for First-inHuman Clinical Trial of PRIMA, its miniaturized sub-retinal implant. Pixium Vision. https://www.pixium-vision.com/file_bdd/dynamic_content/file_pdf_pdf_en/1508344285_Pixium-PRIMAFIH-GB-final.pdf. Published 2017. Accessed October 22, 2019.

84. Palanker D, Le Mer Y, Mohand-Said S, Muqit MMK, Sahel JA. Photovoltaic Restoration of Central Vision in Atrophic Age-Related Macular Degeneration. *Ophthalmology*. 2020.

85. Nayagam DAX, Williams RA, Allen PJ, et al. Chronic electrical stimulation with a suprachoroidal retinal prosthesis: a preclinical safety and efficacy study. *PLoS One*. 2014;9(5):e97182.

86. Shepherd RK, Villalobos J, Burns O, Nayagam DAX. The development of neural stimulators: a review of preclinical safety and efficacy studies. *J Neural Eng*. 2018;15(4):41004.

87. Shannon R V. A model of safe levels for electrical stimulation. *IEEE Trans Biomed Eng*. 1992;39(4):424-426.

88. Ayton LN, Blamey PJ, Guymer RH, et al. First-in-human trial of a novel suprachoroidal retinal prosthesis. *PLoS One*. 2014;9(12):e115239.

89. Allen PJ, Nayagam D, Epp S, et al. A 44 channel suprachoroidal retinal prosthesis: interim safety and stability results for our 2 year clinical trial. *Invest Ophthalmol Vis Sci*. 2020;61(7):2200.

90. Petoe MA, Titchener SA, Shivdasani MN, et al. A 44 channel suprachoroidal retinal prosthesis: initial psychophysical results. *Invest Ophthalmol Vis Sci*. 2019;60(9):4993.

91. Kolic M, Baglin EK, Titchener S, et al. A 44 channel suprachoroidal retinal prosthesis: interim functional vision results. *Invest Ophthalmol Vis Sci*. 2020;61(7):2199.

92. Fujikado T, Kamei M, Sakaguchi H, et al. Testing of Semichronically Implanted Retinal

Prosthesis by Suprachoroidal-Transretinal Stimulation in Patients with Retinitis Pigmentosa. *Invest Ophthalmol Vis Sci*. 2011;52(7):4726-4733. doi:10.1167/iovs.10-6836

93. Fujikado T, Kamei M, Sakaguchi H, et al. Clinical trial of chronic implantation of suprachoroidal-transretinal stimulation system for retinal prosthesis. *Sensors Mater*. 2012;24(4):181-187.

94. Veraart C, Raftopoulos C, Mortimer JT, et al. Visual sensations produced by optic nerve stimulation using an implanted self-sizing spiral cuff electrode. *Brain Res*. 1998;813(1):181-186.

95. Delbeke J, Wanet-Defalque MC, Gérard B, Troosters M, Michaux G, Veraart C. The microsystems based visual prosthesis for optic nerve stimulation. *Artif Organs*. 2002;26(3):232-234.

96. Brelén ME, De Potter P, Gersdorff M, Cosnard G, Veraart C, Delbeke J. Intraorbital implantation of a stimulating electrode for an optic nerve visual prosthesis: case report. *J Neurosurg*. 2006;104(4):593-597.

97. Fitzgibbon T, Taylor SF. Retinotopy of the human retinal nerve fibre layer and optic nerve head. *J Comp Neurol*. 1996;375(2):238-251.

98. Caspi A, Roy A, Dorn JD, Greenberg RJ. Retinotopic to Spatiotopic Mapping in Blind Patients Implanted With the Argus II Retinal Prosthesis. *Investig Ophthalmol Vis Sci*. 2017;58(1):119-127.

99. Stronks HC, Dagnelie G. Phosphene mapping techniques for visual prostheses. In: *Visual Prosthetics*. Springer; 2011:367-383.

100. Veraart C, Wanet-Defalque M-C, Gérard B, Vanlierde A, Delbeke J. Pattern Recognition with the Optic Nerve Visual Prosthesis. *Artif Organs*. 2003;27(11):996-1004. doi:10.1046/j.1525-1594.2003.07305.x

101. Veraart C, Duret F, Brelen M, Delbeke J. Vision rehabilitation with the optic nerve visual prosthesis. In: *Engineering in Medicine and Biology Society, 2004. IEMBS'04. 26th Annual International Conference of the IEEE*. Vol 2. IEEE; 2004:4163-4164.

102. Sakaguchi H, Kamei M, Fujikado T, et al. Artificial vision by direct optic nerve electrode (AV-DONE) implantation in a blind patient with retinitis pigmentosa. *J Artif Organs*. 2009;12(3):206-209.

103. Gaillet V, Cutrone A, Artoni F, et al. Spatially selective activation of the visual cortex via intraneural stimulation of the optic nerve. *Nat Biomed Eng*. 2020;4(2):181-194.

104. Li M, Yan Y, Wu K, et al. Penetrative Optic Nerve-Based Visual Prosthesis Research. In: *Artificial Vision*. Springer; 2017:165-176.

105. Nishida K, Sakaguchi H, Kamei M, et al. Visual sensation by electrical stimulation using a new direct optic nerve electrode device. *Brain Stimul Basic, Transl Clin Res Neuromodulation*. 2015;8(3):678-681.

106. Pezaris JS, Eskandar EN. Getting signals into the brain: visual prosthetics through thalamic microstimulation. *Neurosurg Focus*. 2009;27(1):E6.

107. Nguyen HT, Tangutooru SM, Rountree CM, et al. Thalamic Visual Prosthesis. *IEEE Trans Biomed Eng*. 2016;63(8):1573-1580. doi:10.1109/TBME.2016.2567300

108. Pezaris JS, Reid RC. Simulations of electrode placement for a thalamic visual prosthesis. *IEEE Trans Biomed Eng*. 2008;56(1):172-178.

109. Pezaris JS, Reid RC. Demonstration of artificial visual percepts generated through thalamic microstimulation. *Proc Natl Acad Sci*. 2007;104(18):7670-7675.

110. Lozano AM, Lipsman N, Bergman H, et al. Deep brain stimulation: current challenges and future directions. *Nat Rev Neurol*. 2019;15(3):148-160.

111. Schmidt EM, Bak MJ, Hambrecht FT, Kufta C V, O'rourke DK, Vallabhanath P. Feasibility of a visual prosthesis for the blind based on intracortical micro stimulation of the visual cortex. *Brain*. 1996;119(2):507-522.

112. Fernández E, Normann RA. CORTIVIS Approach for an Intracortical Visual Prostheses BT - Artificial Vision: A Clinical Guide. In: Gabel VP, ed. Cham: Springer International Publishing; 2017:191-201. doi:10.1007/978-3-319-41876-6_15

113. Wang C, Brunton E, Haghgooie S, Cassells K, Lowery A, Rajan R. Characteristics of electrode impedance and stimulation efficacy of a chronic cortical implant using novel annulus electrodes in rat motor cortex. *J Neural Eng*. 2013;10(4):46010.

114. Stensaas SS, Eddington DK, Dobelle WH. The topography and variability of the primary visual cortex in man. *J Neurosurg*. 1974;40(6):747-755. doi:10.3171/jns.1974.40.6.0747

115. Parker RA, Davis TS, House PA, Normann RA, Greger B. Chapter 11 - The functional consequences of chronic, physiologically effective intracortical microstimulation. In: Schouenborg J, Garwicz M, Danielsen N, eds. *Brain Machine Interfaces: Implications for Science, Clinical Practice and Society*. Vol 194. Progress in Brain Research. Elsevier; 2011:145-165. doi:https://doi.org/10.1016/B978-0-444-53815-4.00010-8

116. Niketeghad S, Muralidharan A, Patel U, et al. Phosphene perceptions and safety of chronic visual cortex stimulation in a blind subject. *J Neurosurg*. 2019;1(aop):1-8.

117. Researchers Present Latest Positive Results of Second Sight's Orion Visual Cortical Prosthesis Feasibility Study. http://investors.secondsight.com/news-releases/news-release-details/researchers-present-latest-positive-results-second-sights-orion. Published 2019. Accessed October 24, 2019.

118. Fujikado T, Kamei M, Sakaguchi H, et al. One-year outcome of 49-channel suprachoroidal–transretinal stimulation prosthesis in patients with advanced retinitis pigmentosa. *Invest Ophthalmol Vis Sci*. 2016;57(14):6147-6157.

119. Ayton LN, Rizzo JF, Bailey IL, et al. Harmonization of outcomes and vision endpoints in vision restoration trials: recommendations from the international HOVER taskforce.

Transl Vis Sci Technol. 2020;9(8):25.

120. Treutwein B. Adaptive psychophysical procedures. *Vision Res*. 1995;35(17):2503-2522.

121. Bach M, Wilke M, Wilhelm B, Zrenner E, Wilke R. Basic Quantitative Assessment of Visual Performance in Patients with Very Low Vision. *Invest Ophthalmol Vis Sci*. 2010;51(2):1255-1260. doi:10.1167/iovs.09-3512

122. Stingl K, Bartz-Schmidt K-U, Gekeler F, Kusnyerik A, Sachs H, Zrenner E. Functional outcome in subretinal electronic implants depends on foveal eccentricity. *Invest Ophthalmol Vis Sci*. 2013;54(12):7658-7665.

123. Barry MP, Dagnelie G. Hand-Camera Coordination Varies over Time in Users of the Argus® II Retinal Prosthesis System. *Front Syst Neurosci*. 2016;10. doi:10.3389/fnsys.2016.00041

124. Petoe MA. The Bionic Vision Technologies Suprachoroidal Retinal Prosthesis: Interim Clinical Trial Results. In: *The Eye and the Chip - World Congress on Artificial Vision*. Detroit; 2019.

125. Drasdo N, Fowler CW. Non-linear projection of the retinal image in a wide-angle schematic eye. *Br J Ophthalmol*. 1974;58(8):709.

126. Dacey DM, Petersen MR. Dendritic field size and morphology of midget and parasol ganglion cells of the human retina. *Proc Natl Acad Sci*. 1992;89(20):9666-9670.

127. Kolic M, Baglin E, Titchener SA, et al. A 44 channel suprachoroidal retinal prosthesis: initial functional vision results. *Invest Ophthalmol Vis Sci*. 2019;60(9):4986.

128. Sikder MKU, Shivdasani MN, Fallon JB, et al. Electrically conducting diamond films grown on platinum foil for neural stimulation. *J Neural Eng*. 2019.

129. Zeng Q, Zhao S, Yang H, Zhang Y, Wu T. Micro/Nano Technologies for High-Density Retinal Implant. *Micromachines*. 2019;10(6):419.

130. Flores T, Huang T, Bhuckory M, et al. Honeycomb-shaped electro-neural interface enables cellular-scale pixels in subretinal prosthesis. *Sci Rep*. 2019;9(1):10657.

131. Seo HW, Kim N, Ahn J, Cha S, Goo YS, Kim S. A 3D flexible microelectrode array for subretinal stimulation. *J Neural Eng*. 2019;16(5):56016.

132. Ho E, Lei X, Flores TA, et al. Characteristics of prosthetic vision in rats with subretinal flat and pillar electrode arrays. *J Neural Eng*. 2019.

133. Chang Y-C, Ghaffari DH, Chow RH, Weiland JD. Stimulation strategies for selective activation of retinal ganglion cell soma and threshold reduction. *J Neural Eng*. 2018.

134. Chenais NAL, Leccardi MJIA, Ghezzi D. Capacitive-like photovoltaic epiretinal stimulation enhances and narrows the network-mediated activity of retinal ganglion cells by recruiting the lateral inhibitory network. *J Neural Eng*. 2019.

135. Spencer TC, Fallon JB, Shivdasani MN. Creating virtual electrodes with 2D current steering. *J Neural Eng*. 2018;15(3):35002.

136. Spencer MJ, Kameneva T, Grayden DB, Meffin H, Burkitt AN. Global activity shaping strategies for a retinal implant. *J Neural Eng*. 2019;16(2):26008.

137. McCarthy C, Walker JG, Lieby P, Scott A, Barnes N. Mobility and low contrast trip hazard avoidance using augmented depth. *J Neural Eng*. 2014;12(1):16003.

138. He Y, Huang NT, Caspi A, Roy A, Montezuma SR. Trade-Off Between Field-of-View and Resolution in the Thermal-Integrated Argus II SystemHe et al. *Transl Vis Sci Technol*. 2019;8(4):29. doi:10.1167/tvst.8.4.29

139. Sanchez-Garcia M, Martinez-Cantin R, Guerrero JJ. Indoor Scenes Understanding for Visual Prosthesis with Fully Convolutional Networks. In: *International Joint Conference on Computer Vision, Imaging and Computer Graphics Theory and Applications*. ; 2019.

140. Melanitis N, Nikita KS. Biologically-inspired image processing in computational retina models. *Comput Biol Med*. 2019:103399.

141. Lorach H, Benosman R, Marre O, Ieng S-H, Sahel JA, Picaud S. Artificial retina: the multichannel processing of the mammalian retina achieved with a neuromorphic asynchronous light acquisition device. *J Neural Eng*. 2012;9(6):66004.

142. Sabbah N, Authié CN, Sanda N, Mohand-Said S, Sahel J-A, Safran AB. Importance of Eye Position on Spatial Localization in Blind Subjects Wearing an Argus II Retinal Prosthesis. *Investig Ophthalmol Vis Sci*. 2014;55(12):8259-8266.

143. Brady-Simmons C, Van Der Biest R, Bozeman L. Miami lighthouse for the blind and visually impaired case study: vision rehabilitation for the first Florida resident to receive the Argus II" Bionic Eye". *J Vis Impair Blind*. 2016;110(3):177.

144. Leigh RJ, Zee DS. Eye movements of the blind. *Investig Ophthalmol Vis Sci*. 1980;19(3):328-331.

145. Hafed ZM, Stingl K, Bartz-Schmidt K-U, Gekeler F, Zrenner E. Oculomotor behavior of blind patients seeing with a subretinal visual implant. *Vision Res*. 2016;118:119-131. doi:https://doi.org/10.1016/j.visres.2015.04.006

146. McIntosh BP. Intraocular and extraocular cameras for retinal prostheses: effects of foveation by means of visual prosthesis simulation. 2015.

147. Nasiatka PJ, McIntosh BP, Stiles NRB, et al. An intraocular camera for retinal prostheses: restoring sight to the blind. In: Serpengüzel A, Poon AW, eds. *Optical Processes in Microparticles and Nanostructures*. Vol 6. Singapore: World Scientific; 2011:385.

148. Shivdasani MN, Sinclair NC, Gillespie LN, Petoe MA, Pardinas-Diaz D, Blamey PJ. Making phosphenes meaningful – Image and pattern recognition with a suprachoroidal retinal prosthesis. *Artif Vis*. 2015.

149. Caspi A, Roy A, Wuyyuru V, et al. Eye movement control in Argus II retinal prosthesis users improves performance in a shape localization task. *Investig Ophthalmol Vis Sci*. 2017;58(8):4192.

150. Leigh RJ, Averbuch-Heller L. Nystagmus and related ocular motility disorders. *Walsh Hoyt's Clin neuro-ophthalmology*. 1998;1:1461-1505.

151. Gunton KB, Wasserman BN, DeBenedictis C. Strabismus. *Prim Care*. 2015;42(3):393-407.

152. Slater KD, Sinclair NC, Nelson TS, Blamey PJ, McDermott HJ. neuroBi: a highly configurable neurostimulator for a retinal prosthesis and other applications. *IEEE J Transl Eng Heal Med*. 2015;3:1-11.

153. Lieby P, Scott A, Barnes N, Stacey A, Ayton L, Walker J. Evaluating Lanczos2 image filtering for visual acuity in simulated prosthetic vision. *Investig Ophthalmol Vis Sci*. 2013;54(15):1049.

154. Petoe MA, McCarthy CD, Shivdasani MN, et al. Determining the Contribution of Retinotopic Discrimination to Localization Performance With a Suprachoroidal Retinal Prosthesis. *Investig Ophthalmol Vis Sci*. 2017;58(7):3231-3239.

155. Wiecek EW, Pasquale LR, Fiser J, Dakin S, Bex PJ. Effects of peripheral visual field loss on eye movements during visual search. *Front Psychol*. 2012;3:472.

156. Cornelissen FW, Bruin KJ, Kooijman AC. The influence of artificial scotomas on eye movements during visual search. *Optom Vis Sci*. 2005;82(1):27-35.

157. Vargas-Martín F, Peli E. Eye movements of patients with tunnel vision while walking. *Investig Ophthalmol Vis Sci*. 2006;47(12):5295-5302.

158. Luo G, Vargas-Martin F, Peli E. The role of peripheral vision in saccade planning: learning from people with tunnel vision. *J Vis*. 2008;8(14):25.

159. Turano KA, Geruschat DR, Baker FH, Stahl JW, Shapiro MD. Direction of gaze while walking a simple route: persons with normal vision and persons with retinitis pigmentosa. *Optom Vis Sci*. 2001;78(9):667-675.

160. Cheong AMY, Geruschat DR, Congdon N. Traffic gap judgment in people with significant peripheral field loss. *Optom Vis Sci*. 2008;85(1):26-36.

161. Authié CN, Berthoz A, Sahel J-A, Safran AB. Adaptive gaze strategies for locomotion with constricted visual field. *Front Hum Neurosci*. 2017;11:387.

162. Gilchrist ID, Brown V, Findlay JM, Clarke MP. Using the eye–movement system to control the head. *Proc R Soc London B Biol Sci*. 1998;265(1408):1831-1836.

163. Stahl JS. Adaptive plasticity of head movement propensity. *Exp Brain Res*. 2001;139(2):201-208. doi:10.1007/s002210100749

164. Gauthier M, Obrecht G, Pedrono C, Vercher JL, Stark L. Adaptive optimization of eye-head coordination with degraded peripheral vision. In: J.K. O'Regan AL-S, ed. *Eye Movements: From Physiology to Cognition*. Elsevier; 1987:201-210.

165. Rifai K, Wahl S. Specific eye–head coordination enhances vision in progressive lens wearers. *J Vis*. 2016;16(11):5. doi:10.1167/16.11.5

166. Proudlock FA, Shekhar H, Gottlob I. Age-related changes in head and eye coordination. *Neurobiol Aging*. 2004;25(10):1377-1385.

167. Stahl JS. Amplitude of human head movements associated with horizontal saccades. *Exp Brain Res*. 1999;126(1):41-54.

168. Turano KA, Yu D, Hao L, Hicks JC. Optic-flow and egocentric-direction strategies in walking: Central vs peripheral visual field. *Vision Res*. 2005;45(25-26):3117-3132.

169. Fernando Livschitz [Black Sheep Films]. Rush Hour. https://vimeo.com/106226560. Published 2014.

170. Steinman RM. Effect of target size, luminance, and color on monocular fixation. *JOSA*. 1965;55(9):1158-1164.

171. Wandell BA. *Foundations of Vision*. Sinauer Associates; 1995.

172. Thumser ZC, Adams NL, Lerner AJ, Stahl JS. Probing the mechanism of saccade-associated head movements through observations of head movement propensity and cognition in the elderly. *Exp Brain Res*. 2010;202(4):903-913.

173. Ivanov I V, Mackeben M, Vollmer A, Martus P, Nguyen NX, Trauzettel-Klosinski S. Eye Movement Training and Suggested Gaze Strategies in Tunnel Vision-A Randomized and Controlled Pilot Study. *PLoS One*. 2016;11(6):e0157825.

174. Fuller JH. Head movement propensity. *Exp Brain Res*. 1992;92(1):152-164. doi:10.1007/bf00230391

175. Papageorgiou E, Hardiess G, Wiethölter H, et al. The neural correlates of impaired collision avoidance in hemianopic patients. *Acta Ophthalmol*. 2012;90(3):e198-e205.

176. Hardiess G, Papageorgiou E, Schiefer U, Mallot HA. Functional compensation of visual field deficits in hemianopic patients under the influence of different task demands. *Vision Res*. 2010;50(12):1158-1172.

177. Oommen BS, Smith RM, Stahl JS. The influence of future gaze orientation upon eye-head coupling during saccades. *Exp Brain Res*. 2004;155(1):9-18.

178. Thumser ZC, Oommen BS, Kofman IS, Stahl JS. Idiosyncratic variations in eye–head coupling observed in the laboratory also manifest during spontaneous behavior in a natural setting. *Exp Brain Res*. 2008;191(4):419-434.

179. Caspi A, Roy A, Wuyyuru V, et al. Eye movement control in the Argus II retinal-prosthesis enables reduced head movement and better localization precision. *Invest Ophthalmol Vis Sci*. 2018;59(2):792-802.

180. Grobbel J, Dietzsch J, Johnson CA, et al. Normal values for the full visual field, corrected for age-and reaction time, using semiautomated kinetic testing on the octopus 900 perimeter. *Transl Vis Sci Technol*. 2016;5(2):5.

181. Racette L, Casson EJ. The impact of visual field loss on driving performance: evidence

from on-road driving assessments. *Optom Vis Sci*. 2005;82(8):668-674.

182. Muqit MMK, Velikay-Parel M, Weber M, et al. Six-Month Safety and Efficacy of the Intelligent Retinal Implant System II Device in Retinitis Pigmentosa. *Ophthalmology*. 2019;126(4):637-639. doi:https://doi.org/10.1016/j.ophtha.2018.11.010

183. Beauchamp MS, Oswalt D, Sun P, et al. Dynamic Stimulation of Visual Cortex Produces Form Vision in Sighted and Blind Humans. *Cell*. 2020;181(4):774-783.e5. doi:10.1016/j.cell.2020.04.033

184. Beyeler M, Nanduri D, Weiland JD, Rokem A, Boynton GM, Fine I. A model of ganglion axon pathways accounts for percepts elicited by retinal implants. *Sci Rep*. 2019;9(1):9199.

185. Barnes N, Scott AF, Lieby P, et al. Vision function testing for a suprachoroidal retinal prosthesis: effects of image filtering. *J Neural Eng*. 2016;13(3):36013.

186. Caspi A, Dorn JD, McClure KH, Humayun MS, Greenberg RJ, McMahon MJ. Feasibility study of a retinal prosthesis: spatial vision with a 16-electrode implant. *Arch Ophthalmol*. 2009;127(4):398-401.

187. Manning TS, Britten KH. Motion Processing in Primates. In: *Oxford Research Encyclopedia of Neuroscience*. Oxford University Press; 2017:1-29.

188. Wei W. Neural mechanisms of motion processing in the mammalian retina. *Annu Rev Vis Sci*. 2018;4:165-192.

189. Taylor WR, Smith RG. The role of starburst amacrine cells in visual signal processing. *Vis Neurosci*. 2012;29(1):73-81.

190. Abramian M, Lovell NH, Morley JW, Suaning GJ, Dokos S. Activation of retinal ganglion cells following epiretinal electrical stimulation with hexagonally arranged bipolar electrodes. *J Neural Eng*. 2011;8(3):35004.

191. Marc RE, Jones BW, Watt CB, Strettoi E. Neural remodeling in retinal degeneration. *Prog Retin Eye Res*. 2003;22(5):607-655.

192. Cruz-Martín A, El-Danaf RN, Osakada F, et al. A dedicated circuit links direction-selective retinal ganglion cells to the primary visual cortex. *Nature*. 2014;507(7492):358-361.

193. Fujikado T, Kamei M, Sakaguchi H, et al. Clinical Trial of Chronic Implantation of Suprachoroidal-Transretinal Stimulation System for Retinal Prosthesis. *Sensors Mater*. 2012;24(4):181-187.

194. Reuschel J, Rösler F, Henriques DYP, Fiehler K. Spatial updating depends on gaze direction even after loss of vision. *J Neurosci*. 2012;32(7):2422-2429.

195. Kotecha A, Zhong J, Stewart D, da Cruz L. The Argus II prosthesis facilitates reaching and grasping tasks: a case series. *BMC Ophthalmol*. 2014;14(1):1.

196. Luo YH-L, Zhong JJ, da Cruz L. The use of Argus® II retinal prosthesis by blind subjects to

achieve localisation and prehension of objects in 3-dimensional space. *Graefe's Arch Clin Exp Ophthalmol*. 2015;253(11):1907-1914.

197. Fornos AP, Sommerhalder J, Pittard A, Safran AB, Pelizzone M. Simulation of artificial vision: IV. Visual information required to achieve simple pointing and manipulation tasks. *Vision Res*. 2008;48(16):1705-1718.

198. Hauer MC, Nasiatka PJ, Stiles NR, et al. Intraocular Camera for Retinal Prostheses: Optical Design. In: *Frontiers in Optics*. San Jose, CA: Optical Society of America; 2007. doi:10.1364/FIO.2007.FThT1

199. Sahin FE, McIntosh BP, Nasiatka PJ, Weiland JD, Humayun MS, Tanguay AR. Eye-Tracked Extraocular Camera for Retinal Prostheses. In: *Frontiers in Optics 2015*. San Jose, California: Optical Society of America; 2015:FTu2C.3. doi:10.1364/FIO.2015.FTu2C.3

200. Dagnelie G, Walter M, Yang L. Playing checkers: detection and eye–hand coordination in simulated prosthetic vision. *J Mod Opt*. 2006;53(9):1325-1342. doi:10.1080/09500340600619197

201. Hozumi K, Endo T, Hirota M, et al. Improvement of reaching movement in subjects with retinal implant simulator with gaze feedback system. *Investig Ophthalmol Vis Sci*. 2016;57(12):1958.

202. Barry MP, Diaz-Aguilar S, Yang L, Dagnelie G. Retinal prosthesis users' shifts in hand-camera coordination correlate with changes in eye orientation. *Investig Ophthalmol Vis Sci*. 2017;58(8):4687.

203. Petoe MA, Sinclair NC, Shivdasani MN, et al. The Bionic Vision Australia Suprachoroidal Retinal Prosthesis: Research and Development Update. *Eye Chip - World Congr Artif Vis*. 2016.

204. Endo T, Kanda H, Hirota M, Morimoto T, Nishida K, Fujikado T. False reaching movements in localization test and effect of auditory feedback in simulated ultra-low vision subjects and patients with retinitis pigmentosa. *Graefe's Arch Clin Exp Ophthalmol*. 2016;254(5):947-956.

205. Zimmerman DW, Zumbo BD. Rank transformations and the power of the Student t test and Welch t'test for non-normal populations with unequal variances. *Can J Exp Psychol Can Psychol expérimentale*. 1993;47(3):523.

206. Jammalamadaka SR, Sengupta A. Circular Correlation and Regression. In: *Topics in Circular Statistics*. Vol 5. Singapore: World Scientific; 2001.

207. Berens P. CircStat: a MATLAB toolbox for circular statistics. *J Stat Softw*. 2009;31(10):1-21.

208. Titchener SA, Shivdasani MN, Sinclair NC, et al. Oculomotor Behaviour of Patients Implanted with a Suprachoroidal Retinal Prosthesis During a Spatial Discrimination Task. *Eye Chip - World Congr Artif Vis*. 2016.

209. Zoccolan D, Graham BJ, Cox DD. A self-calibrating, camera-based eye tracker for the recording of rodent eye movements. *Front Neurosci*. 2010;4.

210. Van der Geest JN, Frens MA. Recording eye movements with video-oculography and scleral search coils: a direct comparison of two methods. *J Neurosci Methods*. 2002;114(2):185-195.

211. Kanda H, Satonaka S, Morimoto T, Miyoshi T, Fujikado T. Novel eye-tracking method for retinal prostheses. In: *The Annual Meeting of the Association for Research in Vision and Ophthalmology*. Baltimore, MD; 2017:4188.

212. Corbetta M, Shulman GL. Control of goal-directed and stimulus-driven attention in the brain. *Nat Rev Neurosci*. 2002;3(3):201-215. http://dx.doi.org/10.1038/nrn755.

213. Caspi A, Roy A, Barry MP, Sadeghi R, Kartha A, Dagnelie G. The use of a handheld marker to calibrate a head-mounted eye tracker for visual prostheses. *Invest Ophthalmol Vis Sci*. 2020;61(7):926.

214. Barsingerhorn AD, Boonstra FN, Goossens J. Development and validation of a high-speed stereoscopic eyetracker. *Behav Res Methods*. 2018;50(6):2480-2497.

215. Oommen BS, Stahl JS. Overlapping gaze shifts reveal timing of an eye–head gate. *Exp Brain Res*. 2005;167(2):276-286.

216. Stronks HC, Mitchell EB, Nau AC, Barnes N. Visual task performance in the blind with the BrainPort V100 Vision Aid. *Expert Rev Med Devices*. 2016;13(10):919-931.

217. Yarbus. *Eye Movements and Vision*.; 1967.

218. Coppola D, Purves D. The extraordinarily rapid disappearance of entopic images. *Proc Natl Acad Sci*. 1996;93(15):8001-8004.

219. Rucci M, Iovin R, Poletti M, Santini F. Miniature eye movements enhance fine spatial detail. *Nature*. 2007;447(7146):852-855.

220. Fornos AP, Sommerhalder J, da Cruz L, et al. Temporal Properties of Visual Perception on Electrical Stimulation of the RetinaPerception upon Electrical Stimulation of the Retina. *Investig Ophthalmol Vis Sci*. 2012;53(6):2720-2731.

221. Wang V, Kuriyan AE. Optoelectronic Devices for Vision Restoration. *Curr Ophthalmol Rep*.:1-9.

222. Lohmann TK, Werner C, Raffelberg P, et al. Surgical feasibility and biocompatibility of the OptoEpiret retinal stimulator. *Invest Ophthalmol Vis Sci*. 2019;60(9):4982.

223. Barry MP. Shifting gazes with visual prostheses: Long-term hand-camera coordination. 2018.

224. Vive Pro Eye. https://www.vive.com/eu/product/vive-pro-eye/. Accessed November 14, 2019.

225. Eye Tracking: VR. https://imotions.com/biosensor/eye-tracking-vr/. Accessed November

14, 2019.

226. Kutila M, Jokela M, Markkula G, Rué MR. Driver distraction detection with a camera vision system. In: *2007 IEEE International Conference on Image Processing*. Vol 6. IEEE; 2007:VI-201.

227. Eggert T. Eye movement recordings: methods. In: *Neuro-Ophthalmology*. Vol 40. Karger Publishers; 2007:15-34.

228. Singh H, Singh J. Human eye tracking and related issues: A review. *Int J Sci Res Publ*. 2012;2:1-9.

229. Imai T, Sekine K, Hattori K, et al. Comparing the accuracy of video-oculography and the scleral search coil system in human eye movement analysis. *Auris Nasus Larynx*. 2005;32(1):3-9.

230. Shelhamer M, Roberts DC. Chapter 6 - Magnetic scleral search coil. In: *Vertigo and Imbalance: Clinical Neurophysiologyof the Vestibular System*. Vol 9. Handbook of Clinical Neurophysiology. Elsevier; 2010:80-87. doi:https://doi.org/10.1016/S1567-4231(10)09006-4

231. Robinson DA. A method of measuring eye movemnent using a scleral search coil in a magnetic field. *Bio-medical Electron IEEE Trans*. 1963;10(4):137-145.

232. Whitmire E, Trutoiu L, Cavin R, et al. EyeContact: scleral coil eye tracking for virtual reality. In: *Proceedings of the 2016 ACM International Symposium on Wearable Computers*. ACM; 2016:184-191.

233. Bour LJ, Gisbergen JA, Bruijns J, Ottes FP. The double magnetic induction method for measuring eye movement-results in monkey and man. *Biomed Eng IEEE Trans*. 1984;(5):419-427.

234. Bremen P, Van der Willigen RF, Van Opstal AJ. Using double-magnetic induction to measure head-unrestrained gaze shifts I. Theory and validation. *J Neurosci Methods*. 2007;160(1):75-84. doi:10.1016/j.jneumeth.2006.08.012

235. Bremen P, Van der Willigen RF, Van Wanrooij MM, et al. Applying double-magnetic induction to measure head-unrestrained gaze shifts: calibration and validation in monkey. *Biol Cybern*. 2010;103(6):415-432.

236. Roberts D, Shelhamer M, Wong A. A new wireless search-coil system. In: *Proceedings of the 2008 Symposium on Eye Tracking Research & Applications*. ACM; 2008:197-204.

237. Petoe MA, Williams CE, Millard R, Villalobos J, Seligman PM. Determining eye movement using induction. October 2019.

238. Shin Y, Lim HW, Kang MH, Seong M, Cho H, Kim JH. Normal range of eye movement and its relationship to age. *Acta Ophthalmol*. 2016;94.

239. Caspi A, Roy A, Barry MP, Sadeghi R, Kartha A, Dagnelie G. The use of handheld marker to calibrate a field-programmable gate array based eye tracker for artificial vision system.

In: *2020 42nd Annual International Conference of the IEEE Engineering in Medicine & Biology Society (EMBC)*. ; 2020:3323-3326. doi:10.1109/EMBC44109.2020.9175803

240. Fischer H. Three Main Layers of the Eye. https://commons.wikimedia.org/wiki/File:Three_Main_Layers_of_the_Eye.png. Accessed November 6, 2019.

241. Nieto MP. Human visual pathway. https://commons.wikimedia.org/wiki/File:Human_visual_pathway.svg. Accessed November 7, 2019.

242. Fariss RN, Li Z-Y, Milam AH. Abnormalities in rod photoreceptors, amacrine cells, and horizontal cells in human retinas with retinitis pigmentosa. *Am J Ophthalmol*. 2000;129(2):215-223.

243. Dobelle WH. Artificial vision for the blind by connecting a television camera to the visual cortex. *ASAIO J*. 2000;46(1):3-9.

244. Schuettler M, Stieglitz T, Gross M, et al. Reducing stiffness and electrical losses of high channel hybrid nerve cuff electrodes. In: *2001 Conference Proceedings of the 23rd Annual International Conference of the IEEE Engineering in Medicine and Biology Society*. Vol 1. IEEE; 2001:769-772.

245. Niketeghad S, Pouratian N. Brain machine interfaces for vision restoration: the current state of cortical visual prosthetics. *Neurotherapeutics*. 2019;16(1):134-143.